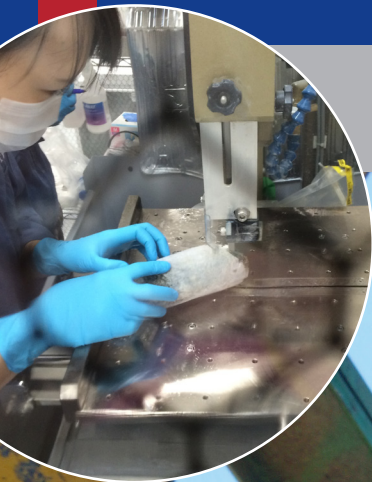
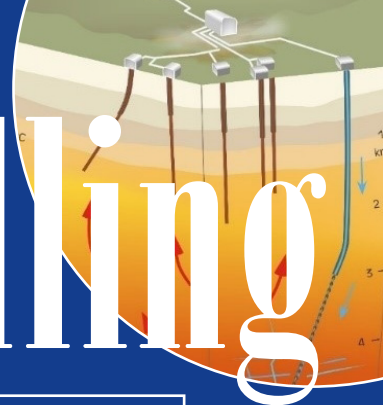


Scientific Drilling



Reports on Deep Earth Sampling and Monitoring

Deep drilling in Iceland for supercritical fluids	1
Drilling into an active mofette in the Czech Republic	13
Autoclave pressure vessels for the deep-sea drill rig MeBo	29
IODP Expedition 357 contamination tracer testing	39
Workshop on Drilling the Ivrea Zone	47
Workshop on Scientific Exploration of Induced Seismicity and Stress	57

Dear reader,

Backed by broad international agreement, the recent COP23 climate conference in Bonn paved the road to phase out coal-based energy generation to reduce atmospheric carbon dioxide. However, regenerative energy resources such as wind and the Sun have a limited capacity to supply the necessary base load energy. In this issue of *SCIENTIFIC DRILLING* the tapping of new geothermal resources with high potential is reported (**pages 1 to 12**), with the IDDP-2 deep geothermal drilling campaign in Iceland reaching supercritical fluids at a depth of 4.5 km. Aside from the scientific themes addressed by IDDP-2, namely the characterization of a mid-ocean ridge submarine black smoker hydrothermal system on land, the utilization of supercritical fluids as a sustainable georesource for energy generation has the potential to outweigh conventional geothermal energy exploitation.

Geofluids were also the target of a drilling project in the western Eger Rift (Czech Republic), where shallow drilling into an active gas emanation (Moffette) served to improve our understanding of the geo-bio interaction in a CO₂-rich environment (**pages 13 to 27**). This drilling also serves as a pilot study for an ICDP-supported multi-well campaign in the area.

Scientific drilling for the deep biosphere is notoriously hampered by sample contamination. Therefore, tracers are deployed to determine influx of surface material. Investigations on tracer concentrations from seabed drills during IODP Expedition 357 (**pages 39 to 46**) provided important information on the quality of core samples taken for deep biosphere exploration and are highly recommended for future applications.

Coring under in situ pressure conditions for sampling and preservation of submarine sediments is examined on **pages 29 to 37**. Deployments of the so-called "MDP" (MeBo pressure vessel) during two offshore expeditions resulted in the recovery of sediment cores with pressure stages equalling in situ hydrostatic pressure, important for many different research fields, including gas hydrates, geotechnics, sedimentology, microbiology, and several others.

The Ivrea-Verbano Zone as one of the most complete, time-integrated crust-upper mantle archives worldwide is a unique drilling target, as discussed recently in a workshop (**pages 47 to 56**). The meeting served to prepare drilling into the deep crust and the Moho transition zone and to test several hypotheses on the formation, evolution, and modification of the continental crust through space and time. A workshop on "Scientific Exploration of Induced Seismicity and Stress, SEISMS" (**pages 57 to 63**) discussed the value of drilling where a fault is instrumented in advance of minor seismic events induced through controlled fluid injection in areas that are feasible from both a societal and scientific standpoint.

We hope to have generated your interest and we hope that you will enjoy reading this volume of *SCIENTIFIC DRILLING*.

Your editors,
**Ulrich Harms, Thomas Wiersberg, Jan Behrmann,
Will Sager, and Tomoaki Morishita**

Aims & scope

Scientific Drilling (SD) is a multidisciplinary journal focused on bringing the latest science and news from the scientific drilling and related programmes to the geosciences community. Scientific Drilling delivers peer-reviewed science reports from recently completed and ongoing international scientific drilling projects. The journal also includes reports on engineering developments, technical developments, workshops, progress reports, and news and updates from the community.

Editorial board

Ulrich Harms (editor in chief),
Thomas Wiersberg, Jan Behrmann,
Will Sager, and Tomoaki Morishita
sd-editors-in-chief@mailinglists.copernicus.org



Additional information

ISSN 1816-8957 | eISSN 1816-3459

 **Copernicus Publications**
The Innovative Open Access Publisher

Copernicus Publications

Bahnhofsallee 1e
37081 Göttingen
Germany
Phone: +49 551 90 03 39 0
Fax: +49 551 90 03 39 70

editorial@copernicus.org
production@copernicus.org

<http://publications.copernicus.org>

View the online library or learn
more about Scientific Drilling on:
www.scientific-drilling.net

Cover figure: Drilling in the Songliao Basin in China reached 6298 m and sets a new benchmark in ICDP drilling. Photo courtesy of Qingtian Lu.

Insert 1: Cutting of a frozen core with ultraclean diamond band saw with frozen stage inside a filtered air clean booth at the Kochi Core Center (Japan). Photograph by Beth Orcutt.

Insert 2: Conceptual model of the Reykjanes Geothermal field in Iceland including the supercritical zone beneath the producing reservoir.

Science Reports

- 1** **The Iceland Deep Drilling Project 4.5 km deep well, IDDP-2, in the seawater-recharged Reykjanes geothermal field in SW Iceland has successfully reached its supercritical target**

G. Ó. Friðleifsson et al.

- 13** **Drilling into an active mofette: pilot-hole study of the impact of CO₂-rich mantle-derived fluids on the geo-bio interaction in the western Eger Rift (Czech Republic)**

R. Bussert et al.

Technical Developments

- 29** Design and deployment of autoclave pressure vessels for the portable deep-sea drill rig MeBo (*Meeresboden-Bohrgerät*)
- 39** Contamination tracer testing with seabed drills: IODP Expedition 357

News & Views

Workshop Reports

- 47** Report on the ICDP workshop DIVE (Drilling the Ivrea-Verbano zone)
- 57** Scientific Exploration of Induced Seismicity and Stress (SEISMS)



The Iceland Deep Drilling Project 4.5 km deep well, IDDP-2, in the seawater-recharged Reykjanes geothermal field in SW Iceland has successfully reached its supercritical target

Guðmundur Ó. Friðleifsson¹, Wilfred A. Elders², Robert A. Zierenberg³, Ari Stefánsson¹, Andrew P. G. Fowler³, Tobias B. Weisenberger⁴, Björn S. Harðarson⁴, and Kiflom G. Mesfin¹

¹HS Orka, Svartsengi, 240 Grindavík, Iceland

²Department of Earth Sciences, University of California, Riverside, CA 92521, USA

³Department of Earth and Planetary Sciences, University of California, Davis, CA 95616, USA

⁴ÍSOR, Grensásvegur 9, 108 Reykjavík, Iceland

Correspondence to: Guðmundur Ó. Friðleifsson (gof@hsorka.is)

Received: 15 June 2017 – Revised: 25 August 2017 – Accepted: 4 September 2017 – Published: 30 November 2017

Abstract. The Iceland Deep Drilling Project research well RN-15/IDDP-2 at Reykjanes, Iceland, reached its target of supercritical conditions at a depth of 4.5 km in January 2017. After only 6 days of heating, the measured bottom hole temperature was 426 °C, and the fluid pressure was 34 MPa. The southern tip of the Reykjanes peninsula is the landward extension of the Mid-Atlantic Ridge in Iceland. Reykjanes is unique among Icelandic geothermal systems in that it is recharged by seawater, which has a critical point of 406 °C at 29.8 MPa. The geologic setting and fluid characteristics at Reykjanes provide a geochemical analog that allows us to investigate the roots of a mid-ocean ridge submarine black smoker hydrothermal system.

Drilling began with deepening an existing 2.5 km deep vertical production well (RN-15) to 3 km depth, followed by inclined drilling directed towards the main upflow zone of the system, for a total slant depth of 4659 m (~4.5 km vertical depth). Total circulation losses of drilling fluid were encountered below 2.5 km, which could not be cured using lost circulation blocking materials or multiple cement jobs. Accordingly, drilling continued to the total depth without return of drill cuttings. Thirteen spot coring attempts were made below 3 km depth. Rocks in the cores are basalts and dolerites with alteration ranging from upper greenschist facies to amphibolite facies, suggesting that formation temperatures at depth exceed 450 °C.

High-permeability circulation-fluid loss zones (feed points or feed zones) were detected at multiple depth levels below 3 km depth to bottom. The largest circulation losses (most permeable zones) occurred between the bottom of the casing and 3.4 km depth. Permeable zones encountered below 3.4 km accepted less than 5 % of the injected water. Currently, the project is attempting soft stimulation to increase deep permeability. While it is too early to speculate on the energy potential of this well and its economics, the IDDP-2 is a milestone in the development of geothermal resources and the study of hydrothermal systems. It is the first well that successfully encountered supercritical hydrothermal conditions, with potential high-power output, and in which on-going hydrothermal metamorphism at amphibolite facies conditions can be observed. The next step will be to carry out flow testing and fluid sampling to determine the chemical and thermodynamic properties of the formation fluids.

1 Introduction

The Iceland Deep Drilling Project (IDDP) is a long-term project (<https://www.iddp.is>) aimed at greatly increasing the production of usable geothermal energy by drilling deep enough to reach the supercritical conditions believed to exist beneath high-temperature geothermal fields in Iceland. When the IDDP consortium was formed in the year 2000, three geothermal fields in Iceland were chosen as suitable locations to search for supercritical resources, Krafla in the northeast of Iceland, and Hengill and Reykjanes in the southwest (Friðleifsson et al., 2003; see Fig. 1). The first attempt to drill into a supercritical reservoir was made in 2008–2009 in the Krafla caldera (IDDP-1), but the well did not attain supercritical fluid pressures because drilling was suspended at too shallow of a depth (Elders et al., 2011). This was because drilling intercepted 900 °C rhyolite magma at a depth of only 2100 m. However, the IDDP-1 was completed with a liner set above the rhyolite intrusion. When the well was tested, it produced superheated 452 °C steam at 140 bar pressure, and had a flow rate and pressure sufficient to generate about 35 MWe. After 2 years of flow testing, repair of the surface installations was necessary, and the well had to be quenched due to failure of the master valves. Unfortunately, this caused a collapse of the well casing and the well was abandoned.

In 2013, as reported previously in this journal (Friðleifsson et al., 2013), the IDDP began planning to drill a deep exploratory/research well, the IDDP-2, in the Reykjanes geothermal field in SW Iceland, where HS Orka generates up to 100 MWe of electric power. From a scientific perspective, this location is of great interest because the Reykjanes peninsula is the landward extension of the Mid-Atlantic Ridge (Fig. 1).

The exposed rocks in Iceland date back to about 16 Ma, the oldest rocks being exposed farthest to the west and farthest to the east, and include about 100 central volcanic complexes of different ages. In Fig. 1 we only show the active central volcanoes associated with on-going rifting at a slow spreading rate of 1.8 cm yr⁻¹. The active rift systems typically show an evolution characterized by development of central volcanoes near the spreading segment centers. Central volcanoes often mature to develop rhyolitic volcanism and calderas over time frames of about 1 My before drifting out of the active spreading zone and cooling down. Many of the high-temperature geothermal areas in Iceland are associated with central volcanoes, for example the Krafla volcano, which displays extensive rhyolitic volcanism and caldera collapse (e.g., Friðleifsson et al., 2003), and which was the site of the IDDP-1 drill hole. The Reykjanes system is in an early rifting stage and has not developed into a central volcano, while the Hengill central volcano, the proposed site for IDDP-3 drilling, is considered to be in an intermediate stage of development as it has not generated large volumes of felsic rock and has yet to develop a caldera.

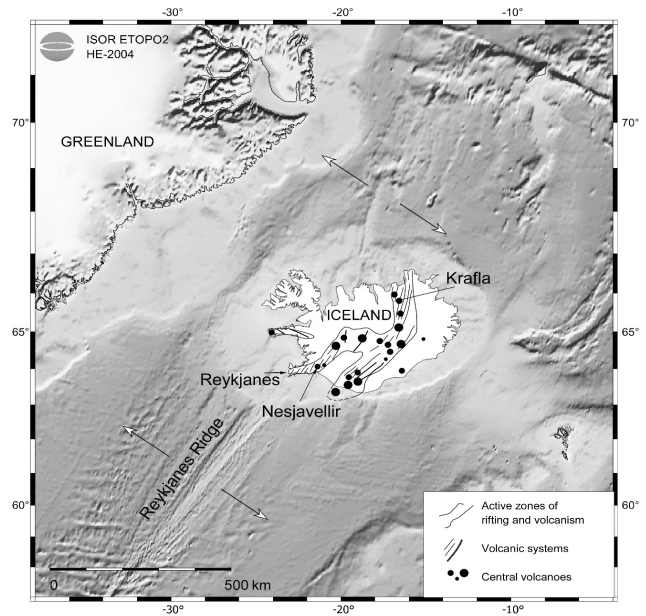


Figure 1. The location of Iceland on the Mid-Atlantic Ridge. The arrows show the spreading directions on the Reykjanes ridge to the south and the Kolbeinsey Ridge to the north. Iceland's neo-volcanic zone with its active central volcanoes and the location of the three high-temperature hydrothermal systems of Reykjanes, Nesjavellir (in the Hengill volcano), and Krafla, targeted for IDDP deep drilling, are also shown.

The drilling target for each of the IDDP sites is to reach supercritical conditions. The critical point of fresh water, which characterizes the Krafla and Hengill fields, occurs at 374 °C and 22.1 MPa. The reservoir fluids currently produced from the Reykjanes field have a salinity of seawater, which has a critical point of 406 °C at 29.8 MPa (Bischoff and Rosenbauer, 1988). As described below, it is already clear that conditions at the bottom of the IDDP-2 well measured during drilling exceed the critical point of seawater. A geothermal well producing from a supercritical geothermal reservoir has the potential to generate power outputs on an order of magnitude greater than conventional high-temperature wells (at 240–340 °C) assuming the same volumetric flow rate of steam (Albertsson et al., 2003; Friðleifsson et al., 2014a).

The Reykjanes hydrothermal resource is a two-phase geothermal system to about 1500 m depth, where temperature follows the boiling point curve with increasing depth and both liquid and vapor are present, below which the temperatures are approximately constant to about 3 km depth, with the highest recorded downhole temperature of about 320 °C (Friðleifsson et al., 2014b). The depth to the bottom of the hydrothermal reservoir is not known, while 3 km depth has been used in reservoir modeling so far for the convection system. The primary motivation for the Reykjanes field operator to undertake such a challenging drilling operation as IDDP-2

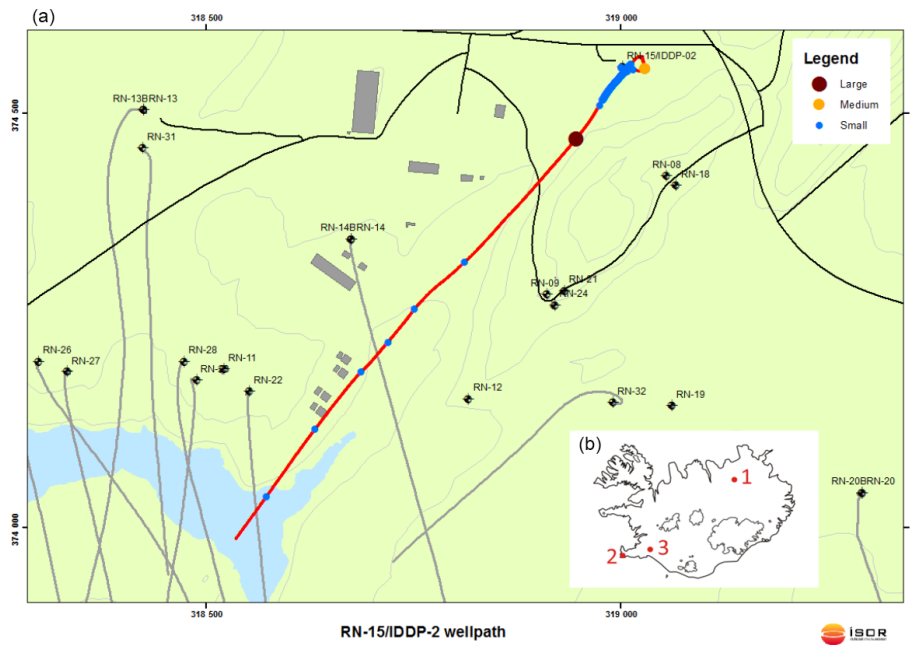


Figure 2. The locations and tracks of wells in the Reykjanes geothermal field (Weisenberger et al., 2017). The red line shows the track of well RN-15/IDDP-2. The relative size of the circulation loss zones are shown with circles (see legend). The inset (bottom right) shows the location of the geothermal fields at Krafla (1), Reykjanes (2), and Hengill (3).

was to address several basic questions important for the future development of the geothermal resource:

- i. What is the nature and location of the base of the Reykjanes hydrothermal reservoir? Is it possibly heated by superheated steam from below?
- ii. Can deeper heat sources be exploited by injecting fluid into the hot rocks beneath the current production zone?
- iii. Will productive permeability be found at these great depths within the approximate center of the fault-related upflow zone?
- iv. Does a hydrothermal reservoir at supercritical condition exist at 4–5 km depth under the Reykjanes well field or does it lie even deeper? Alternatively, will we be dealing with hot dry rocks at those depths?
- v. What is the ultimate heat source of this saline ocean-floor-related hydrothermal system?

In December 2015, the plans for the IDDP-2 were accepted as a part of the European Union Horizon 2020 program DEEPEGS (Deployment of Deep Enhanced Geothermal Systems for Sustainable Energy Business, grant no. 690771). DEEPEGS is a major effort to speed up the development of enhanced geothermal systems within Europe and worldwide, for both high- and low-enthalpy systems.

A drill site was selected on the north side of the Reykjanes drill field (Fig. 2) making use of an existing production

well RN-15 as a “well of opportunity”. In 2004, RN-15 was drilled vertically to a depth of 2500 m with a production casing cemented down to 794 m, and open hole below. The well was suitably sited within the Reykjanes geothermal system for a deepening as an inclined IDDP well, and the potential risk for affecting other production wells during the drilling and cementing operations to 3 km depth was relatively small. Therefore, after serious consideration of the economics as well, IDDP was offered the opportunity to deepen well RN-15. The well is now identified as RN-15/IDDP-2. The RN-15 was cooled down slowly, deepened with a $12\frac{1}{4}$ ” bit to 3000 m, and a new production casing was cemented in place. Drilling then continued with $8\frac{1}{2}$ ” rotary bits towards a target depth of 5 km. We planned to drill $8\frac{1}{2}$ ” spot cores over about 10 % of the total drilling interval.

The RN-15/IDDP-2 passed a significant milestone in geothermal research by reaching a slant depth of 4659 m on 25 January 2017, after 168 days of drilling. Drilling achieved its initial targets to: (a) drill deep enough to reach supercritical conditions (4 to 5 km), (b) measure the fluid temperature and pressure, (c) search for permeable zones, and (d) recover drill cores.

2 The Reykjanes drill field

Prior to the IDDP-2, the deepest producing geothermal wells existing at Reykjanes were about 2.5 km deep. Figure 2 is a map showing the deviated track of well RN-15/IDDP-2, as it was drilled, together with the tracks of existing wells. Ver-

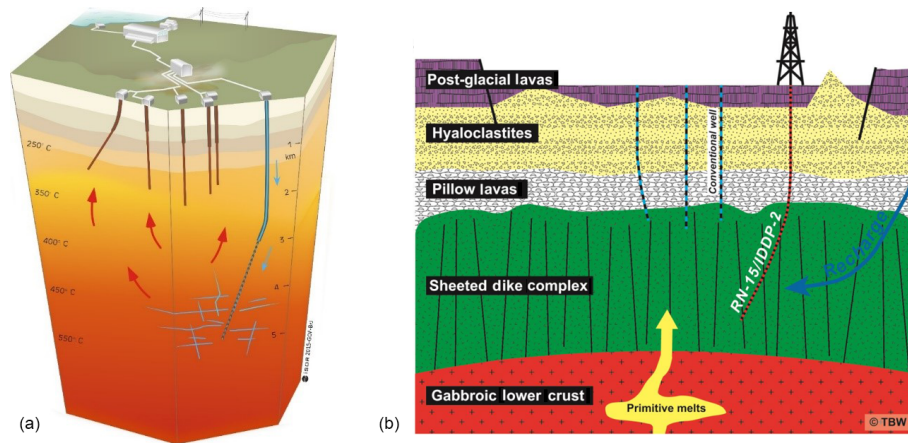


Figure 3. (a) Conceptual model of the roots of the Reykjanes Geothermal field indicating existing wells (brown) and the planned track of the IDDIP-2 well (blue) to intersect the supercritical zone beneath the producing reservoir. (b) Schematic lithological model of the crust beneath the Reykjanes peninsula, which, below a thin apron of subaerial lava flows of Holocene age, is mostly composed of subglacial and marine tuffs, shallow marine sediments, and pillow basalts down to 2–3 km depth, increasingly intruded by dikes with increasing depth. This culminates in a sheeted dike complex which extends for several kilometers, presumably underlain by a gabbroic lower crust.

tical wells are represented by dots only. Figure 3a is a simplified conceptual model of the Reykjanes drill field, showing the well RN-15/IDDIP-2 directionally drilled towards 5 km depth and ending under the main drill field at temperatures anticipated to range from 400–500 °C. Figure 3b is a schematic lithological diagram (Weisenberger et al., 2017), based on lithological logs from about 34 drill holes. Below a pile of several Holocene subaerial lava flows, the rock formations are composed of shallow marine sediments and tuffs, with intervals of pillow basalt and breccia, emplaced in the last ~ 0.5 Ma (Friðleifsson and Richter, 2010). The dike intensity increases dramatically with increasing depth and reaches $\sim 100\%$ below approximately 3 km depth. This sheeted dike complex is presumably underlain by gabbroic lower crust, a model that conforms to typical “classical” ophiolite (Anonymous, 1971). Although the Reykjanes ridge is a slow spreading ridge, it is magmatically robust due to the influence of the Iceland hotspot. Enhanced magmatism results in much thicker crust (~ 16 km) compared to normal mid-ocean ridges (Weir et al., 2001). While the ophiolite conceptual model (Fig. 3b) has been assumed for the Reykjanes field, the RN-15/IDDIP-2 well is the first to confirm the presence of a thick sheeted dike section (see below). The nature of the lower crust and the depth to any large gabbroic intrusions is unknown.

3 Drilling the RN-15/IDDIP-2

The Iceland Drilling Company (IDC) began deepening well RN-15 on 11 August 2016, using the rig Thor (Þór), a Benteq 350-ton drilling rig with an electric top drive (MH PTD-500-AC). On 8 September after 29 working days, drilling to 3000 m depth was completed (Table 1). Well RN-15 had

an existing $13\frac{3}{8}$ " production casing cemented from 0 to 793.8 m. An additional production casing (anchor casing) of $9\frac{7}{8}$ " (from surface to 445 m) and $9\frac{5}{8}$ " (2932.4 m) was run into the hole and cemented (see Table 1) (Weisenberger et al., 2016).

The RN-15/IDDIP-2 was drilled vertically from 2500 m down to 2750 m, and below that drilled directionally to the southwest to intersect the main upflow zone of the Reykjanes system. The bottom of the well is at a vertical depth of about 4500 m, and is situated 738 m southwest of the wellhead.

Cables with eight thermocouples from Petrospec Engineering were attached to the outside of the casing string as it was run into the hole. The thermocouples were rated to tolerate up to 600 °C. They were expected to enable continuous measurement of temperatures at 341, 641, 941, 1541, 1841, 2141, 2341, and 2641 m depths. The thermocouple at 2141 m was damaged during insertion of the casing. In addition, a pressure/temperature sensor was installed at 1241 m depth, and a fiber optic cable for temperature, strain, and seismic measurements was installed by GFZ Potsdam (Geoforschung Zentrum) to 841 m depth, supported by two EU funded programs (IMAGE and GEOWELL) together with DEEPEGS, HS Orka, and Statoil. Data from these sensors were used to evaluate the progress of the cementing operation.

Reverse cementing, with $\sim 150\text{ m}^3$ of cement pumped down the annulus between the casing and the borehole, was completed on 6 September, followed by two separate down-hole cement bond logging trips inside the casing, which indicated that a proper cementing job had been achieved. The result is the longest production casing ever installed in any Icelandic high-temperature geothermal field.

Drilling in formations below 3000 m in the production part of the well began on 17 September (the 38th workday), and

Table 1. Drilling and casing depths in well RN-15 and RN-15/IDDP-2.

ID	Drill rig	Phase	Depth (m)	Depth reference	Bit size	Casing type	Casing depth (m)	Casing-depth reference
RN-15	Saga	Pre-drilling	86.5	Saga RF	26''	22 $\frac{1}{2}$ ''	84.4	Ground surface
RN-15	Jötunn	1. phase	300	Jötunn RF	21''	18 $\frac{5}{8}$ ''	292.8	Ground surface
RN-15	Jötunn	2. phase	804	Jötunn RF	17 $\frac{1}{2}$ ''	13 $\frac{3}{8}$ ''	793.8	Ground surface
RN-15	Jötunn	3. phase	2507	Jötunn RF	12 $\frac{1}{4}$ ''			
RN-15/IDDP-2	Thor	3. phase	3000	Thor RF	12 $\frac{1}{4}$ ''	9 $\frac{7}{8}$ ''	0–445	Ground surface
						9 $\frac{5}{8}$ ''	445–2932.4	Ground surface

Table 2. Overview of the 13 core runs attempted in well RN-15/IDDP-2 at Reykjanes. ROP is rate of penetrations.

Core run	Start	Coring interval (m)	Cored length (m)	Drilling time (h)	ROP (m h ⁻¹)	Core recovered (m)
1	18/09/2016	3068.7–3074.1	5.4	7.12	0.8	
2	04/10/2016	3177.6–3179.0	1.4	2	0.7	
3	30/10/2016	3648.0–3648.9	0.9	5	0.2	0.52
4	02/11/2016	3648.9–3650.7	1.8	10.25	0.2	
5	11/11/2016	3865.5–3869.8	4.3	8.5	0.6	3.85
6	12/11/2016	3869.8–3870.2	0.4	2.5	0.2	0.15
7	22/11/2016	4089.5–4090.6	1.1	2.25	0.5	0.13
8	28/11/2016	4254.6–4255.3	0.7	5.5	0.1	0.28
9	06/12/2016	4308.7–4309.9	1.2	3	0.4	
10	07/12/2016	4309.9–4311.2	1.3	8.25	0.2	0.22
11	16/01/2017	4634.2–4642.8	8.6	1.25	6.9	7.58
12	17/01/2017	4642.8–4652.0	9.2	1	9.2	9
13	19/01/2017	4652.0–4659.0	7	0.75	9.3	5.58
Total			43.3			27.31
Core recovery about						63 %

was concluded on 26 January 2017 (the 168th workday) at 4659 m (Fig. 4). Various challenges arose as the drilling progressed: there were weather delays, problems with hole stability that required frequent reaming, and the drilling assembly became stuck several times. These instances were successfully resolved as they happened. However, the major unsolved problem was a near-complete loss of circulation just below the 9 $\frac{5}{8}$ '' production casing shoe (2931 m) that could not be cured with lost circulation materials or by 12 successive attempts to seal the loss zone with cement. As cementing was not successful, drilling had to continue without any return of drill cuttings to the surface from deeper than 3200 m, except for drill cuttings that were intermittently sampled between 3000 and 3200 m depth (Weisenberger et al., 2017).

Consequently, the drill cores are the only deep rock samples recovered from the well.

Figure 4 shows that after the delays attempting to condition the well by repeated cementing, the drilling itself more or less followed the scheduled path, despite several problems on the way down such as stuck drill string, weather delays, etc.

We had considerable difficulties in recovering drill cores in most of the first 10 core runs, and only a total of 27.3 m of core was retrieved in 13 attempts, or about 63 % recovery of the cored intervals (Table 2). We were using an IDDP-designed 8 $\frac{1}{2}$ '' coring tool, with 9.7 m long core barrel (Skinner et al., 2010), which had yielded good core recoveries in RN-17B, an inclined 8 $\frac{1}{2}$ '' hole from 2800 m depth, and also from three successive core runs below a 9 $\frac{5}{8}$ '' liner in well

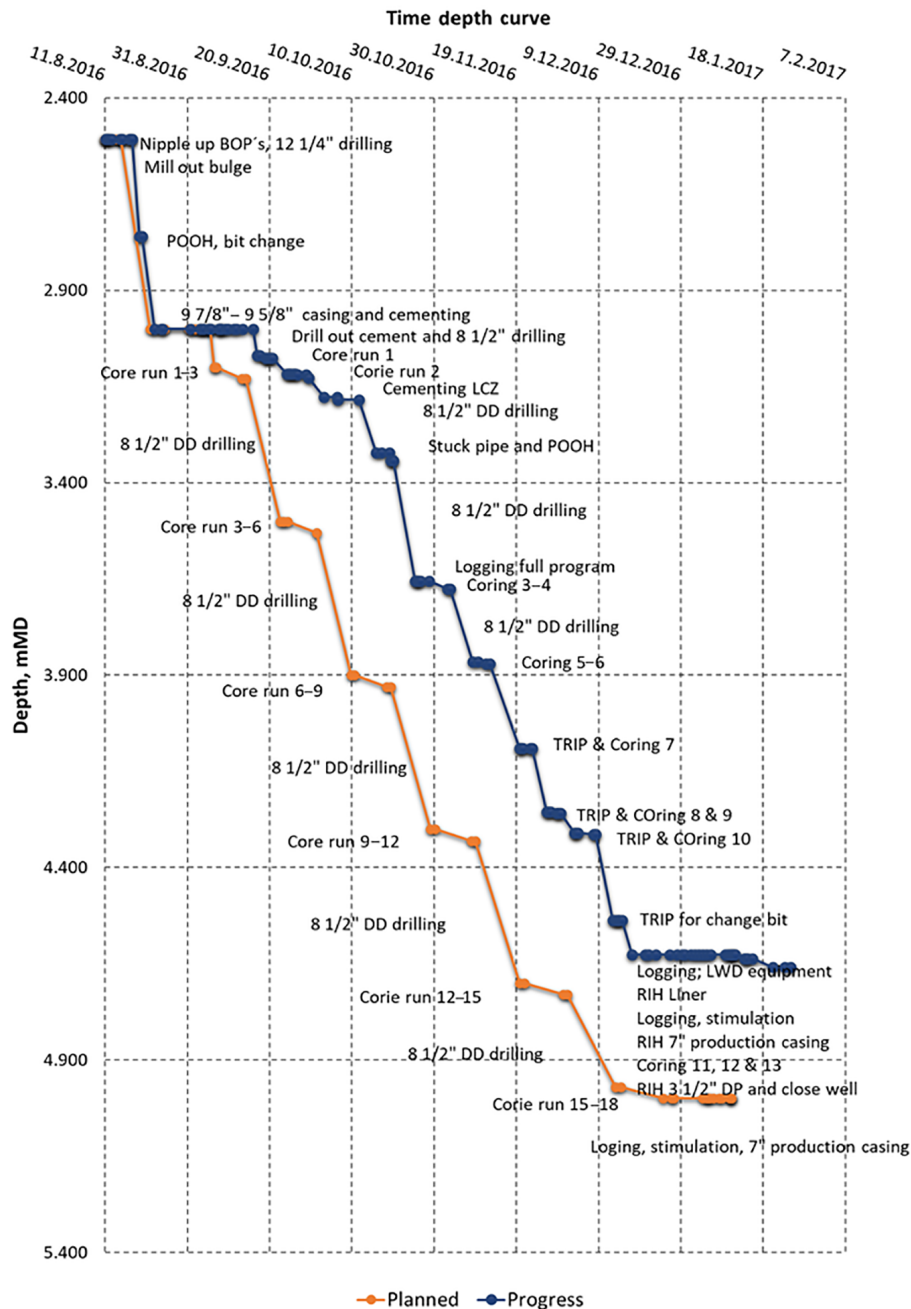


Figure 4. Actual drilling progress of the RN-15/IDDP-2 drill hole (blue) compared to the drilling schedule (orange).

RN-30 at Reykjanes from similar depth to RN-17B (Fowler et al., 2015; Fowler and Zierenberg, 2016). Table 2 gives an overview of the core recovery in 10 core runs with the IDDP 8 1/2" coring tool and 3 successive core runs with the 6" Baker Hughes tool at the bottom of IDDP-2, beneath the 7" liner. Prior to coring with the 6" tools, an 8 m deep 6" pilot hole was drilled with a tri-cone bit from 4626 to 4634 m to clean out the bottom fill after casing and to condition the well.

A comprehensive analysis of the poor performance of our 8 1/2" specially designed coring tool assembly in the IDDP-

2 will appear elsewhere, but there could be several possible reasons for its poor performance. The special feature of our IDDP coring tool is its allowance for much greater water passage (up to 40 L s^{-1}) for cooling extremely hot rock formation, an order of magnitude higher flow rate than that possible using conventional coring tools. Another characteristic feature of our tool is the relatively soft coring bits, designed for single use only.

Possible reasons for the poor performance of the 8 1/2" coring assembly are (a) the inclination of the hole, which in-

creased with increasing depth; (b) possible dog-legs in the hole, which may have damaged the relatively soft drill bits banging against the well wall on running in; (c) rapid cooling leading to thermal fracturing of the formation; and (d) the diameter of the coring tool and reamers, which exceeded the diameter of the heavy drill collars by an inch. Accordingly, the coring bottom-hole-assembly (BHA) was stiffer than the drill collar BHA alone while rotary drilling. Three stabilizers were put in the BHA above the coring tool. In some cases, the $8\frac{1}{2}$ " tri-cone bit may have been slightly under-sized, adding to the problems. We also often had to ream the hole for considerable lengths before getting to the bottom of the hole; in other cases, fill in the hole may have hindered good coring performance. We attempted to overcome the problems by shortening the core barrel from 10 to 5 m, cutting off all the stabilizers on the BHA, and using only one stabilizer above a heavy drill collar and the BHA. After that modification (in core run 4), we improved the situation considerably and retrieved 3.85 m of core in a 5 m long barrel, compared to the 0 to 0.5 m in preceding runs with the 10 m barrel. However, the situation did not improve sufficiently to satisfy our need for drill cores. Nevertheless, recovering tens of centimeters of core from depths in the field that were previously not sampled made a huge difference scientifically, compared to having no rock samples at all.

Finally, after casing the well with a 7" perforated liner, a Baker Hughes 6" coring tool with a PCD bit (poly crystalline diamond) resulted in very satisfying core recovery at the very bottom of the well. The immediate lesson learned is that in the future we should probably use a slimmer coring assembly in inclined wells, such as drilling 6" in an $8\frac{1}{2}$ " hole, or $8\frac{1}{2}$ " in a $12\frac{1}{4}$ " hole, etc.

4 Geophysical and chemical logging during drilling

We had great expectations for temperature data from the thermocouples installed outside the casing (see above). At first, they seemed to work properly but as time passed, and for unknown reasons, they ceased to transmit data to the surface display, although the casing had not heated above 100 °C. The fiber optic cable may still be operational, but will not be used until the well heats up. A gas spectrophotometer and sampling device on the flowline was provided and set up by the ICDP-OSG at GFZ, and conductivity and pH sensors were set up by ISOR and HS Orka. These devices were kept operational throughout the drilling of the well. However, they provided no useful data during drilling because, as explained above, there was total loss of circulation throughout almost the entire drilling operation.

Conventional downhole geophysical logs were attained after drilling to 3000 m depth, and also when the well was 3648 m deep. Normal resistivity, neutron and natural gamma, and sonic logs were obtained from a casing depth to 3440 m. A televiwer log was attempted but had poor quality (Weisenberger et al., 2016, 2017). Close to the end of drilling, when the well was 4626 m deep, special LWD (logging while drilling) tools were hired from Weatherford International and used for the first time in Iceland. The logging suite consisted of natural gamma, temperature, pressure, and multi-frequency resistivity from casing to 4615 m. Micro-resistivity imaging was obtained to 4490 m (good quality) and acoustic velocity to 3045 m. The results will be described elsewhere. Following this, and after only 6 days of heating (3 January 2017), the temperature measured at the bottom of the well was ~ 426 °C with a fluid pressure of 34 MPa, and good indications of permeability at depth (at ~ 3400 , ~ 4375 , ~ 4550 m) based on inflections in the downhole temperature profile (Fig. 5). The fluid at the bottom of the well at that time was inferred to be a mixture of injected water and formation fluids. Both the temperature and the pressure indicate that the bottom fluid was at supercritical conditions during the logging operation. Accordingly, one of the main objectives of the IDDP drilling project was achieved, i.e., to drill into supercritical fluid conditions.

In addition to the major loss zone at 3360–3380 m, there are less permeable loss zones further downhole. There are several feed points below the 2931 m casing shoe all masked by a large feed zone near 3400 m and 6 smaller feed points at 3820, 3990, 4100, 4200, 4375, and 4550 m, and possibly also at the very bottom of the well below the depth of the temperature log (Fig. 5). It is clear from the deepest drill cores that we had some open space in fractures containing pristine supercritical fluid down to the bottom of the well 4659 m.

The 7" perforated hanging liner was inserted to the bottom after the pressure–temperature (PT) logging run of 3 January 2017. Subsequently, a 7" sacrificial casing was lowered from the surface down to 1300 m and cemented up to the surface. Casing shoes were then drilled out and the well was deepened using 6" bits, ending with three successive coring runs down to the 4659 m final depth. After the deepest coring run, a $3\frac{1}{2}$ " drill string was lowered to the bottom of the hole. The aim was to enhance the permeability deep in the hole by pumping in cold water for several months through the $3\frac{1}{2}$ " drill string. There are already some positive indications of enhancement of injectivity. Tests made after the last coring runs showed that cold water injection increased the injectivity index from 1.7 to $3.1 \text{ L s}^{-1} \text{ bar}^{-1}$. We expect that continued deep stimulation with cold water is likely to further improve the fracture permeability at depth. While this “soft stimulation” is going on, a surface test bed, with two parallel flowlines, will be designed and constructed for long-term flow testing. Only after these fluid handling and flow tests are concluded will we be able to determine the nature of the formation fluids, their enthalpy and flow characteristics, and hence estimate their engi-



Reykjanes Well IDDP-2

3. january 2017
HI/HCS

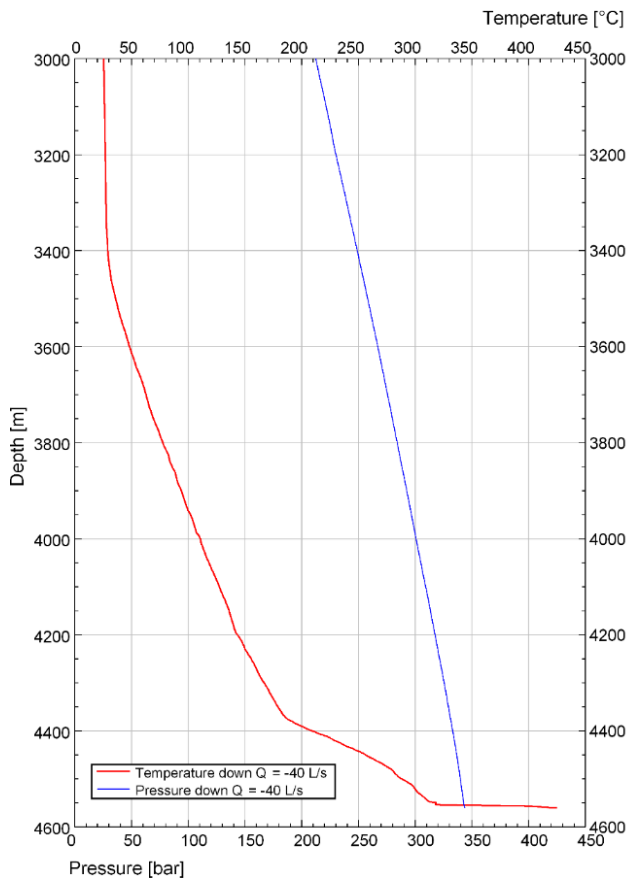


Figure 5. Temperature and pressure log to 4560 m depth in IDDP-2 after only 6 days of heating. As can be seen from the temperature profile, the well is far from thermal equilibrium because of cold water injection. When thermal recovery is complete, it is likely that temperatures will exceed the estimated 426 °C measured at the bottom of the hole. The PT logging was done with a K-10 logging tool, which was calibrated to only 380 °C (Weisenberger et al., 2017).

neering and economic potential. The total loss of circulation below 3 km depth was unexpected but the existence of large permeability, a kilometer deeper than the current production zones at Reykjanes, may have implications for the future development of the geothermal resource that are independent of supercritical production.

5 Lithology and alteration

A detailed description of the lithologic section drilled in the IDDP-2 well is hampered by total circulation loss below ~3200 m and is based on preliminary observations of recovered drill cores (Table 2). Despite these limitations, a relatively coherent picture of downhole lithology and hydrothermal alteration is apparent, and is generally

consistent with observations from the deepest holes drilled into in situ oceanic crust at fast-spreading ridges by the Deep Sea Drilling Project (DSDP)/Ocean Drilling Program (ODP)/Integrated Ocean Drilling Program (IODP), wells 504B (Costa Rica Rift, Galapagos Spreading Center) and well 1256B (Guatemala Basin, eastern tropical Pacific) (Alt et al., 1986, 2010; Anderson et al., 1982).

The upper 2500 m of the IDDP-2 well was drilled in 2004 as the former production well RN-15, which is described by Jónsson et al. (2010). Cuttings recovered during deepening of the well down to the lost circulation zone at 3200 m are described by Weisenberger et al. (2017). Here we focus on the drill core recovered at spot intervals in the depth interval between 3648 and 4659 m.

6 Primary lithology

Analysis of drill cuttings indicates that the uppermost section of RN-15 down to about 1400 m is dominantly volcanic rock with interbedded zones of basalt flows, basalt breccia, pillow lavas, and hyaloclastite. Basaltic intrusions increase in frequency downhole below ~1400 m, and mixed intrusive and extrusive rocks continue to at least 3200 m. Variably rounded cobbles and fragments of volcanic rock derived from below the casing depth 2940 m were recovered as rubble on top of several of the cores. It is likely that many of these were derived from an enlarged eroded section of the drill hole around ~3360 m depth, coincident with a major circulation loss zone in the well. The zone from ~1400 to ~3500 m depth is, therefore, interpreted as the transition zone between overlying volcanic rocks and an underlying sheeted dike complex (Fig. 6). The preliminary interpretation of the lithological structure and major alteration mineral zones identified in IDDP-2 compared to DSDP/ODP/IODP holes 504B (Costa Rica Rift, Galapagos Spreading Center) and 1256D (Guatemala Basin, eastern tropical Pacific) is presented on Fig. 6.

The shallowest cored interval extends from 3648.00 to 3648.52 m and recovered sections of three dikes separated by two chilled margins that indicate that at least the upper two dikes are half-dikes intruded by the underlying dike. Lithologic interpretation based on sparse core recovery is subject to large uncertainty, however, all of the underlying drill core can be reasonably interpreted to have come from a sheeted dike complex with no definitive evidence that they represent either coarse-grained basalt from flow interiors or thick intrusive sills or fine-grained gabbro bodies. Interpretation of the downhole geophysical logs may provide further evidence of the nature of the lithologies in-between the cored intervals as well as orientations of the contacts between intrusive units. Cores 5 and 6 recovered a relatively coarse-grained diabase with no apparent systematic grain-size variation extending from 3865.50 to 3869.95 m. Cores 11–13 provide the most continuous recovery, with four half-dikes separated by three

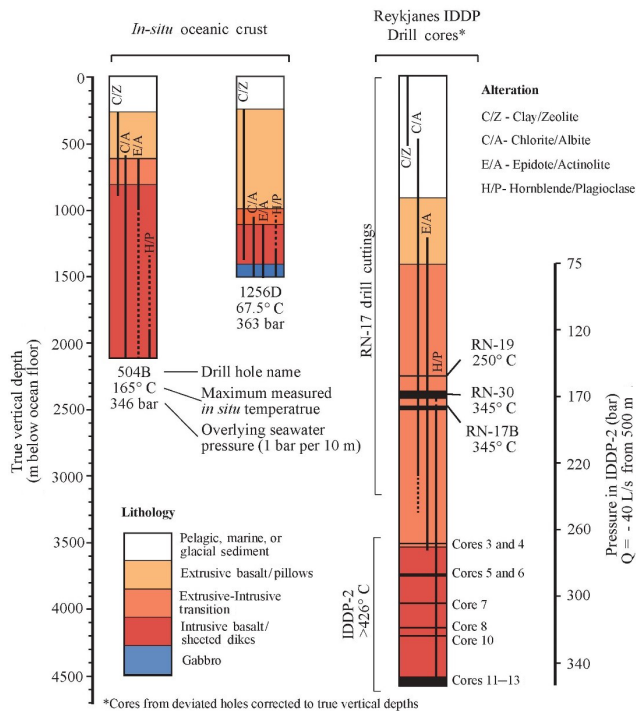


Figure 6. Simplified alteration and lithology logs of RN-15/IDDP-2 compared to the two deepest DSDP/ODP/IODP drill holes completed in situ oceanic crust (Hole 504B and Hole 1256D). Maximum temperature and pressure conditions are indicated. The structure of the Reykjanes geothermal system differs from 504B and 1256D in that the transition zone between the upper pillow basalt section and lower sheeted dike section is greatly expanded at Reykjanes. On a broad scale, alteration mineral sequences in the active Reykjanes system vary predictably as a function of depth in the crust and temperature. Overprinting alteration mineral sequences in rocks from Holes 504B and 1256D reflect time-integrated changes in hydrothermal conditions as rocks tectonically migrated away from active hydrothermal conditions at the spreading center. Data for DSDP/ODP/IODP holes from Alt et al. (2010); Anderson et al. (1982); and Marks et al. (2010). Data for shallower portions of Reykjanes from Marks et al. (2010); Fowler et al. (2015); and Fowler and Zierenberg (2016).

chilled margins recovered between 4634.20 and 4656.00. The thickest half-dike extends 14.4 m downhole implying a minimum thickness greater than 9 m, given the inclination of the drill hole of approximately 40° and assuming the dike is vertical.

All the recovered dikes show similar primary mineralogy with subequal concentrations of plagioclase and clinopyroxene accompanied by 3–6 % titanomagnetite. The only apparent exceptions are the uppermost half-dike in core 11, which appears from hand specimen descriptions to contain $\sim 2\%$ euhedral green partially altered olivine crystals, and the half-dike in the lowermost 1.5 m of core 12, which is described as containing approximately 15 % dark blocky clinopyroxene (2–3 mm) and 20 % finer-grained beer-bottle brown or-

thopyroxene (~ 2 mm). Given that all recovered cores are overprinted by hydrothermal alteration, estimates of original mineral percentages are uncertain. Plagioclase tends to be slightly coarser-grained (3–4 mm), elongated, and more euhedral compared to clinopyroxenes, which tends to occur interstitial to the plagioclase matrix.

Irregular patches and vein-like segregations of more differentiated felsic melt are a minor component of some of the dikes and become increasingly common downcore. The first noted occurrence of these segregations is in core 5, which shows a few irregular discontinuous lighter colored veins characterized by an increased abundance of late-stage igneous plagioclase, some of which appears cloudy due to symplectic intergrowth with very fine-grained quartz. Clinopyroxene is less abundant in these veins, and some formed as thin (≤ 1 mm) elongated prisms up to 5 mm long. All of the pyroxene in this core interval has been replaced by hydrothermal amphibole. Core 10 contains a 3 cm thick plagioclase-quartz-clinopyroxene-titanomagnetite segregation vein, where quartz occurs as coarser-grained crystal as well as symplectic intergrowths with plagioclase. Cores 11–13 show an increased abundance of felsic segregation patches, irregular veinlets and veins up to 5 cm thick (Fig. 7), and many of these include green to brown biotite as a primary igneous mineral, which in some veins is more abundant than clinopyroxene. Preliminary examination of thin sections reveals that accessory apatite is more abundant in the felsic segregations. Some felsite veins have euhedral zircon crystals up to 2 mm in length. Rock of rhyolitic compositions, although common in other Icelandic volcanic centers such as Krafla (e.g., Jónasson, 2007), have not been observed previously at Reykjanes.

7 Alteration and hydrothermal veining

The assemblage of alteration minerals observed in cuttings from RN-15 (Jónsson et al., 2010) and the upper section of IDDP-2 above the lost circulation zone (Weisenberger et al., 2017) is consistent with the downhole prograde alteration assemblages described by Tómasson and Kristmannsdóttir (1972). Cuttings from the production reservoir of the Reykjanes field show epidote-actinolite facies alteration characterized by replacement, open-space filling veins, and vug-filling alteration minerals dominated by chlorite, epidote, actinolite, albite, and quartz.

The upper-most core samples from IDDP-2 (core 3, 3648 m) are pervasively altered and intensively veined by epidote, amphibole, plagioclase (with or without quartz) with chlorite-rich vein selvages. Igneous clinopyroxene is completely replaced by amphibole and chlorite. Igneous plagioclase shows patchy alteration to albite, epidote, and chlorite. Titanomagnetite is partially replaced by magnetite and titanite. Minor phases include pyrite, pyrrhotite, and intermediate solid solution Cu-Fe sulfide. Hydrothermal clinopyrox-



Figure 7. A piece of core from the RN-15/IDDP-2 well from 4634.40 to 4634.55 m depth, showing felsite veins and conjugate sets of older fractures/veins. The red color of the felsite relates to hematic stain formed from a mixture of supercritical vein fluid with cold oxidizing drilling fluid (see text for further discussion).

ene is present in veins and groundmass replacement of the fine-grained to formerly glassy quenched dike margins. The epidote veins are somewhat anastomosing and dip in multiple directions. Some veins show clear cross-cutting relationships while others merge into composite veins. In contrast to alterations observed in overlying cuttings, textures indicative of open-space fracture fillings are absent and quartz is much less abundant, occurring as a minor phase in the veins. Actinolite is the dominant amphibole, but is locally replaced by hornblende. Plagioclase in the veins is calcic, ranging to near end-member anorthite. The presence of hornblende and calcic plagioclase is an indication that rocks have reached PT conditions of the amphibole alteration facies, but the rocks have not reached equilibrium. Overprinting of epidote-actinolite facies by amphibole facies alteration is an indication of prograde expansion of the hydrothermal system and/or subsidence of these rocks to higher PT conditions.

The alteration observed in the deeper sections of core, starting with core 5 at 3865 m, is consistent with amphibolite facies alteration. Epidote and chlorite are not present and quartz, if present, is a minor phase. In most of the deeper cores, igneous clinopyroxene is pervasively to completely altered to amphibole, but igneous plagioclase generally appears to be unaltered. Actinolite persists at depth, but hornblende becomes increasingly abundant downhole. Albitization of plagioclase is minor to absent. The dominant vein minerals are amphibole and calcic plagioclase, which can occur separately or together. Plagioclase-rich veins may contain minor amounts of quartz, but quartz is absent from most hydrothermal veins and is most common in and adjacent to the felsite segregation patches and veins/dikelets. Although most of the cores show pervasive alteration, cross-cutting veins are volumetrically a very minor component of the rock. The veins tend to be thin (1–4 mm), irregular, and discontinuous and lack evidence of filling of open space, consistent with formation in the brittle/ductile transition zone. Trace amounts of hydrothermal biotite and clinopyroxene are noted as shallow as core 8 (4254 m).

The most continuous core recovery was achieved at the bottom of the hole from 4634 to 4659 m. Most of the dikes in this section show pervasive alteration of igneous clinopyrox-

ene to hornblende, but relict igneous pyroxene is preserved in some dikes. Hydrothermal biotite is less abundant than amphibole, but is intergrown with hornblende in the deeper rocks. Igneous plagioclase retains its morphology and growth zoning patterns but is locally cloudy and dusted with iron oxide and vapor-rich inclusions. Hydrothermal veining is very minor for most of this interval but there are local zones of millimeter scale, cross-cutting hornblende and hornblende plus plagioclase veins. Thin (1–2 mm wide) discontinuous, anastomosing veinlets of plagioclase and quartz that may be accompanied by hornblende and/or biotite branch off the felsite segregation veins/dikelets, and the distinction between igneous and hydrothermal deposition/alteration is obscure at present. One mineralized open fracture was recovered along the margin of a 3 cm wide felsite vein (4637.19 m). The fracture was covered by coarse-grained euhedral hydrothermal biotite (Fig. 8a) that was overgrown by later, fine-grained euhedral quartz (Fig. 8b), including doubly terminated prismatic crystals. The fracture and the adjacent core surfaces were stained and locally coated by hematite that, based on textural relations, clearly formed during the drilling process by oxidation of ferrous iron bearing formation fluid interacting at high temperature with oxygenated surface water pumped downhole for cooling. Similar hematite staining is increasingly abundant in patchy intervals downhole, becoming very common in core 13. The hematite staining is restricted to surfaces cut by the core bit or pre-existing fracture surfaces and is not present on post-coring fractures or the interior of the core that was cut for examination. Sulfides (pyrrhotite and/or intermediate solid solution Cu-Fe sulfide) and hydrothermal magnetite are minor, but commonly observed, alteration phases in the deepest cores.

8 Significance of the IDDP-2

The IDDP-2 cores include the first samples recovered from active, supercritical geothermal conditions in a seawater-recharged hydrothermal system analogous to the roots of deep-sea black smoker systems. The lithological section underlying the presently exploited hydrothermal system at Reykjanes is typical of sheeted complexes in oceanic crust and ophiolites. Logging measurements confirm that permeable feed zones are present at temperature and pressure conditions in excess of the critical point of seawater in the deepest section of the well.

The geological environment of the Reykjanes geothermal field is of great interest to the scientific community, situated as it is on the landward extension of the Mid-Atlantic Ridge that forms part of the world-encircling system of divergent plate boundaries, or oceanic spreading centers (Elders and Friðleifsson, 2010). These are regions of frequent volcanic eruption, high heat flow, and submarine hot springs. Base-metal sulfide scales that form in drill holes and production pipes are similar to seafloor massive sulfide deposits

(a)



(b)



Figure 8. (a) Euhedral hydrothermal biotite books, approximately 1 mm across, coating fracture surface in RN-15/IDDP-2 (4637.81 m depth). Exposed crystals were stained red by hematite during the coring operation. (b) Open-space filling quartz, up to 4 mm in length, overgrowing hydrothermal biotite (black crystals) in RN-15/IDDP-2 (4637.81 m depth). Exposed crystals were stained red by hematite during the coring operation.

(Hardardóttir et al., 2012). The IDDP-2 is a unique opportunity to examine the roots of a black smoker.

In the future, our demonstration that it is possible to drill into a supercritical zone could have a large impact on the economics of high-temperature geothermal resources worldwide, wherever young volcanic rocks occur (Dobson et al., 2017). By extending the available economic reservoir downwards, we can extend the lifetimes of existing producing fields. As higher enthalpy fluids have greater power conversion efficiencies, fewer turbines are required for a given power output. Similarly, as fewer wells are needed for a given output, we can increase the productivity of a geothermal field without increasing its environmental footprint.

More information on the IDDP can be found at www.iddp.is and at www.deepeg.eu.

Data availability. Our underlying research data is partly kept at the following link: <https://www.icdp-online.org/projects/world/europe/iceland/details/> and at an internal IDDP website at icdp-online for the IDDP science team only – until published.

Competing interests. The authors declare that they have no conflict of interest.

Acknowledgements. The IDDP-2 was funded by HS Orka, Landsvirkjun, Orkuveita Reykjavíkur, and the National Energy Authority in Iceland, together with Statoil, the Norwegian oil and gas company. The IDDP has also received funding from the EU H2020 (DEEPEGS, grant no. 690771), and science funding from ICDP and NSF. In 2005, funding for IDDP to obtain spot cores at Reykjanes and elsewhere was provided by ICDP and the US NSF (grant no. 05076725), which is greatly appreciated. Successful coring attempts exist from wells RN-17B, RN-19, RN-30, and now from RN-15/IDDP-2, Iceland.

Edited by: Tomoaki Morishita

Reviewed by: Robert O. Fournier and one anonymous referee

References

- Albertsson, A., Bjarnason, J.Ö., Gunnarsson, T., Ballzus, C., and Ingason, K.: Part III: Fluid handling and evaluation, in: Iceland Deep Drilling Project, Feasibility Report, edited by: Friðleifsson, G. Ó., Orkustofnun Report OS-2003-007, 32 pp., available at: <http://www.os.is/gogn/Skyrslur/OS-2003/OS-2003-007.pdf>, 2003.
- Alt, J. C., Honnorez, J., Laverne, C., and Emmermann, R.: Hydrothermal alteration of a 1 km section through the upper oceanic crust, Deep Sea Drilling Project Hole 504B: Mineralogy, chemistry and evolution of seawater-basalt interactions, *J. Geophys. Res.*, 91, 10309–10335, 1986.
- Alt, J. C., Laverne, C., Coggon, R. M., Teagle, D. A. H., Banerjee, N. R., Morgan, S., Smith-Duque, C. E., Harris, M., and Galli, L.: Subsurface structure of a submarine hydrothermal system in oceanic crust formed at the East Pacific Rise, ODP/IODP Site 1256, *Geochem. Geophys. Geosy.*, 11, Q10010, <https://doi.org/10.1029/2010GC003144>, 2010.
- Anderson, R. N., Honnorez, J., Becker, K., Adamson, A. C., Alt, J. C., Emmerman, R., Kempton, P. D., Kinoshita, H., Laverne, C., Mottl, M. J., and Newmarks, R. L.: Hole 504B, the first reference section over 1 km through Layer 2 of the oceanic crust, *Nature*, 300, 589–594, 1982.
- Anonymous: Penrose Field Conference on Ophiolites, *Geotimes*, 17, 24–25, 1972.
- Bischoff, J. L. and Rosenbauer, R. J.: Liquid-vapor relations in the critical region of the system NaCl–H₂O from 380 °C to 414 °C: A refined determination of the critical point of seawater, *Geochim. Cosmochim. Acta*, 52, 2121–2126, 1988.

- Dobson, P., Asanuma, H., Huenges, E., Polletto, F. Reinsch, T., and Sanjuan, B.: Supercritical Geothermal Systems – A Review of Past Studies and Ongoing Research Activities. Proceedings, 41st Workshop on Geothermal Reservoir Engineering Stanford University, Stanford, California, 13–15 February, 1–13, 2017 SGP-TR-212, 2017.
- Elders, W. A. and Friðleifsson, G. Ó.: Implications of the Iceland Deep Drilling Project for improving understanding of hydrothermal processes at slow spreading mid-ocean ridges. In: Diversity of Hydrothermal Systems on Slow Spreading Ocean Ridges, American Geophysical Union, Geoph. Monog. Ser., 188, 91–112, 2010.
- Elders, W. A., Friðleifsson, G. Ó., Zierenberg, R. A., Pope, E. C., Mortensen, A. K., Guðmundsson, Á., Lowenstern, J. B., Marks, N. E., Owens, L., Bird, D. K., Reed, M., Olsen, N. J., and Schiffman, P.: Origin of a rhyolite that intruded a geothermal well while drilling in a basaltic volcano, at Krafla, Iceland, *Geology*, 39, 231–234, 2011.
- Fowler, A. P. G. and Zierenberg, R. A.: Elemental changes and alteration recorded by basaltic drill core samples recovered from in-situ temperatures up to 345 °C in the active, seawater-recharged Reykjanes Geothermal System, Iceland, *Geochem. Geophys. Geos.*, 17, <https://doi.org/10.1002/2016GC006595>, 2016.
- Fowler, A. P. G., Zierenberg, R. A., Schiffman, P., Marks, N., and Friðleifsson, G. Ó.: Evolution of fluid–rock interaction in the Reykjanes geothermal system, Iceland: Evidence from Iceland Deep Drilling Project core RN-17B, *J. Volcanol. Geotherm. Res.*, 302, 47–63, 2015.
- Friðleifsson, G. Ó. and Richter, B.: The geological significance of two IDDP-ICDP spot cores from the Reykjanes geothermal field, Iceland, Proceedings of the World Geothermal Congress 2010, Bali, Indonesia, p. 6, available at: www.iddp.is, 2010.
- Friðleifsson, G. Ó., Ármannsson, H., Árnason, K., Bjarnason, I. P., and Gíslason, G.: IDDP Feasibility Report. Iceland Deep Drilling Project, Part I Geosciences – Site Selection. Orkustofnun, Report, OS-2003-007, 103 pp., available at: <http://www.os.is/gogn/Skyrslur/OS-2003/OS-2003-007.pdf>, 2003.
- Friðleifsson, G. Ó., Elders, W. A., and Bignall, G.: A plan for a 5 km-deep borehole at Reykjanes, Iceland, into the root zone of a black smoker on land, *Sci. Dril.*, 16, 73–79, <https://doi.org/10.5194/sd-16-73-2013>, 2013.
- Friðleifsson, G. Ó., Elders, W. A., and Albertsson A.: The Concept of the Iceland Deep Drilling Project, *Geothermics*, 49, 2–8, 2014a.
- Friðleifsson, G. Ó., Sigurdsson, Ó., Þorbjörnsson, D., Karlsdóttir, R., Gíslason, P., Albertsson, A., and Elders, W. A.: Preparation for drilling well IDDP-2 at Reykjanes, *Geothermics*, 49, 119–126, 2014b.
- Hardardóttir, H., Hannington, M., Hedenquist, J., Kjarsgaard, I., and Hoal, K.: Cu-rich scales in the Reykjanes geothermal systems, *Econ. Geol.*, 105, 1143–1155, 2012.
- Jónasson, K.: Silicic volcanism in Iceland: composition and distribution within the active volcanic zones, *J. Geodynam.*, 43, 101–117, 2007.
- Jónsson, S. S., Sigurgeirsson, M. A., Sigurðsson, Ó., and Ingólfsson, H.: Reykjanes –Hóla RN-15, 3. phase: Drilling of the production part from 804 m to 2507 m (in Icelandic), ÍSOR Report 2010/050.69 pp., 2010.
- Marks, N., Schiffman, P., Zierenberg, R., Franzson, H., and Friðleifsson, G. Ó.: Hydrothermal alteration in the Reykjanes geothermal system: Insights from Iceland deep drilling program well RN-17, *J. Volcanol. Geoth. Res.*, 189, 172–190, 2010.
- Skinner, A., Bowers, P., Þórhallsson, S., Friðleifsson, G. Ó., and Guðmundsson, H.: Extreme coring, designing and operating a core barrel for the Iceland Deep Drilling Project, *GeoDrilling Int.*, 2010, 18–22, 2010.
- Tómasson, J. and Kristmannsdóttir, H.: High temperature alteration minerals and thermal brines, Reykjanes, Iceland, *Contributions to Mineralogy and Petrology*, 36, 123–134, 1972.
- Weir, N. R. W., White, R. S., Bandsdóttir, B., Einarsson, P., Shimamura, H., Shiobara, H., and the RISE Fieldwork Team: Crustal structure of the northern Reykjanes Ridge and Reykjanes Peninsula, southwest Iceland, *J. Geophys. Res.*, 106, 6347–6368, 2001.
- Weisenberger, T. B., Kästner, F., Nielsson, S., Harðarson, B. S., Kristinsson, B., Ingólfsson, H., Stefánsson, H. Ö., Jónasson, H., and Vilhjálmsson S.: Well Report – RN-15/IDDP-2, Drilling of Well RN-15/IDDP-2 in Reykjanes – Continuation of Phase 3 from 2509 m down to 3000 m, Iceland GeoSurvey, report, ÍSOR-2016/053, 2016.
- Weisenberger, T. B., Harðarson, B. S., Kästner, F., Gunnarsdóttir, S. H., Tulinius, H., Guðmundsdóttir, V., Einarsson, G. M., Pétursson, F., Vilhjálmsson, S., Stefánsson, H. Ö., and Nielsson S.: Well Report – RN-15/IDDP-2, Drilling in Reykjanes – Phase 4 and 5 from 3000 to 4659, ISOR 2017/016, 277 pp., 2017.



Drilling into an active mofette: pilot-hole study of the impact of CO₂-rich mantle-derived fluids on the geo–bio interaction in the western Eger Rift (Czech Republic)

Robert Bussert¹, Horst Kämpf², Christina Flechsig³, Katja Hesse⁴, Tobias Nickschick^{2,3}, Qi Liu⁵, Josefine Umlauf³, Tomáš Vylita⁶, Dirk Wagner⁵, Thomas Wonik⁴, Hortencia Estrella Flores³, and Mashal Alawi⁵

¹Institute of Applied Geosciences, Technische Universität Berlin, 13355 Berlin, Germany

²GFZ German Research Centre for Geosciences, Section 3.2: Organic Geochemistry, 14473 Potsdam, Germany

³Institute for Geophysics and Geology, University of Leipzig, 04103 Leipzig, Germany

⁴Leibniz Institute for Applied Geophysics, 30655 Hannover, Germany

⁵GFZ German Research Centre for Geosciences, Section 5.3: Geomicrobiology, 14473 Potsdam, Germany

⁶Balneological Institute, 360 01 Karlovy Vary, Czech Republic

Correspondence to: Robert Bussert (r.bussert@tu-berlin.de)

Received: 19 April 2017 – Revised: 20 July 2017 – Accepted: 15 August 2017 – Published: 30 November 2017

Abstract. Microbial life in the continental “deep biosphere” is closely linked to geodynamic processes, yet this interaction is poorly studied. The Cheb Basin in the western Eger Rift (Czech Republic) is an ideal place for such a study because it displays almost permanent seismic activity along active faults with earthquake swarms up to M_L 4.5 and intense degassing of mantle-derived CO₂ in conduits that show up at the surface in form of mofettes. We hypothesize that microbial life is significantly accelerated in active fault zones and in CO₂ conduits, due to increased fluid and substrate flow. To test this hypothesis, pilot hole HJB-1 was drilled in spring 2016 at the major mofette of the Hartoušov mofette field, after extensive pre-drill surveys to optimize the well location. After drilling through a thin caprock-like structure at 78.5 m, a CO₂ blowout occurred indicating a CO₂ reservoir in the underlying sandy clay. A pumping test revealed the presence of mineral water dominated by Na⁺, Ca²⁺, HCO₃⁻, SO₄²⁻ (Na-Ca-HCO₃-SO₄ type) having a temperature of 18.6 °C and a conductivity of 6760 μS cm⁻¹. The high content of sulfate (1470 mg L⁻¹) is typical of Carlsbad Spa mineral waters. The hole penetrated about 90 m of Cenozoic sediments and reached a final depth of 108.50 m in Palaeozoic schists. Core recovery was about 85 %. The cored sediments are mudstones with minor carbonates, sandstones and lignite coals that were deposited in a lacustrine environment. Deformation structures and alteration features are abundant in the core. Ongoing studies will show if they result from the flow of CO₂-rich fluids or not.

1 Introduction

Microbial processes in the “deep biosphere” and their interaction with geological processes are a matter of ongoing debate. Microbial habitats extend down to great depths beneath the earth’s surface. However, cell counts and detailed characterizations of the microbial community structure in the continental deep biosphere are rare and mostly related to investigations in oil reservoirs (Youssef et al., 2009), geothermal aquifers (Alawi et al., 2011; Lerm et al., 2013) or gold

mines (Deflaun et al., 2007; Takai et al., 2001; Trimarco et al., 2006). A few continental drilling campaigns have focused on the deep biosphere (Fredrickson et al., 1997; Onstott et al., 1998; Zhang et al., 2005), though the state of knowledge reached is still in the early stages. In deep saline aquifers intended for CO₂ capture and geological storage (CCS), changes in the microbial community caused by injected CO₂ can induce mineral dissolution and precipitation or the formation of biofilms (Onstott, 2005; Mitchell et al.,

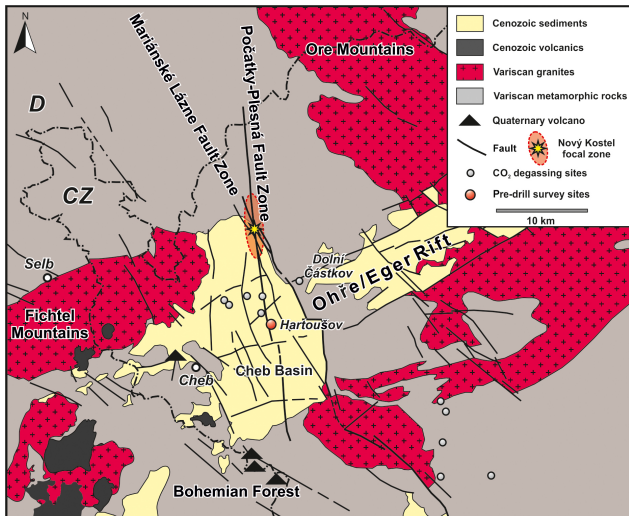


Figure 1. Geological map of the Cheb Basin and surroundings, based on Flechsig et al. (2008) and Dahm et al. (2013).

2009), and might affect long-term storage efficiency and reliability (Morozova et al., 2010; Gulliver et al., 2016; Pellizzari et al., 2016).

In the scope of the International Continental Scientific Drilling Program (ICDP) project “Drilling the Eger rift: Magmatic fluids driving the earthquake swarms and the deep biosphere” (Dahm et al., 2013), one focus is to determine to which extent the microbial communities are conditioned by the mantle-derived CO₂ degassing and how the microbial activity is potentially affected by seismic events such as swarm earthquakes. As a pre-examination, a research project “Microbial processes in the deep biosphere of the CO₂-dominated active fault zone in NW Bohemia” started in 2016 and included a 108.5 m deep drilling (Alawi et al., 2015). We assume that in active fault zones, due to an intensified substrate support, microbial processes are significantly accelerated compared to other deep subsurface ecosystems. Similar to black smokers in the deep sea, active fault zones might represent “hot spots” of microbial life in the deep subsurface (Alawi et al., 2015). The combination of intense CO₂-rich mantle degassing, ongoing seismic activity including earthquake swarms and microbiological activity that occurs in the Cheb Basin (western Eger Rift, Czech Republic; Fig. 1) is exceptional and allows the study of bio-geo interactions as part of active geodynamic processes in the lithosphere (Kämpf et al., 1989, 2005, 2007, 2013; Wagner et al., 2007; Bräuer et al., 2007, 2008, 2011, 2014; Dahm et al., 2013; Fischer et al., 2014, 2017; Alawi et al., 2015; Schuessler et al., 2016).

About 10 km south of the Nový Kostel focal zone epicentral area (Fig. 1), strong subcontinental mantle-dominated CO₂ degassing occurs in the Bublák and Hartoušov mofette fields (Bräuer et al., 2003, 2014; Kämpf et al., 2013; Nickschick et al., 2015, 2017). Mofettes are places where



Figure 2. The major wet mofette in Hartoušov is located in the direct vicinity of the drill site. At the upper and lower part of the mofette bubbles of CO₂-rich gas are visible.

geogenic CO₂ ascends through conduits from the mantle to the surface (Fig. 2). The CO₂ conduits are regarded as important structures of lithospheric mantle–crust interaction via mantle fluids. However, both rock–fluid and geo–bio interactions in these structures are hardly understood.

Microbial growth in the deep subsurface is limited by factors such as temperature, pH, redox potential, gas concentration, water and substrate availability (Kallmeyer and Wagner, 2014). The conditions for life in the deep biosphere are extreme in comparison to most surface environments: no light is available for photosynthesis, typically much higher temperatures than in surface habitats prevail, the availability of water and of organic carbon is severely restricted, and high gas pressures occur. The exchange of substances is crucially reduced since it is coupled to water availability and to diffusion processes. Therefore, microbial activities are slowed and microbial turnover times are strongly decreased (Lomstein et al., 2012). However, microbes can survive long periods of starvation by reducing their metabolism or forming spores (Goldscheider et al., 2006; Hubert et al., 2009). Interestingly, there are hints that the microbial turnover in active fault zones is significantly accelerated in comparison to the ordinary terrestrial deep biosphere. Eight weeks after an earthquake swarm occurred in the northwestern part of the Cheb Basin, the amount of microbiologically produced methane increased significantly and persisted for more than two years (Bräuer et al., 2005, 2007). The authors assume that hydrogen was released from a fractured granitic aquifer during seismic activity and became available for microorganisms. In the same region, Schuessler et al. (2016) explain recurring changes in iron isotope signatures of mineral spring water by a combination of abiotic and biotic processes triggered by swarm earthquakes. CO₂ as the dominating gas in the Cheb Basin might liberate organic compounds (Glombitza et al., 2009; Sauer et al., 2012); enhance the dissolution, transformation and precipitation of minerals (Rempel et al., 2011); and could thereby affect the availability of substrates for microorganisms. These examples lead to the question of

whether and how geodynamic processes such as earthquakes can trigger microbiological activity by transport of substrates and changes in environmental conditions. Our main interests are to determine to which extend the microbial communities are conditioned by the mantle-derived CO₂, how the microbial activity is potentially affected by seismic activity such as earthquake swarms, and if active fault zones, due to an intensified substrate support, lead to significantly accelerated microbial activity compared to other deep subsurface ecosystems.

The present pilot-hole study that precedes the ICDP drilling project “Drilling the Eger Rift” (<http://web.natur.cuni.cz/uhigug/icdp>; Dahm et al., 2013) focuses on the interaction between lithospheric geodynamic activity driven by magma generation and magma/fluid escape beneath the Cheb Basin in the western Eger Rift and the microbial communities of the deep biosphere in the upper crust.

Here we describe the 108.5 m deep drilling of well HJB-1 into an active CO₂ conduit in the Cheb Basin, located at the northern part of the Hartoušov mofette field. It was intended to core as continuously as possible down to the bottom of the lacustrine succession. The operational challenges were manifold, starting with the logistics and technical feasibility of the drilling to the high standards we require with regard to assessing sample contamination through infiltration of drill mud. Because of the potential risk of a spontaneous gas/fluid blowout during drilling, extra safety measures including the application of a blowout gas preventer, high-density bentonite-based drill mud and gas alarm techniques had to be employed.

2 Geological background

The Cheb Basin represents the shallow western part of the Cenozoic Ohře/Eger Rift, the easternmost segment of the European Cenozoic Rift System that has developed in response to intraplate stresses exerted from the Alps, and possibly to thermal doming (Malkovský, 1987; Rajchl et al., 2009). The basin is located at the intersection of the ENE–WSW trending Eger Rift with the N–S striking Regensburg–Leipzig–Rostock zone respectively its major local segments, the Počátky–Plesná Fault zone and the Mariánské Lázně Fault zone (Fig. 1; Bankwitz et al., 2003). It is underlain by Palaeozoic metamorphics and granites (Hecht et al., 1997; Fiala and Vejnar, 2004) and bounded on its eastern side by the morphologically distinct scarp of the Mariánské Lázně Fault zone (Peterek et al., 2011), and to the west and to the south by the Fichtel (Smrčiny) Mountains and the Oberpfalz Forest.

The fill of the Cheb Basin consists of less than 300 m of continental sediments. Sedimentation started in the Eocene with the local deposition of clays and sands, possibly in maars, referred to as the Staré Sedlo Formation (Fm.; Špičáková et al., 2000; Pešek, 2014). Following a phase of

uplift and erosion, sedimentation commenced with the deposition of gravels, sands and clays of the Oligocene (Chattian) to Early Miocene (Early Aquitanian) Lower Argillaceous-Sandy Fm. (Pešek et al., 2014). In the Lower Miocene, the coal-bearing Main Seam Fm. formed in an alluvial landscape enclosing extensive wetlands. Subsequently, a large lake developed in which the clay-dominated Cypris Fm. was deposited (Rojik, 2004). After a hiatus, sedimentation started again in the Pliocene with lacustrine clays, sands and gravels of the Vildštejn Fm. and continued without an obvious break into the Quaternary (Pešek et al., 2014).

In the surrounding of the Eger Rift, volcanism was temporarily active during the Cenozoic. In the Quaternary, volcanic activity formed two small scoria cones with lava flows and a just recently discovered explosive maar structure (Mršina et al., 2007, 2009; Flechsig et al., 2015; Ulrych et al., 2016). Ongoing tectonic activity in the Cheb Basin is manifested by earthquake swarms that concentrate along the northern segment of the Mariánské Lázně Fault zone (Fig. 1). The strongest registered earthquakes reached local magnitudes of M_L 4.5 (Fischer et al., 2014). Active fault zones very likely represent migration pathways for the degassing of mantle-derived CO₂ that causes intense mofette activity (Kämpf et al., 2013; Nickschick et al., 2015, 2017), while the ascent of magmas and the fluid activity probably constitute the forcing mechanisms of the seismic activity (Bräuer et al., 2003, 2008, 2011, 2014; Dahm et al., 2008; Fischer et al., 2014).

3 Hydrogeological background

Numerous mineral water springs occur in the Cheb Basin. In spa towns such as Františkovy Lázně the springs are used for illness prevention, and rehabilitation and consequently their catchment areas are safeguarded as protection zones. The springs are linked to gas-saturated and highly mineralized waters of an aquifer located at the eastern margin of the Mariánské Lázně Fault zone. Most mineral waters are of the Carlsbad Spa type, i.e., Na-HCO₃(SO₄Cl) to Na(Ca)-HCO₃(SO₄). Total dissolved solids are highly variable and range from a few mg L⁻¹ to over 20 g L⁻¹. The components are of a complex origin with both exogenous (oxidative and hydrolytic) and endogenous (hydrolytic and possibly fossil and evaporitic) contributions (Egeter et al., 1984; Dvořák, 1998; Paces and Smejkal, 2004).

4 Microbiological background

Microorganisms involved in all major global biogeochemical cycles exist in the deep biosphere. They are capable of catalyzing reactions between gases, fluids, sediments and rocks, thus enhancing mineral alteration as well as precipitation. Depending on respective subsurface environmental conditions, (hyper-)thermophilic and halotolerant microor-

ganisms were identified. Abundant metabolic groups are for example methanogenic archaea and sulfate-reducing bacteria, and strains from both of these taxa are able to obtain their carbon solely from CO₂ (Alawi et al., 2011). McMahon and Chapelle (1991) highlight that more than 90 % of the 16S ribosomal DNA sequences recovered from hydrothermal waters circulating through deeply buried igneous rocks in Idaho are related to hydrogenotrophic methanogenic microorganisms. Geochemical characterization indicates that hydrogen is the primary energy source for this methanogen-dominated microbial community. These results demonstrate that hydrogen-based microbial communities do occur in earth's deep biosphere. Considering increased hydrogen concentrations during seismic periods in the Cheb Basin (Bräuer et al., 2005) one might conclude that the microbial activity is potentially positively correlated to hydrogen availability, and therefore increased seismicity. We assume that a proliferating primary production based on methanotrophic archaea might provide the starting point for a secondary heterotrophic microbial community. As Alawi (2014) has shown elsewhere, such microorganisms produce energy-rich organic polymers that might be subsequently degraded by fermentative processes and thereby can close the carbon cycle by the emission of CO₂ as well as H₂. Acetate which is produced by acetogenic bacteria may then become a valuable substrate for Fe^{III}, Mn^{III,IV} and SO₄²⁻ reducing microorganisms as well as acetoclastic methanogens (Alawi, 2014). In addition, first analyses of the microbial communities in wetland soils of the Bublák mofette field in the Cheb Basin show that both bacteria and archaea are able to incorporate ¹³C-labeled CO₂ (Beulig et al., 2015, 2016). Hence, an effect of the increased CO₂ concentrations on the composition of the microbial community seems very likely. Despite various indicators for geo-bio interactions in the deep biosphere, it remains to be understood precisely how geological processes influence microbial activities in the deep subsurface and what role these processes have played in the geological evolution of the earth through time.

5 Pre-drilling site surveys

During the last years several geophysical, soil gas and gas flux analyses were performed to understand the patterns of CO₂ degassing at the Hartoušov mofette field. Well sections of prior boreholes drilled in the region, made available by the Czech Geological Survey (<http://www.geology.cz/extranet-eng/services/data>), provided provisional information on the near sub-surface sediments but detailed data on the mofette field were first acquired in a scientific drill campaign in 2007 (Flechsigg et al., 2008). The objective of the pre-drill surveys was to understand the structural and sedimentological control of CO₂ degassing and to determine an optimal drill site of intense degassing underlain by a conduit.

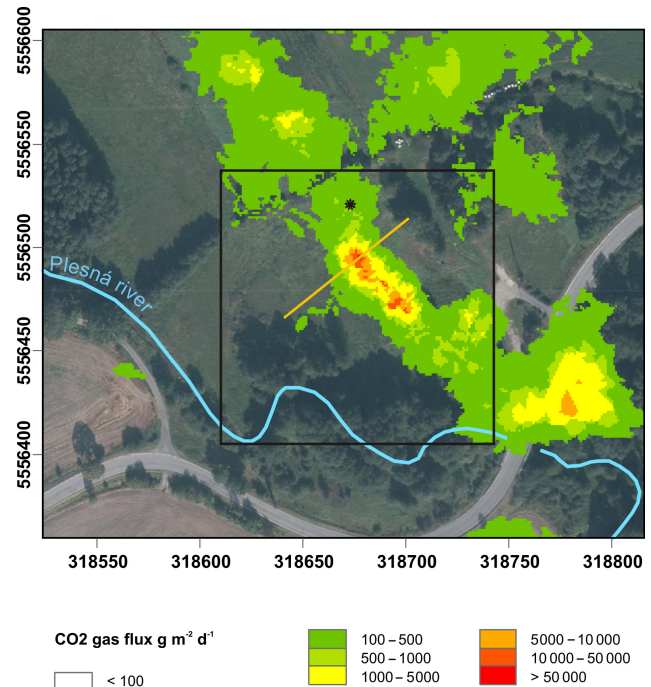


Figure 3. Location of the ICDP drill HJB-1 (black star) in the Hartoušov mofette field, with CO₂ gas flux mapping results of Nickschick et al. (2015). The black rectangle shows the area of passive seismic noise measurements (Fig. 6 and Sect. 5.3; matched field processing, MFP). The location of the geoelectrical profile in Fig. 5 is indicated by the orange line. Coordinates are in UTM zone 33N.

5.1 CO₂ mapping

Mapping of the temporal and spatial pattern of mantle-related CO₂ degassing in the Hartoušov mofette field (Fig. 3) revealed distinct differences in the spatial pattern of emitted CO₂, with low emission rates in a north–south trending zone in the southern part of the mofette field and heavy degassing in the central and northern part (Schütze et al., 2012; Kämpf et al., 2013; Rennert and Pfan, 2016; Nickschick et al., 2015, 2017). This led Nickschick et al. (2015) to hypothesize that sinistral strike-slip fault movement causes the opening of pull-apart structures, in which intense mantle-derived CO₂ degassing occurs in conduits. For the total area of 0.35 km² Nickschick et al. (2015) estimate that between 23 and 97 t of CO₂ are emitted each day.

The results of Nickschick et al. (2015) formed a major basis for the selection of the drill site of HJB-1 (Fig. 3). Located in the central part of the Hartoušov mofette field, CO₂ emission rates here can vary considerably, but are generally high (Nickschick et al., 2015). During a test study in 2012, we measured daily CO₂ gas fluxes on the spot that later became the drill site. Emission rates varied between ~ 14 and 43 kg m⁻² d⁻¹ (Fig. 4) with a mean rate of 27.5 ± 9.5 kg m⁻² d⁻¹ in the observation period. Because of

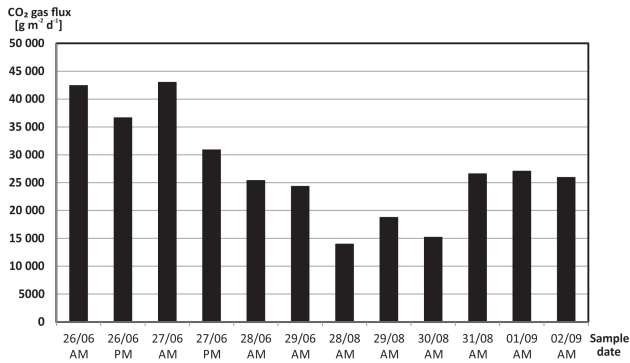


Figure 4. Variations in the CO₂ gas flux at the drill site of HJB-1 measured in 2012.

the continuously high CO₂ gas fluxes, the site proved an ideal location for HJB-1.

5.2 Geoelectrical near-surface surveys

The main objective of geophysical surveys in the Hartoušov mofette field was to detect and characterize subsurface structures that potentially represent fluid pathways or domains of fluid–rock interaction. We used preferentially electrical resistivity tomography (ERT), since the resistivity of rocks is notably sensitive to the presence of fluids. To retrieve a detailed conductivity image of the mofette field, modern ERT inversion and modeling techniques were applied (Günther et al., 2006; Günther and Rücker, 2009).

Combined with sedimentological studies and CO₂ soil gas measurements, the ERT surveys provided an image of near-surface structures down to a depth of ~100 m underneath the mofette field (Flechsigt et al., 2008, 2010; Schütze et al., 2012; Nickschick et al., 2015, 2017). The detected structures are, most probably, directly or indirectly caused by CO₂ flow because the geophysical subsurface anomalies not only correlate positively with areas of high CO₂ but also with sediment properties such as elevated organic carbon (C_{org}) and pyrite contents, and with the occurrence of dispersed quartz pebbles in fine-grained sediments. The sedimentological properties are likely related to chemical and physical conditions caused by high concentrations of CO₂ in the sediments, and to high gas pressure. Near-surface features such as low-permeability beds seem to influence primarily the variation in CO₂ degassing linked to meteorological conditions. The presence of such beds could cause the temporal accumulation of CO₂ in underlying porous sand layers.

ERT was also used in time-lapse mode to detect temporal changes in subsurface resistivity, caused by fluctuating relations of the gaseous to liquid phase, and was combined with repeated soil gas measurements (Nickschick et al., 2017). To evaluate the stability of subsurface degassing structures over time, repeated measurements were carried out (Nickschick et al., 2017). Two repeated 2D-ERT surveys in 2007 and

2016 at the central mofette (Fig. 5) indicated small-scale near-surface (< 2 m depth) variations in the resistivity, caused by meteorological and seasonal influences, while a distinct anomaly below the central mofette at 45–55 m correlates positively with a zone of high-intensity soil degassing (Fig. 3). The detected changes suggest that CO₂ degassing sites are not steady structures; instead, their architecture changes over time spans of days to years (Nickschick et al., 2017).

5.3 Matched Field Processing (MFP) for noise source localization

Subsurface CO₂ flow is often accompanied by gas bubble collapses that act as ambient noise sources and produce seismic signals. With the help of dense small-aperture instrumental arrays and matched field processing (MFP) techniques, the noise sources can be located (Vandemeulebrouck et al., 2010; Corciulo et al., 2012; Flores Estrella et al., 2016). The data are typically displayed as a 3-D probability map that illustrates the distribution of noise sources within and beneath the array. In this way, degassing spots such as mofettes can be detected, and their corresponding subsurface feeding channels can be imaged (Flores Estrella et al., 2016).

In May 2015 we measured continuous seismic noise with an instrumental array of 25 stations (vertical geophones connected to REF TEK Texan recorders) covering 1 ha surface area in the Hartoušov mofette field. The normalized MFP output shows three clearly defined surface maxima (values ~ 1; Fig. 6a). Including areas with medium MFP amplitude (values between 0.35 and 0.6), the sources form a NW–SE trending zone of increased noise activity. While the northernmost source is only visible down to a depth of 10 m (Fig. 6b), the other two sources are still recognizable in the 10–18 m depth interval but continuously decay below 18 m in amplitude and they widen. In the depth interval 18–30 m another source appears in between, but contrary to the other ones it shows a steady amplitude increase with depth.

The measurements suggest the presence of two major fluid channels to the NE of the array that reach from the surface down to a depth of at least 30 m. Another channel in the northernmost part of the array is limited to the uppermost 10 m. A fourth channel seems to exist between the two major channels starting at 18 m depth and continuously increases in MFP amplitude with depth. The deep-seated channel might form the main feeder channel for the near-surface channels.

5.4 Shallow wells

The borehole HJB-1 was placed in an area in which the two exploratory drillings HJ-3 and HJ-4 were conducted in 1993, exploring the presence of groundwater of deeper aquifers closer to the crossing of faults. Next, direct information on the shallow subsurface sediments in the Hartoušov mofette field was gained in an exploratory drill campaign in 2007 when five shallow wells reached depths of up to 9 m

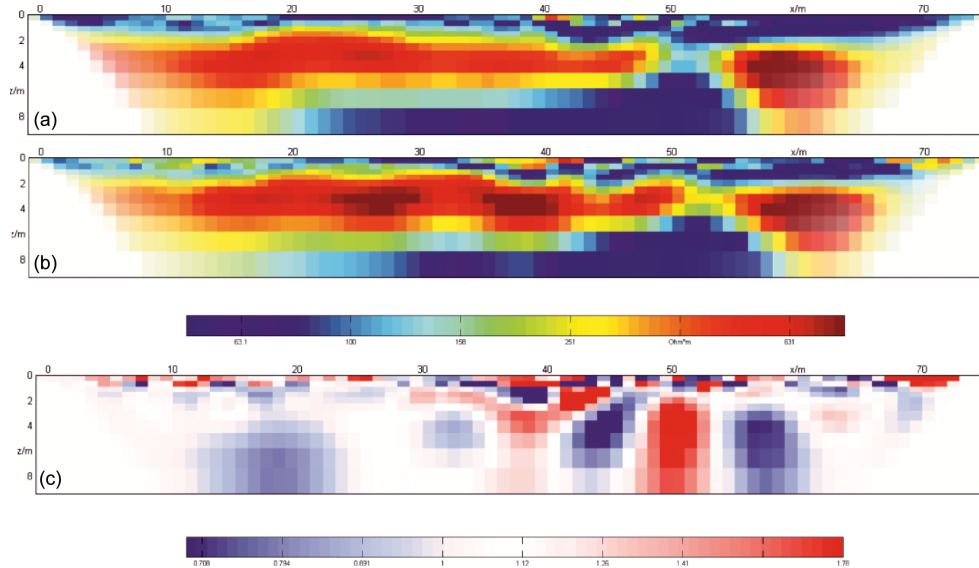


Figure 5. Results of repeated 2-D resistivity surveys at the central mofette in Hartoušov, (a) inversion model of the resistivity (Ωm) distribution measured in May 2007, (b) inversion model of the resistivity distribution measured in October 2016 (inversion code DC2DInvRes) and (c) relative change in the subsurface resistivity by inversion of the ratio of data from the initial (2006) and later (2016) data sets. A variation of 1 means that the resistivity has not changed, a variation of 1.2 represents an increase of 20 %.

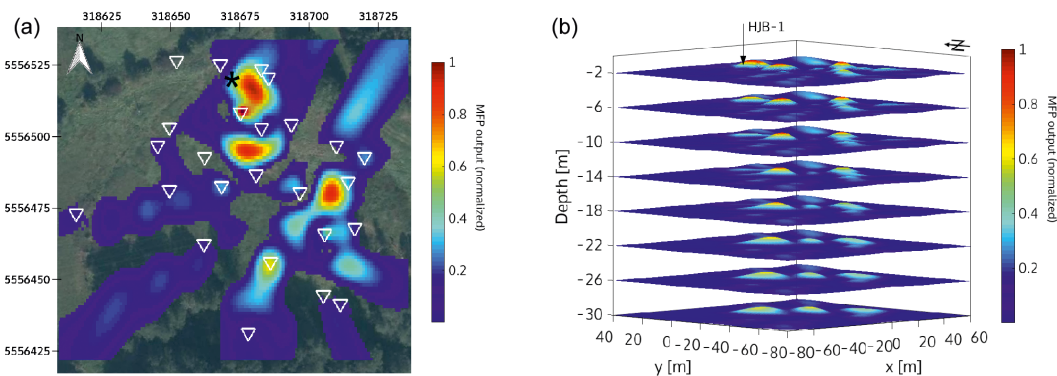


Figure 6. matched field processing (MFP) results (normalized) for the array deployed in May 2015 in the Hartoušov mofette field. (a) Surface plot. The white triangles indicate the position of stations. The black star shows the location of HJB-1. (b) 3-D depth plot (0–30 m).

(Flechsigt et al., 2008). The main objective of the campaign was to compare near-surface sediments underneath an active mofette with sediments in reference sites likely not affected by CO_2 emissions. The authors assumed that sediments in mofette sites are influenced by accelerated silicate weathering due to acidifying and leaching effects of CO_2 , decelerated decomposition of organic matter, and enhanced preservation and possibly formation of sulfides and sulfates. Another purpose of the pilot-hole was to corroborate the interpretation of geoelectrical lines measured at that time.

The drillings showed that the uppermost sediments in the mofette field consist of Quaternary fluvial channel and flood plain deposits of the Plesná river, while the lower section is made up of Pliocene lacustrine clays. Drilling in the

central mofette site revealed the occurrence of dispersed pebbles in fine-grained sediments and confirmed the presence of a domal uplift of the Pliocene clays already recognized in geoelectrical data (Flechsigt et al., 2008). Laboratory analyses showed increased C_{org} and pyrite contents of the sediments in areas of high CO_2 degassing. The results of the drilling campaign supported the hypothesis that in areas of high CO_2 degassing, such as mofettes, physical and mineralogical properties of sediments can be significantly influenced by CO_2 .

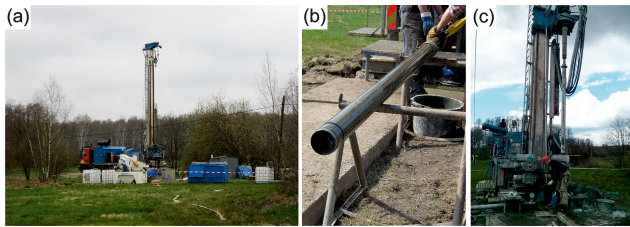


Figure 7. (a) Drill site of HJB-1 in Hartoušov; (b) core barrel display after recovery; (c) geophysical logging operations.

6 Drilling and coring, hydraulic and geochemical analyses, logging operations, and sampling

The drill site of HJB-1 (Fig. 7) is located in the protection zone of natural healing resources of the spa town of Františkovy Lázně (Franzensbad) but likewise in the protected area of natural water accumulation of the Cheb Basin and the Slavkovský Forest. Thus, drilling permissions had to be obtained from the State Land Office of the Czech Republic, Ministry of Public Health, Regional Authority of the Karlovy Vary Region (OŽPaZ) and the District Mining Bureau for the region of Karlovy Vary. Because of difficult terrain conditions, it was necessary to build a gravel track to allow the heavy drilling lorry to access the drilling location. The drilling operator was the company SG Geoprůzkum České Budějovice.

6.1 Drilling and coring

Drilling started on 30 March 2016 and lasted until 27 April 2016. First, a steel casing with a diameter of 324 mm was cemented down to a depth of 8 m. Next, a conductor pipe of diameter 219 mm was fitted and cemented down to 15.50 m below surface level. On the inner casing (219 mm) a preventive slide valve (preventer) DN 300 mm was installed. Then the hole was drilled near-vertically and reached a final depth of 108.50 m utilizing a core drilling system Drillmec G-25 with a cutting diameter from 450 to 275 mm installed on a Tatra 815 drilling lorry. For the coring, a Terracore S Geobor wireline core barrel system (Atlas Copco) was used (inner diameter 96.1 mm). Cores were retrieved in PVC liners of 3 m length. Pure bentonite was used as a drilling mud additive. Drilling was conducted under strict contamination control using fluorescein in the drilling mud as a contamination tracer, as tested before at the CO₂-sequestration site in Ketzin (Brandenburg, Germany) (Pellizzari et al., 2013). The concentration of fluorescein in the drilling mud was kept constant at 5 mg L⁻¹.

Drilling was performed through the gate valve so that the drilling crew was able to overcome problems of pressurized CO₂ in the drilling shaft. Pressure signs, which were expected in the project, occurred in the form of smaller and larger gas eruptions after drilling through the ceiling formed

by the Cypris Fm. The first eruption of CO₂ occurred at a depth of 78.5 m when about 0.3 m³ of clay was flushed to surface, and acoustic signs of CO₂ emission became loud. Afterwards, until the final depth was reached, dense bentonite mud (~ 1150 kg m⁻³) was used, while the drilling mud initially had a density of ~ 1100 kg m⁻³. Mud loss was high in the Quaternary deposits and in the claystones of the Cypris Fm., and particularly in the interval of 27 to 45 m.

On the 28 April 2016 the drilling string was pulled out of the hole and geophysical logging was performed. On the 2 May 2016 the first borehole cleaning was realized by using airlift of debris; an annulus was used for filling the stem with drinking water and the air was pushed using airlift tubes with a diameter of 72 mm. The stem was purified from the residual mud and dressed with a PVC-U casing with a diameter of 114 mm. In sections 58.50 to 63.50 m, 68.50 to 83.50 m and 88.50 to 103.50 m a perforated PVC-U casing was fitted. The bottom of the borehole was equipped with a full casing with a length of 5 m. Subsequently, the casing was backfilled using washed gravel. Pressure on the gridiron is monitored online (on average 510 kPa or 5.1 bar) by H. Woith (GFZ Potsdam). Today, the wellhead is closed by a gas-tight seal and flange mounted gauge. During the drilling, the groundwater level was irregularly monitored. A very shallow aquifer was reached at 0.60 m below surface, then an aquifer in the upper part of the Cypris Fm., and finally a deep aquifer below 81.50 m in the Main Seam Fm. 24 h after reaching the final depth, the groundwater level in the well was at 4.20 m below surface. Hydraulic properties of the aquifer system were checked using short-time pumping and recovery tests. The borehole was left open for long-term online monitoring of the casing-head pressure. Until today, the borehole forms an active ascent path for gases. Since no cores were recovered in the uppermost 9 m, a dry drilling (HAR-2R) was performed immediately after HJB-1 was drilled. The dry drilling allowed the retrieval of uncontaminated shallow-core samples.

6.2 Hydraulic and geochemical analyses

A 24 h pumping test was performed after a mechanical gas-separator and an automatic measuring station were fitted to the wellhead to monitor groundwater level and flow, conductivity and temperature of pumped water. Subsequently, short-time hydrodynamic tests with a maximum tapping phase of 22 h were completed using a submersible pump (Grundfos SQ 2 70). The effective yield value of the liquid phase was 0.15 L s⁻¹, while the yield of the gaseous phase was significantly higher, on average 0.5 L s⁻¹, with a maximum of 2.92 L s⁻¹. The coefficient of determination between the water level and the yield of the gaseous phase amounted to 0.67; the coefficient of determination between the yields of liquid phase and gaseous phase yields was at 0.89 during the short-term tests. The specific yield value amounted to $2.9 \times 10^{-5} \text{ m}^2 \text{ s}^{-1}$. Transmissivity was around $7.8 \times 10^{-6} \text{ m}^2 \text{ s}^{-1}$ during non-steady flow at the end of the short-term hydro-

Table 1. Comparison of the chemical parameters of the recovered mineral water in HJB-1. The sampling date was 10 May 2016 (20:00 LT, end of recovery test). A comparison to the chemistry of two typical mineral waters from western Bohemia is shown (Karlovy Vary: spring Vřídlo (Sprudel), borehole BJ-35, 55.2 m deep and Františkovy Lázně: spring Adler, borehole 33 m deep).

Water source	K (mg L ⁻¹)	Na (mg L ⁻¹)	Ca (mg L ⁻¹)	Mg (mg L ⁻¹)	Cl (mg L ⁻¹)	SO ₄ (mg L ⁻¹)	HCO ₃ (mg L ⁻¹)	Fe (mg L ⁻¹)	Mineralization (mg L ⁻¹)
HJB-1	44.2	1080	411	85.1	229	1470	2420	13.7	5870
Karlovy Vary	90.2	1670	118	42.9	592	1610	2180	1.3	6422
Františkovy Lázně	21.9	921	48.4	11.2	398	1119	671	14.3	3306

dynamic test, just before eruption. Thus, the Variscan mica schists and basal Cenozoic sediments seem to be weakly to slightly permeable. Less permeable rocks were reached after approximately 10 h of pumping. The tests suggest the presence of a major fluid ascending channel located in a permeable fault zone. Reaching a significant fault in basal layers of the basin and its fundament is also supported by a large spreading of the gas phase after penetrating the ceiling formed by less permeable strata of the Cypris Fm.

Starting at a depth of approximately 78.5 m, after penetrating a carbonate-rich layer approximately 30–40 cm in thickness, significant circulation of gas-saturated groundwater was observed, and bursts of gaseous CO₂ and water occurred at the wellhead. Gas analysis measured 99.90 vol. % CO₂, 0.0831 vol. % N₂ and 0.00558 vol. % O₂. We assume that the sand-bearing sediments directly underneath this caprock-like structure form a reservoir for mantle-derived CO₂. Physicochemical parameters of groundwater recovered from the basal aquifer (approximately at a depth of 79–85 m) were measured during the pumping tests (Table 1). After cleaning the borehole, samples were taken for chemical and microbiological analysis of liquid and or gaseous phases. The subthermal mineral water had a temperature of up to 18.6 °C. The water was highly gas-saturated with about 1892 mg L⁻¹ of free dissolved CO₂, and heavily mineralized with an electrical conductivity of around 6800 µS cm⁻¹. The pH was about 6.4.

The content of H₂SiO₃ in the groundwater of the basal aquifer is very high, with up to 112 mg L⁻¹, as is the Fe content with up to 13.7 mg L⁻¹. The groundwater of the basal aquifer is of the Na-Ca-HCO₃-SO₄ type, typical of the Františkovy Lázně Spa and its mineral waters. Its composition is mainly influenced by intense hydrolysis of aluminosilicate minerals probably caused by CO₂, and, given the relatively high concentration of chloride ions, by a fossil component (Na-Cl) related to an evaporitic closed lacustrine basin represented by the claystones of the Cypris Fm. (unit 3 in Fig. 8). A high content of sulfate is typical of Karlovy Vary Spa mineral waters and might reflect, at least partly, the dissolution of evaporites such as Na₂SO₄ (Paces and Smejkal, 2004).

6.3 Logging operations

Logging data were acquired in eight runs to ensure complete well coverage without losing data due to sensor off-sets in stacked tool strings. Most tools were combined with a gamma ray (GR) probe to allow an accurate depth alignment. Since borehole stability was a concern, the spectral GR was run before pulling out the drill pipe, logging downwards at 2 m min⁻¹. A bismuth germanate (BGO) scintillation crystal within the tool allowed us to determine the amount of natural radioactivity within the formation and additionally a splitting into thorium (Th), potassium (K) and uranium (U) based on discrete energy peaks. After run 1, the drill pipe was pulled and all consecutive measurements were acquired in open hole. Run 2 consisted of a probe recording the environmental parameters of the borehole fluid including temperature, pressure, conductivity, salinity, pH, oxygen saturation and chloride content. A magnetic susceptibility probe was run in combination with GR in runs 3 and 4 in two intervals. An overlap was logged to allow for proper depth alignment and splicing of the two runs. In run 4, a different gain was used for the susceptibility probe. To compensate for the difference between both measurements, a multiplier was utilized to homogenize the data before splicing. Due to the presence of a conductor pipe at approximately 15 m, no open hole data could be gained above that depth. Since the data of run 3 and 4 were acquired logging upwards and in open hole, they were used as depth reference. All other measurements were matched with these runs using either a linear or an interactive depth shift. Run 5 provided a focused electric resistivity measurement followed by formation velocity in run 6. The sonic data were reprocessed by picking the first arrivals of the near and far detectors and recalculating delta time compressional and primary velocity (V_p). A dipmeter probe was logged in run 7 providing four pad conductivities in four directions, caliper data and borehole navigation data. Microsusceptibility was the last measurement proving to be a higher-resolution log than the standard susceptibility in runs 3 and 4, with a vertical resolution of about 2 cm. It will be used in the future for a better correlation with core data. To complete the logging suite, Prague University acquired gamma density and neutron porosity data.

The composite log is presented in Fig. 8 together with a lithology obtained from core data. The core depth and litho-

logical boundaries were adjusted on the basis of the logging data, especially in areas of low core recovery. The borehole was drilled vertically with a slight north trend and a deviation of 1–2°. The GR log indicates a gradual decrease in clay content towards the surface. Especially the weathered schists near total depth feature high thorium contents. Susceptibility is generally low but shows several peaks throughout Miocene deposits. Within the weathered Paleozoic schist an increase in gamma ray, sonic velocity and resistivity can be noted indicating higher clay content and likely a higher compaction. The dipmeter shows several conductivity spikes within the Miocene that could be related to minor fractures or cracks. The sonic wavelets indicate several chevrons that probably developed for the same reason.

6.4 Sampling

At the well site, the laboratory container of GFZ Potsdam (BUGLAB) was installed to allow subsampling under optimal conditions. Equipped with refrigerators as well as with –80 °C freezers, the container permitted optimal storage conditions for biological samples. Below 20 m depth, the sediment was too consolidated for subsampling with cutoff syringes and consequently whole round cores (8 cm long, still in plastic liner) were cut. To preserve the samples, different techniques were used. Core material assigned for cultivation-based analyses were stored in CO₂-flushed gas-tight bags, while samples intended for geochemical analyses were stored in N₂-flushed bags, and samples reserved for molecular biological studies were frozen in the field at –80 °C. By now, segments of the core have been transferred to project partners to analyze the microbiology, sedimentology and mineralogy as well as to perform geochemical analyses. Because the perimeter of the core most likely was contaminated by drilling mud, it was discarded. This so-called inner coring was performed under aseptic conditions at the GFZ Potsdam. More than 300 samples are currently processed in this way. From each core meter about 60 cm were retained as whole round cores for sedimentological and mineralogical analyses and to perform core logging. All cores were photographed at the GFZ (Fig. 9).

6.5 Contamination control

To assess drill-mud penetration into cores the tracer fluorescein was extracted from the cut-off rim and the inner core according to the protocol from Pellizzari et al. (2013; Fig. 10). Sediment samples were ground using a mortar so that 0.250 g of the powder was mixed with 600 µL buffer (50 mM TRIS, pH 9) in a 2 mL reaction tube. The tubes were placed on a vortex and mixed for 30 min at maximum speed. Then, the sediment samples were centrifuged at 20 800 × *g* for 10 min and the supernatant was transferred to a 1.5 mL reaction tube. The extraction procedure was then repeated. The supernatants were combined, centrifuged and transferred to a

clean tube. The fluorescein content was measured in triplicate using 96-well plates processed using a filter fluorometer (CLARIOstar® OPTIMA, BMG LABTECH, Germany). The quantification of fluorescein indicates that 5 out of 45 inner core samples (after inner-coring) were contaminated by drill mud. Generally sandy (highly permeable) samples showed a higher degree of contamination in comparison to clay-rich samples.

7 Initial core description

In total, 85 % of the 108.5 m hole was available in the form of core halves for inspection and sampling. Major gaps exist primarily in the uppermost 30 m. The core was split in half lengthwise and subsequently photographed at the GFZ Potsdam, followed by a visual core description. The recovered core is severely affected by drilling disturbance. Partly, it shows a conspicuous banding composed of relatively dark mudstones typically 2–5 cm thick and of lighter colored homogeneous and comparatively soft mud mostly 0.5–2.5 cm thick (Fig. 9g and f). Although the banding resembles rhythmic bedding, close inspection reveals that it results from the injection of drilling mud along preexisting bedding planes. Drilling mud was also injected into the core along sub-vertical, natural and drilling-induced fractures, while in the basal interval of the core the mud has intruded highly-altered or weathered mica schists. Thus, careful examination of the core is vital to identify artificial “false bedding” and to differentiate natural and drilling-induced deformation structures.

The core is composed of five units (Fig. 9):

The lowermost unit 1 from ~108.5 to ~89.8 m consists of highly altered or weathered Palaeozoic mica schists (Fig. 9a). According to preliminary XRD measurements, the schists are principally composed of kaolinite, muscovite/illite, siderite and quartz. Kaolinite likely has formed under near-surface weathering conditions during Mesozoic–Early Cenozoic time (Störr, 1976). The common presence of siderite might either be related to an alteration under reducing conditions and elevated *p*CO₂, hence possibly to fluids rich in CO₂, or to a formation during the influence of an overlying freshwater swamp.

Unit 2 from ~89.8 to ~79.0 m is made up primarily of massive to crudely bedded grey to brown and sandy to peaty mudstones with abundant mottles and nodules (Fig. 9b). The mineralogy is dominated by kaolinite, siderite, quartz and anatase. Thin lignite layers and abundant lignite coal fragments as well as the presence of root structures and possible soil horizons suggest deposition in a swamp environment. The unit might represent the Main Seam Fm. (Lower Miocene).

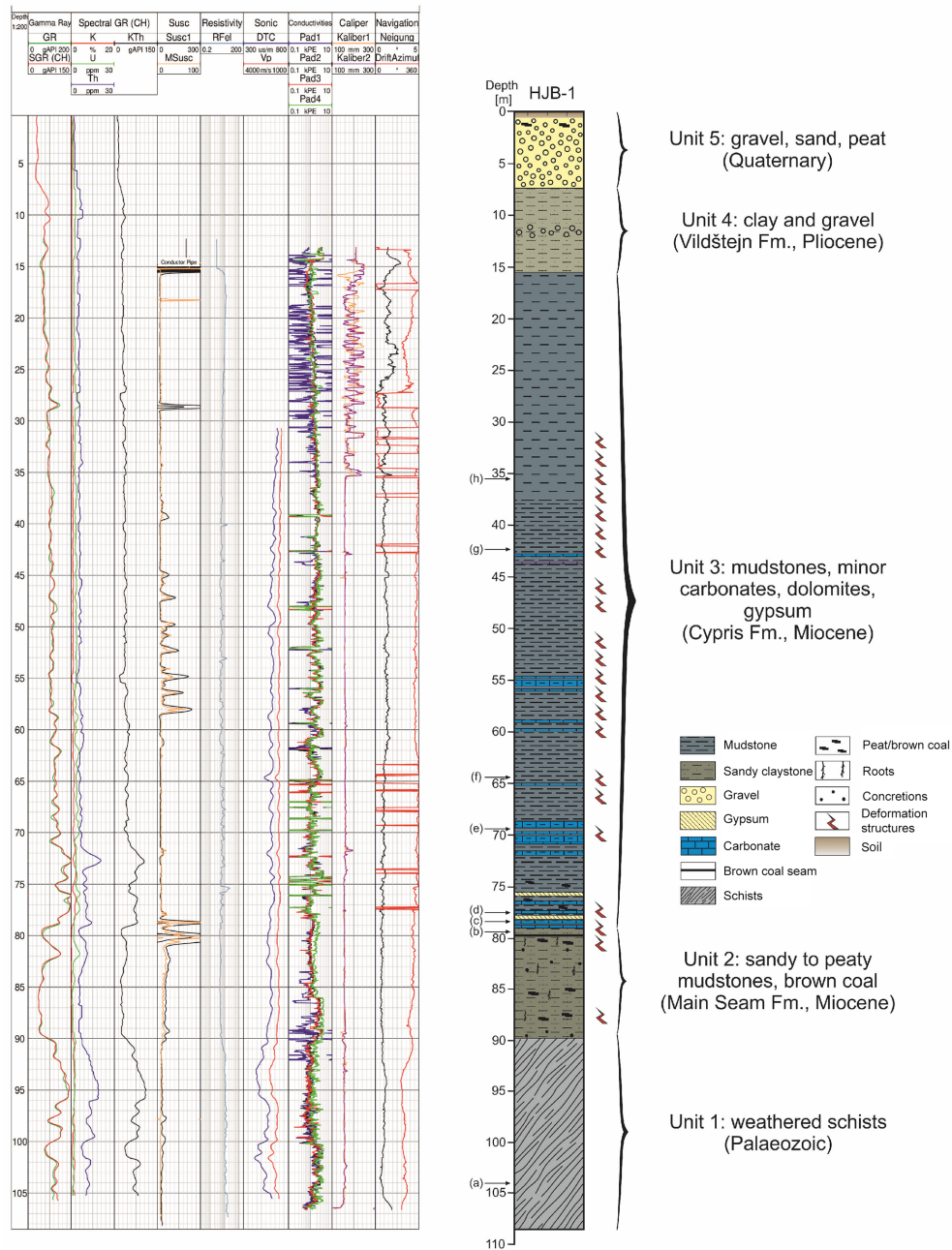


Figure 8. Logging data of well HJB-1 and summary stratigraphy based on initial core description results. Positions of cores in Fig. 9 are indicated by corresponding labels (a–h) and arrows.

Upward, following unit 3 from about 79.0 to ~ 15.5 m is dominated by grey to green mudstones. The relatively heterogeneous lower part of the unit consists of calcareous, sandy or peaty mudstones that are interbedded with thin peloidal or bioclastic carbonates, dolomite beds and gypsum layers (Fig. 9c, d, e). The overlying part up to ~ 37.5 m consists primarily of laminated or thin bedded mudstones (Fig. 8, while the uppermost part of the unit up to ~ 15.5 m is made up of massive to crudely bedded mudstones. Laminated mud-

stones were most likely deposited in a relatively deep lake with dysoxic to anoxic bottom-water conditions. The planar lamination from a few millimeters up to 2 cm thick might have formed due to seasonal changes in the bioproductivity or in the water stratification, whereas thin detrital carbonate beds up to 5 cm thick possibly represent event layers such as turbidites. The mudstones of the whole core interval are made up of clay minerals such as muscovite/illite, kaolinite, smectite and mixed-layers, and of quartz, K-feldspars, pyrite,

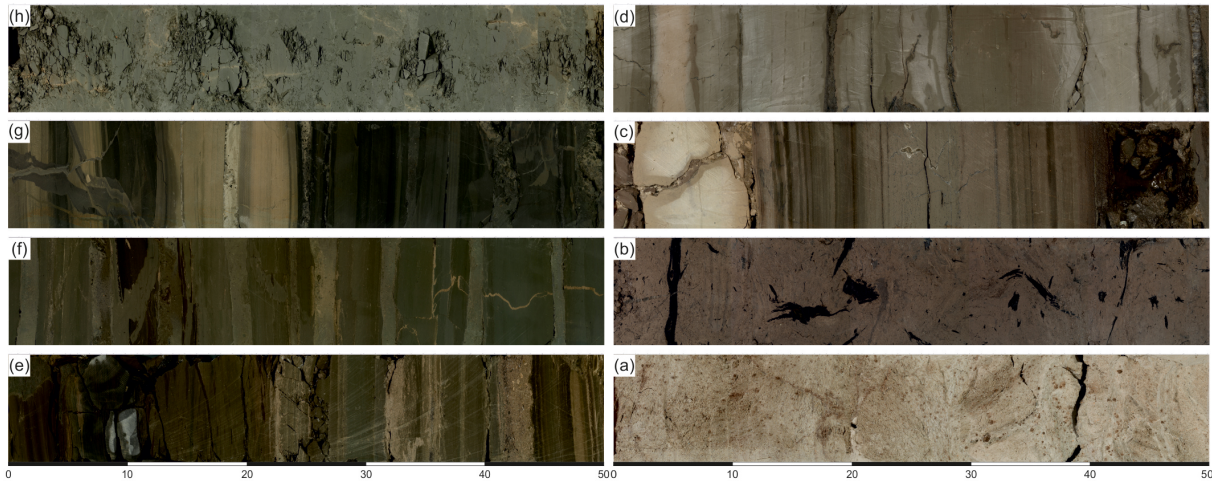


Figure 9. Representative lithologies in core HJB-1. (a) Palaeozoic schists with siderite concretions (104.16–104.66 m); (b) sandy mudstone with lignite coal (79.50–80.00 m); (c) interbedded sandy mudstones, calcareous mudstones and carbonates (78.50–79.00 m); (d) calcareous mudstones with gypsum layers and injection structures (77.61–78.11 m); (e) interbedded laminated mudstones and peloidal to bioclastic carbonates (69.56–70.06 m); (f) “false bedded” mudstones (light colored regular banding represents injected drilling mud) with natural injection structures (64.55–65.05 m); (g) laminated mudstones with natural deformation structures and “false bedding” (~ 42.00–42.46 m and (h) massive mudstones (~ 35.15–35.60 m). Scale is in centimeters.

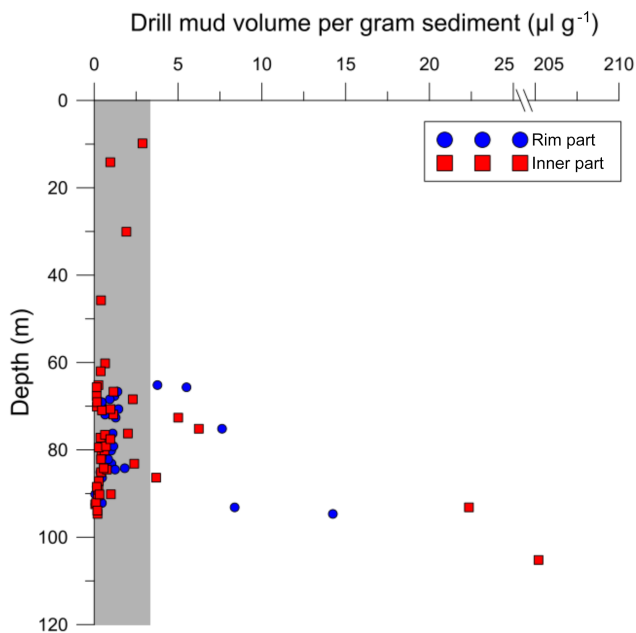


Figure 10. Contamination assessment of drill mud in cores. The grey area indicates the background noise of the fluorometric measurements of fluorescein (evaluated with core material obtained at the same site but without addition of fluorescein). 5 out of 45 inner core samples (red squares) are contaminated by drill mud.

zeolites, gypsum and analcime. Greigite occurs in several layers in the middle part of the mudstone interval according to petrophysical well site observation (magnetic susceptibility), but its presence is not yet confirmed by XRD. The pres-

ence of gypsum and analcime suggests a saline-alkaline lacustrine depositional environment, while the common occurrence of pyrite implies suboxic conditions during early diagenesis. However, the formation of these minerals might also be influenced by CO₂-rich fluids or microbial activity during diagenesis (e.g., Chen et al., 2016). The whole mudstone-dominated unit 3 likely correlates to the Cypris Fm.

Unit 4 between ~ 15.5 and ~ 7.2 m consists of green to brown clay and of minor gravel probably correlative to the Vildštejn Fm. Unit 5, representing the uppermost sediments down to a depth of ~ 7.2 m, is made up of predominantly moderately to poorly sorted sand to gravel with minor peat, most likely Quaternary channel and floodplain deposits of the nearby Plesná river.

Natural deformation structures such as microfaults, dikes and sills as well as irregular intrusions are abundant in several core intervals but are best visible in the laminated mudstones of unit 3. Most of the structures seem to have formed by hydrofracturing, sediment fluidization and injection as a result of excessive pore fluid pressure. Carbonate and gypsum cements are infrequently associated with the deformation structures and the host rock in the surrounding partly has changed its color or is bleached. Whether the deformation structures, cements and color changes are related to the flow of CO₂-rich fluids is the subject of ongoing investigations.

8 Conclusions, ongoing studies and open questions

Pilot hole HJB-1 drilled into an active mofette has proved as a successful test for upcoming well projects planned in the scope of the ICDP project “Drilling the Eger Rift”

(<http://web.natur.cuni.cz/uhigug/icdp>). First microbiological investigations including activity tests for microbial methane production, DNA extractions and cultivation experiments are ongoing. Microbial DNA was extractable from all samples and is currently analyzed through Illumina MiSeq 16S rDNA sequencing and quantitative PCR. A new procedure for the recovery of DNA from deep subsurface sediment samples was recently established by Alawi et al. (2014). With this method, DNA can be extracted from sediments with a low bacterial abundance, where commercial DNA extraction kits fail. Furthermore, with this technique it is possible to separate extracellular and intracellular DNA, and therefore to distinguish between fossil and modern microbial communities. Additionally, it is planned to perform community analyses based on Shotgun metagenomic sequencing for selected samples (in cooperation with P. Kyslik, Academy of Sciences of the Czech Republic). This method allows the identification of genes from all organisms present in the sediment, regardless of their taxa and specificity of PCR primers. For anaerobic culturing, the focus is set on methanogenic archaea and sulfate-reducing bacteria. Both metabolic groups are cultivated in a liquid anaerobic media and are inoculated inside an anaerobic chamber (glovebox). Growth is monitored by methane production and changing sulfate concentrations. Using different media compositions and temperatures, defined enrichment cultures have already been obtained and will be further characterized physiologically in detail. Pure cultures are a prerequisite for further laboratory experiments to gain deeper insights into the link to mineralogical processes such as mineral precipitation and alteration under varying conditions. Further on molecular biological analyses will be complemented by biomarker analyses at the Deutsches GeoForschungsZentrum GFZ (K. Mangelsdorf). Diversity of soil fungal communities will be analyzed by P. Baldrian (Academy of Sciences of the Czech Republic).

The core shows many features that might result from the flow of mantle-derived CO₂ e.g., deformation structures and alteration features, which are the subject of upcoming petrographic and geochemical studies. Further pending questions are to distinguish between Mesozoic–Cenozoic deep chemical weathering of Palaeozoic mica schists and alteration due to CO₂ flow or hydrothermal influence, the contribution of pyroclastics to the basin fill, and the palaeoenvironmental information contained in the Cenozoic lake sediments, in particular in the finely laminated (varved) interval of the Cypris Fm.

Ongoing geophysical studies, notably seismic (TU Freiberg), geoelectric (University of Leipzig) and magnetotelluric surveys (GFZ Potsdam) focus on examining the subsurface structure beneath the Hartoušov degassing area. The drill core from well HJB-1 provides essential information on the basin's sediments for these studies whereas the geophysical surveys will help to better understand the findings of the drill.

Data availability. The data used in this paper that stems from pilot hole HJB-1 are in the process of being interpreted in detail for various research targets. When these analyses are finished, and the related publications are submitted, the data will be deposited in reliable public depositories for access. However, at the current state of the projects the raw data cannot be made accessible for public use. When available, details of the data depositories can be obtained by contacting the corresponding author.

Competing interests. The authors declare that they have no conflict of interest.

Acknowledgements. We thank the German Research Foundation (DFG) for financial support of the project (grants AL 1898/1 and KA 902/16). The project AL 1898/1 was funded by the DFG Priority Programme 1006, International Continental Scientific Drilling Program (ICDP). Technical expertise and supervision of drilling operations by Bernhard Prevedel (GFZ Potsdam) is highly appreciated. Special thanks go to the drilling, logging and sampling crews in the field, in particular to Thomas Grelle and Carlos Lehne (both LIAG) and to Maria Börger, Susanne Boteck, Oliver Burckhardt, Patryk Krauze, Kai Mangelsdorf and Mareike Noah (all GFZ Potsdam). Alexander Wendt (University of Greifswald) photographed the core and preliminary XRD analyses were done by Sandro Wobeser (University of Potsdam) in the scope of his Bachelor thesis.

Edited by: Thomas Wiersberg

Reviewed by: Luca Pizzino and one anonymous referee

References

- Alawi, M.: Microbes in geo-engineered systems: geomicrobiological aspects of CCS and Geothermal Energy Generation, in: *Microbial Life of the Deep Biosphere*, (Life in Extreme Environments), edited by: Kallmeyer, J. and Wagner, D., De Gruyter, Berlin, 203–224, 2014.
- Alawi, M., Lerm, S., Vetter, A., Wolfgramm, M., Seibt, A., and Würdemann, H.: Diversity of sulfate-reducing bacteria in a plant using deep geothermal energy, *Grundwasser*, 16, 105–112, 2011.
- Alawi, M., Schneider, B., and Kallmeyer, J.: A procedure for separate recovery of extra- and intracellular DNA from a single marine sediment sample, *J. Microbiol. Meth.*, 104, 36–42, 2014.
- Alawi, M., Nickschick, T., and Kämpf, H.: Mikrobiologische Prozesse in CO₂-Aufstiegskanälen, *System Erde*, 5, 28–33, <https://doi.org/10.2312/GFZ.syserde.05.01.5>, 2015.
- Bankwitz, P., Schneider, G., Kämpf, H., and Bankwitz, E.: Structural characteristics of epicentral areas in Central Europe: study case Cheb Basin (Czech Republic), *J. Geodyn.*, 35, 5–32, 2003.
- Beulig, F., Heuer, V. B., Akob, D. M., Viehweger, B., Elvert, M., Herrmann, M., Hinrichs, K. U., and Küsel, K.: Carbon flow from volcanic CO₂ into soil microbial communities of a wetland mofette, *ISME J.*, 9, 746–759, 2015.
- Beulig, F., Urich, T., Nowak, M., Trumbore, S. E., Gleixner, G., Gilfillan, G. D., Fjelland, K. E., and Küsel, K.: Altered carbon turnover processes and microbiomes in soils under long-

- term extremely high CO₂ exposure, *Nature Microbiol.*, 1, 15025, <https://doi.org/10.1038/nmicrobiol.2015.25>, 2016.
- Bräuer, K., Kämpf, H., Strauch, G., and Weise, S. M.: Isotopic evidence (³He/⁴He, ¹³C/CO₂) of fluid-triggered intraplate seismicity, *J. Geophys. Res.-Sol. Ea.*, 108, 2070, <https://doi.org/10.1029/2002JB002077>, 2003.
- Bräuer, K., Kämpf, H., Faber, E., Koch, U., Nitzsche, H.-M., and Strauch, G.: Seismically triggered microbial methane production relating to the Vogtland NW Bohemia earthquake swarm period 2000, Central Europe, *Geochem. J.*, 39, 441–450, 2005.
- Bräuer, K., Kämpf, H., Koch, U., Niedermann, S., and Strauch, G.: Seismically induced changes of the fluid signature detected by a multi-isotope approach (He, CO₂, CH₄, N₂) at the Wettingquelle, Bad Brambach (central Europe), *J. Geophys. Res.*, 112, B04307, <https://doi.org/10.1029/2006JB004404>, 2007.
- Bräuer, K., Kämpf, H., Niedermann, S., Strauch, G., and Tesař, J.: The natural laboratory NW Bohemia – comprehensive fluid studies between 1992 and 2005 used to trace geodynamic processes, *Geochem. Geophys.*, 9, Q04018, <https://doi.org/10.1029/2007GC001921>, 2008.
- Bräuer, K., Kämpf, H., Koch, U., and Strauch, G.: Monthly monitoring of gas and isotope compositions in the free gas phase at degassing locations close to the Nový Kostel focal zone in the western Eger Rift, Czech Republic, *Chem. Geol.*, 290, 163–176, <https://doi.org/10.1016/j.chemgeo.2011.09.012>, 2011.
- Bräuer, K., Kämpf, H., and Strauch, G.: Seismically triggered anomalies in the isotope signatures of mantle-derived gases detected at degassing sites along two neighbouring faults in NW Bohemia, central Europe, *J. Geophys. Res.-Sol. Ea.*, 119, 5613–5632, 2014.
- Chen, F., Turchyn, A., Kampman, N., Hodell, D., Gázquez, F., Maskell, A., and Bickle, M.: Isotopic analysis of sulfur cycling and gypsum vein formation in natural CO₂ reservoir, *Chem. Geol.*, 436, 72–83, 2016.
- Corciulo, M., Roux, P.-F., Campillo, M., Dubucq, D., and Kuperman, W. A.: Multiscale matched-field processing for noise-source localization in exploration geophysics, *Geophysics*, 77, 33–41, 2012.
- Dahm, T., Fischer, T., and Hainzl, S.: Mechanical intrusion models and their implications for the possibility of magma-driven swarms in NW Bohemia Region, *Stud. Geophys. Geod.*, 52, 529–548, 2008.
- Dahm, T., Hrubcová, P., Fischer, T., Horálek, J., Korn, M., Buske, S., and Wagner, D.: Eger Rift ICDP: an observatory for study of non-volcanic, mid-crustal earthquake swarms and accompanying phenomena, *Sci. Dril.*, 16, 93–99, <https://doi.org/10.5194/sd-16-93-2013>, 2013.
- Deflaun, M. F., Fredrickson, J. K., Dong, H., Pfiffner, S. M., Onstott, T. C., Balkwill, D. L., Streger, S. H., Stackebrandt, E., Knoessen, S., and van Heerden, E.: Isolation and characterization of a *Geobacillus thermoleovorans* strain from an ultra-deep South African gold mine, *Syst. Appl. Microbiol.*, 30, 152–164, 2007.
- Dvořák, J.: Hydrogeology and the genesis of mineral waters of the Carlsbad type in western Bohemia, *Münchener Geologische Hefte*, B8, 63–69, 1998.
- Egerter, H.-G., Plötner, G., Dvořák, J., and Jordan, H.: Geochemische Beziehungen in vogtländisch-westböhmisches Mineralwässern, *Abhandlungen der Sächsischen Akademie der Wissenschaften zu Leipzig, mathematisch-naturwissenschaftliche Klasse*, 56, 1–60, 1984.
- Fiala, J. and Vejnar, Z.: The lithology, geochemistry, and metamorphic gradation of the crystalline basement of the Cheb (Eger) Tertiary Basin, Saxothuringian Unit, *Bull. Geosci.*, 79, 41–52, 2004.
- Fischer, T., Horálek, J., Hrubcová, P., Vavryčuk, V., Bräuer, K., and Kämpf, H.: Intracontinental earthquake swarms in west-Bohemia and Vogtland: A review, *Tectonophysics*, 611, 1–27, 2014.
- Fischer, T., Matyskac, C., and Heinicke, J.: Earthquake-enhanced permeability – evidence from carbon dioxide release following the ML3.5 earthquake in West Bohemia, *Earth Planet. Sc. Lett.*, 460, 60–67, <https://doi.org/10.1016/j.epsl.2016.12.001>, 2017.
- Flechsigt, Ch., Bussert, R., Rechner, J., Schütze, C., and Kämpf, H.: The Hartoušov Mofette Field in the Cheb Basin, Western Eger Rift (Czech Republic): a comparative geoelectric, sedimentologic and soil gas study of a magmatic diffuse degassing structure, *Zeitschr. Geol. Wiss.*, 36, 177–193, 2008.
- Flechsigt, C., Fabig, T., Rücker, C., and Schütze, C.: Geoelectrical investigations in the Cheb basin/W-Bohemia: An approach to evaluate the near-surface conductivity structure, *Stud. Geophys. Geod.*, 54, 417–437, 2010.
- Flechsigt, C., Heinicke, J., Mrlina, J., Kämpf, H., Nickschick, T., Schmidt, A., Günther, T., Rücker, C., and Seidel, E.: Integrated geophysical and geological methods to investigate the inner and outer structures of the Quaternary maar Mýtina (W-Bohemia Czech Republic), *Int. J. Earth Sci.*, 104, 2087–2105, 2015.
- Flores Estrella, H., Umlauf, J., Schmidt, A., and Korn, M.: Locating mofettes using seismic noise records from small dense arrays and matched field processing analysis in the NW Bohemia/Vogtland Region, Czech Republic, *Near Surf. Geophys.*, 14, 327–335, 2016.
- Fredrickson, J. K., McKinley, J. P., Bjornstad, B. N., Long, P. E., Ringelberg, D. B., White, D. C., Krumholz, L. R., Suffita, J. M., Colwell, F. S., Lehman, R. M., Phelps, T. J., and Onstott, T. C.: Pore-size constraints on the activity and survival of subsurface bacteria in a Late Cretaceous shale-sandstone sequence, north-western New Mexico, *Geomicrobiol. J.*, 14, 183–202, 1997.
- Glombitza, C., Mangelsdorf, K., and Horsfield, B.: A novel procedure to detect low molecular weight compounds released by alkaline ester cleavage from low maturity coals to assess its feedstock potential for deep microbial life, *Organic Geochem.*, 40, 175–183, 2009.
- Goldscheider, N., Hunkeler, D., and Rossi, P.: Review: Microbial biocenoses in pristine aquifers and an assessment of investigative methods, *Hydrogeol. J.*, 14, 926–941, 2006.
- Günther, T. and Rücker, C.: Advanced inversion strategies using a new geophysical inversion and modelling library. Paper presented at the 15th European Meeting of Environmental and Engineering Geophysics, Dublin, Ireland, 7–9 September 2009.
- Günther, Th., Rücker, C., and Spitzer, K.: Three-dimensional modelling and inversion of dc resistivity data incorporating topography – II. Inversion, *Geophys. J. Int.*, 166, 506–517, <https://doi.org/10.1111/j.1365-246X.2006.03011.x>, 2006.
- Gulliver, D. M., Lowry, G. V., and Gregory, K. B.: Comparative study of effects of CO₂ concentration and pH on microbial communities from a saline aquifer, a depleted oil reservoir, and a freshwater aquifer, *Environ. Engineer. Sci.*, 33, 806–816, 2016.

- Hecht, L., Vignerresse, J. L., and Morteani, G.: Constraints on the origin of zonation of the granite complexes in the Fichtelgebirge (Germany and Czech Republic): Evidence from a gravity and geochemical study, *Geol. Rundsch.*, 86, 93–109, <https://doi.org/10.1007/pl00014669>, 1997.
- Hubert, C., Loy, A., Nickel, M., Arnosti, C., Baranyi, C., Brüchert, V., Ferdelman, T., Finster, K., Christensen, F. M., de Rezende, J. R., Vandieken, V., and Jorgensen, B. B.: A constant flux of diverse thermophilic bacteria into the cold Arctic seabed, *Science*, 325, 1541–1544, 2009.
- Kämpf, H., Strauch, G., Vogler, P., and Michler, W.: Hydrologic and hydrochemic changes associated with the December 1985/January 1986 earthquake swarm activity in the Vogtland/NW Bohemia seismic area, *Z. Geol. Wissenschaft.*, 17, 685–698, 1989.
- Kämpf, H., Peterek, A., Rohrmüller, J., Kumpel, H. J., and Geissler, W. H.: The KTB deep crustal laboratory and the western Eger Graben, in: *GeoErlangen 2005/Exkursionsführer*, edited by: Koch, R. and Röhling, H. G., *Schriftreihe der Deutschen Gesellschaft für Geowissenschaften*, 40, 37–108, 2005.
- Kämpf, H., Geissler, W. H., and Bräuer, K.: Combined gas-geochemical and receiver function studies, of the Vogtland/NW-Bohemia intraplate mantle degassing field Central Europe, in: *Mantle Plumes – A Multidisciplinary Approach*, edited by: Ritter, J. R. R. and Christiansen, U. R., Springer-Verlag, Berlin-Heidelberg-New York, 127–158, 2007.
- Kämpf, H., Bräuer, K., Schumann, J., Hahne, K., and Strauch, G.: CO₂ discharge in an active, non-volcanic continental rift area (Czech Republic): Characterisation (delta C-13, He-3/He-4) and quantification of diffuse and vent CO₂ emissions, *Chem. Geol.*, 339, 71–83, <https://doi.org/10.1016/j.chemgeo.2012.08.005>, 2013.
- Kallmeyer, J. and Wagner, D. (Eds.): *Microbial Life of the Deep Biosphere, (Life in Extreme Environments; 1)*, Berlin, De Gruyter, XVII, 325 pp., 2014.
- Lerm, S., Westphal, A., Miethling-Graff, R., Alawi, M., Seibt, A., Wolfgramm, M., and Würdemann, H.: Thermal effects on microbial composition and microbiologically induced corrosion and mineral precipitation affecting operation of a geothermal plant in a deep saline aquifer, *Extremophiles*, 17, 311–327, 2013.
- Lomstein, B. A., Langerhuus, A. T., D'Hondt, S., Jorgensen, B. B., and Spivack, A. J.: Endospore abundance, microbial growth and necromass turnover in deep sub-seafloor sediment, *Nature*, 484, 101–104, 2012.
- Malkovský, M.: The Mesozoic and Tertiary basins of the Bohemian Massif and their evolution, *Tectonophysics* 137, 31–42, 1987.
- McMahon, P. B. and Chapelle, F. H.: Microbial production of organic acids in aquitard sediments and its role in aquifer geochemistry, *Nature*, 349, 233–235, 1991.
- Mitchell, A. C., Phillips, A. J., Hiebert, R., Gerlach, R., Spangler, L. H., and Cunningham, A. B.: Biofilm enhanced geologic sequestration of supercritical CO₂, *Int. J. Greenh. Gas Control*, 3, 90–99, 2009.
- Morozova, D., Wandrey, M., Alawi, M., Zimmer, M., Vieth, A., Zettlitzer, M., Würdemann, H., & Grp, C. S.: Monitoring of the microbial community composition in saline aquifers during CO₂ storage by fluorescence in situ hybridisation. *Int. J. Greenh. Gas Control*, 4, 981–989, 2010.
- Mrlina, J., Kämpf, H., Geissler, W. H., and van den Bogaard, P.: Proposed Quaternary maar structure at the Czech/German boundary between Mýtina and Neualbentreuth (western Eger Rift, Central Europe): geophysical, petrochemical and geochronological indications, *Zeitschr. Geol. Wissenschaft.*, 35, 213–230, 2007.
- Mrlina, J., Kämpf, H., Kroner, C., Mingram, J., Stebich, M., Bräuer, A., Geissler W.H., Kallmeyer, J., Matthes, H., and Seidl, M.: Discovery of the first Quaternary maar in the Bohemian Massif, Central Europe, based on combined geophysical and geological surveys, *J. Volc. Geoth. Res.*, 182, 97–112, 2009.
- Nickschick, T., Kämpf, H., Flechsig, Ch., Mrlina, J., and Heinicke, J.: CO₂ degassing in the Hartousov mofette area, western Eger Rift, imaged by CO₂ mapping and geoelectrical and gravity surveys, *Int. J. Earth Sci.*, 104, 2107–2129, <https://doi.org/10.1007/s00531-014-1140-4>, 2015.
- Nickschick, T., Flechsig, Ch., Meinel, C., Mrlina, J., and Kämpf, H.: Architecture and temporal variations of a terrestrial CO₂ degassing site using electrical resistivity tomography and CO₂ gas measurements, *Int. J. Earth Sci.*, <https://doi.org/10.1007/s00531-017-1470-0>, 2017.
- Onstott, T. C.: Impact of CO₂ injections on deep subsurface microbial ecosystems and potential ramifications for the surface biosphere, in: *Carbon Dioxide Capture for Storage in Deep Geologic Formations – Results from the CO₂ Capture Project, v. 2: Geologic Storage of Carbon Dioxide with Monitoring and Verification*, edited by: Benson, S. M., Elsevier Science, London, 1217–1250, 2005.
- Onstott, T. C., Phelps, T. J., Colwell, F. S., Ringelberg, D., White, D. C., Boone, D. R., McKinley, J. P., Stevens, T. O., Long, P. E., Balkwill, D. L., Griffin, W. T., and Kieft, T.: Observations pertaining to the origin and ecology of microorganisms recovered from the deep subsurface of Taylorsville Basin, Virginia, *Geomicrobiol. J.*, 15, 353–385, 1998.
- Paces, T. and Smejkal, V.: Magmatic and fossil components of thermal and mineral waters in the Eger River continental rift (Bohemian massif, central Europe), in: *Water-Rock Interaction*, edited by: Wanty, R. B. and Seal II., R. R., Taylor and Francis Group, London, 167–172, 2004.
- Pellizzari, L., Neumann, D., Alawi, M., Voigt, D., Norden, B., and Würdemann, H.: The use of tracers to assess drill-mud penetration depth into sandstone cores during deep drilling: method development and application, *Environ. Earth Sci.*, 70, 3727–3738, 2013.
- Pellizzari, L., Morozova, D., Neumann, D., Klapperer, S., Kasina, M., Zettlitzer, M., and Würdemann, H.: Comparison of the microbial community composition of the well and saline aquifer fluids and of rock cores at the Ketzin CO₂ storage site – results of geochemical and molecular biological characterisation, *Environ. Earth Sci.*, 75, 1323, <https://doi.org/10.1007/s12665-016-6111-6>, 2016.
- Pešek, J., Brož, B., Brzobohatý, R., Dašková, J., Doláková, N., Elznic, A., Fejfar, O., Franců, J., Hladilová, Š., Holcová, K., Honěk, J., Hoňková, K., Kvaček, J., Kvaček, Z., Macůrek, V., Mikuláš, R., Opluštil, S., Rojčík, P., Spudil, J., Svobodová, M., Sýkorová, I., Švábenická, L., Teodoridis, V., and Tomanová-Petrová, P.: Tertiary basins and lignite deposits of the Czech Republic, *Czech Geological Survey, Prague*, 260 pp., 2014.
- Peterek, A., Reuther, C. D., and Schunk, R.: Neotectonic evolution of the Cheb Basin (Northwestern Bohemia, Czech Republic) and its implications for the late Pliocene to Recent crustal deforma-

- tion in the western part of the Eger Rift, *Zeitschr. Geol. Wissenschaft.*, 349, 335–365, 2011.
- Rajchl, M., Uličný, D., Grygar, R., and Mach, K.: Evolution of basin architecture in an incipient continental rift: the Cenozoic Most Basin, Eger Graben (Central Europe), *Basin Res.*, 21, 269–294, 2009.
- Rempel, K. U., Liebscher, A., Heinrich, W., and Schettler, G.: An experimental investigation of trace element dissolution in carbon dioxide: Applications to the geological storage of CO₂, *Chem. Geol.*, 289, 224–234, 2011.
- Rennert, T. and Pfanz, H.: Hypoxic and acidic soils on mofette fields, *Geoderma*, 280, 73–81, <https://doi.org/10.1016/j.geoderma.2016.06.019>, 2016.
- Rojik, P.: New stratigraphic subdivision of the Tertiary in the Sokolov Basin in Northwestern Bohemia, *J. Czech Geol. Survey*, 49, 173–185, 2004.
- Sauer, P., Glombitza, C., and Kallmeyer, J.: A system for incubations at high gas partial pressure, *Front. Microbiol.*, 3, 1–9, 2012.
- Schuessler, J. A., Kämpf, H., Koch, U., and Alawi, M.: Earthquake impact on iron isotope signatures recorded in mineral spring water, *J. Geophys. Res.*, 121, 8548–8568, 2016.
- Schütze, C., Sauer, U., Beyer, K., Lamert, H., Bräuer, K., Strauch, G., Flechsig, C., Kämpf, H., and Dietrich, P.: Natural analogues: a potential approach for developing reliable monitoring methods to understand subsurface CO₂ migration processes, *Environ. Earth Sci.*, 67, 411–423, <https://doi.org/10.1007/s12665-012-1701-4> 2012.
- Špičáková, A., Ulěny, D., and Kouldelková, G.: Tectonosedimentary evolution of the Cheb Basin (NW Bohemia, Czech Republic) between Oligocene and Pliocene: a preliminary note, *Stud. Geophys. Geod.*, 44, 556–580, 2000.
- Störr, M.: Zur Kenntnis der jungmesozoisch–tertiären Formation der Verwitterungskruste in der DDR, *Schriftenreihe geologische Wissenschaften*, 5, 231–241, 1976.
- Takai, K., Moser, D. P., Onstott, T. C., Spoelstra, N., Pfiffner, S. M., Dohnalkova, A., and Fredrickson, J. K.: *Alkaliphilus transvaalensis* gen. nov., sp. nov., an extremely alkaliphilic bacterium isolated from a deep South African gold mine, *Int. J. Syst. Evol. Microbiol.*, 51, 1245–1256, 2001.
- Trimarco, E., Balkwill, D., Davidson, M., and Onstott, T. C.: In situ enrichment of a diverse community of bacteria from a 4–5 km deep fault zone in South Africa, *Geomicrobiol. J.*, 23, 463–473, 2006.
- Ulrych, J., Krmíček, L., Tomek, Č., Lloyd, F. E., Ladenberger A., Ackerman, L., and Balogh, K.: Petrogenesis of Miocene alkaline volcanic suites from western Bohemia: whole rock geochemistry and Sr–Nd–Pb isotopic signatures, *Chem. Erde-Geochem.*, 76, 77–93, 2016.
- Vandemeulebrouck, J., Roux, P., Gouédard, P., Legaz, A., Revil, A., Hurst, A. W., Bolève, A., and Jardani, A.: Application of acoustic noise and self-potential localization techniques to a buried hydrothermal vent (Waimangu Old Geyser site, New Zealand), *Geophys. J. Int.*, 180, 883–890, 2010.
- Wagner, C., Mau, M., Schloemann, M., Heinicke, J., and Koch, U.: Characterization of the bacterial flora in mineral waters in upstreaming fluids of deep igneous rock aquifers, *J. Geophys. Res.*, 112, G01003, <https://doi.org/10.1029/2005JG000105>, 2007.
- Youssef, N., Elshahed, M. S., and McInerney, M. J.: Chapter 6 Microbial processes in oil fields: culprits, problems, and opportunities, in: *Advances in Applied Microbiology*, edited by: Allen, S. S., Laskin, I., and Geoffrey, M. G., Academic Press, 141–251, 2009.
- Zhang, G., Dong, H., Xu, Z., Zhao, D., and Zhang, C.: Microbial diversity in ultra-high-pressure rocks and fluids from the Chinese Continental Scientific Drilling Project in China, *Appl. Environ. Microbiol.*, 71, 3213–3227, 2005.



Design and deployment of autoclave pressure vessels for the portable deep-sea drill rig MeBo (*Meeresboden-Bohrgerät*)

Thomas Pape^{1,2}, Hans-Jürgen Hohnberg^{2,3}, David Wunsch³, Erik Anders³, Tim Freudenthal²,
Katrin Huhn², and Gerhard Bohrmann^{1,2}

¹Department of Geosciences at the University of Bremen, Klagenfurter Str. 4, 28359 Bremen, Germany

²MARUM – Center for Marine Environmental Sciences at the University of Bremen, Leobener Str. 8, 28359
Bremen, Germany

³Corsyde International GmbH & CO. KG, Reuchlinstr. 10–11, 10553 Berlin, Germany

Correspondence to: Thomas Pape (tpape@marum.de)

Received: 22 January 2017 – Revised: 27 April 2017 – Accepted: 8 May 2017 – Published: 30 November 2017

Abstract. Pressure barrels for sampling and preservation of submarine sediments under in situ pressure with the robotic sea-floor drill rig MeBo (*Meeresboden-Bohrgerät*) housed at the MARUM (Bremen, Germany) were developed. Deployments of the so-called “MDP” (MeBo pressure vessel) during two offshore expeditions off New Zealand and off Spitsbergen, Norway, resulted in the recovery of sediment cores with pressure stages equaling in situ hydrostatic pressure. While initially designed for the quantification of gas and gas-hydrate contents in submarine sediments, the MDP also allows for analysis of the sediments under in situ pressure with methods typically applied by researchers from other scientific fields (geotechnics, sedimentology, microbiology, etc.). Here we report on the design and operational procedure of the MDP and demonstrate full functionality by presenting the first results from pressure-core degassing and molecular gas analysis.

1 Introduction

Pressure coring is currently the only method that enables precise off-site analysis of gas and gas hydrate volumes contained in marine sediments. Because the manufacture of pressure-coring tools and their operational application are technically challenging, pressure vessels have only been in use for the last few decades. A review of pressure-coring systems used for offshore research from various platforms in the past and today is presented elsewhere (Abid et al., 2015 and references cited therein). These include the Dynamic Autoclave Piston Corer (DAPC) which is frequently in use for pressure coring of shallow (down to 2.65 m below the sea floor, hereafter m b.s.f.) gas-hydrate-bearing sediments at the MARUM – Center for Marine Environmental Sciences since the early 2000s (e.g., Abegg et al., 2008; Heeschen et al., 2007; Pape et al., 2011a).

In 2005, the sea-floor drill rig MARUM-MeBo70 (acronym for *Meeresboden-Bohrgerät*, German for sea-floor

drill rig), initially designed to obtain non-pressurized sediment cores from a depth of up to 70 m b.s.f., was operated for the first time (Freudenthal and Wefer, 2007, 2013). MeBo70 is a robotic drill remotely controlled from conventional research vessels via an umbilical cable that allows for sampling of the sea bed by push core or rotary core drilling. Compared to those of drilling vessels, the advantages of sea-floor drill rigs are optimal control over the drilling process at the sea floor, great flexibility in use from various vessels, and time and cost efficiency. For lowering sampling tools and measurement devices into the well, the comparably fast wireline drilling technique is used (Freudenthal and Wefer, 2013). In 2014 the second MeBo generation, MARUM-MeBo200, which allows core drillings to be conducted down to 200 m b.s.f. by means of wireline technology, was additionally taken into use. Gas-hydrate-bearing sediments from depths exceeding 10 m b.s.f. in the eastern Black Sea (unpublished data) and in the Gulf of Guinea (Sultan et al., 2014; Wei et al., 2015) were recovered in 2011 with MeBo70 for

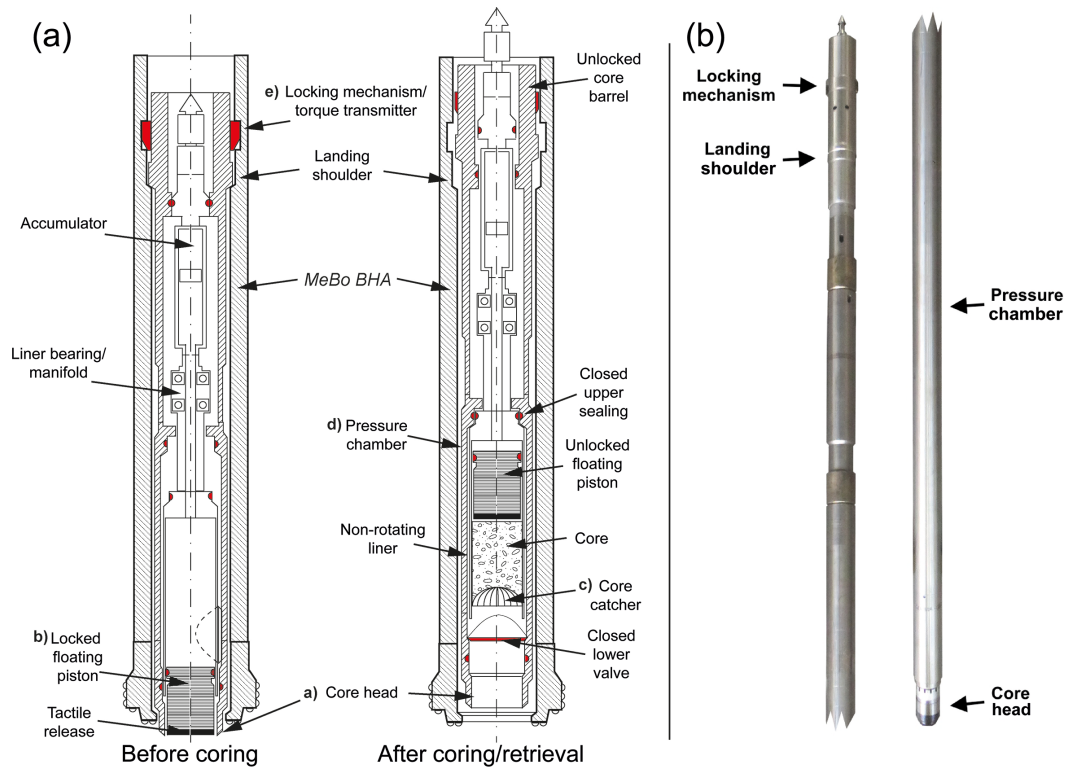


Figure 1. (a) Scheme and working principle of the MeBo pressure vessel (MDP; not in scale). BHA = bottom hole assembly. (b) Photograph of the MDP (left: top part; right: bottom part).

qualitative analysis. However, during both sampling campaigns, sediments below the maximum penetration depth of the DAPC eluded analysis of accurate gas volumes since appropriate techniques were unavailable.

Recently, a pressure-core barrel has been developed within the German collaborative project “SUGAR” for use with both systems, MeBo70 and MeBo200. The pressure-core barrel, called MDP (German for *MeBo-Druckkern-Probennnehmer*), is employed like a wireline inner core barrel. Pressure coring with the MDP was successfully carried out during two subsequent deep-sea cruises with MeBo200 (east of New Zealand) and MeBo70 (west of Spitsbergen) in 2016. Hence, a system is now available that allows for the recovery of pressurized sediment cores with both MeBo systems and for subsequent quantitative sampling of gas from these. Here we report on the design and deployment of the MDP and demonstrate their complete functionality by presenting first results from pressure coring and pressure-core processing.

2 Design and deployment

2.1 Design, specifications, and operational procedure

The MDP principally consists of (a) a cutting shoe or core head cutting the sediment core with the required core diameter, (b) a floating piston using hydrostatic pressure to force

the penetration of the sediment core into the core barrel, (c) a core catcher that inhibits loss of sediment before the valve is closed, (d) a pressure housing and a valve that closes after the coring process in order to keep the in situ pressure within the core barrel, and (e) a latching device that ensures the correct position of the pressure-core barrel within the MeBo drill string and that activates the closing of the valve when the core barrel is pulled with an “overshot” using the wire-line technique (Fig. 1). Titanium was used to manufacture all pressure-holding parts, which facilitates future imaging of pressurized sediment cores by computerized tomography.

As a consequence of required implementations of several activation and lifting mechanisms, the MDP core barrel has a shorter length and a smaller diameter compared to conventional MeBo core barrels (Table 1), resulting in a smaller liner volume. In order to support sediment intrusion into the liner, a piston system has been developed which allows the cutting of a core that has a relatively small diameter compared to the borehole diameter. This system is based on using the physical principle of the increasing hydrostatic pressure when lowering the MeBo from the vessel to the sea floor. A sealed atmosphere within the MDP generates a differential pressure, which at the time of coring drives the piston upwards with the relative downward movement of the drill string. Usage of the differential pressure to support sediment intrusion while coring soft sediments is a unique method

Table 1. Specifications of the conventional core barrels and the MDP operated with MeBo70 or MeBo200.

Specification		Conventional barrel – MeBo70/MeBo200	MDP – MeBo70/MeBo200
Barrel outer diameter	(mm)	73/73	73/73
Barrel length, approx.	(mm)	3400/4300	3400/4300
Core diameter	(mm)	55/55	45/45
Maximum core length	(mm)	2500/3500	1300/1300
Maximum core volume	(L)	5.94/8.32	2.07/2.07
Operating pressure	(MPa)	n/a / n/a	20/20

n/a = not applicable

(Hohnberg, 2010, patent pending). The piston is locked mechanically before operation and released when a touch sensor strikes the sediment at the drill-hole bottom at the beginning of the coring process. During coring the piston is driven upwards by the hydrostatic pressure at the depth of the borehole. This procedure allows the application of a drilling speed that is higher than that of conventional corers and supports receipt of high-quality cores with comparably high recovery rates (see Sect. 3.2). It adopts the advantages of piston coring but minimizes the adverse impact on the recoverable core-length-to-tool-length ratio. A damping system positioned above the piston regulates the raising velocity of both the piston and the incoming sediment core. After the core has been cut, the overshot is lowered into the drill string in the same way as in the recovery procedure of conventional MeBo core barrels. Once the overshot is latched onto the MDP locking mechanism, the wireline is pulled. Before unlocking the MDP the sealing mechanisms are released by an additional axial lift in the upper part of the tool. Closing of valves at the top and the bottom section of the pressure chamber assures pressure-tight recovery of the core under near in situ pressure. Furthermore, a special pre-configured accumulator is activated in order to compensate for potential changes in pressure due to temperature fluctuations throughout the recovery process and to ensure pressure tightness of the system, thus preserving near in situ pressure during recovery and storage. During pre-configuration the internal pressure of the accumulator is adjusted to as close to the hydrostatic down-hole pressure as possible. A significant higher initial pressure (“overcharge”) should be avoided since it lasts on the core and may lead to sample alteration and misinterpretations of core properties.

2.2 Deployments and operations with MeBo200 and MeBo70

The MDPs were successfully deployed, with both MeBo200 and MeBo70, during two campaigns in deep-sea areas in 2016. Cruise SO247 with the German RV *Sonne* in spring 2016 off New Zealand (Huhn, 2016) provided excellent opportunities for trial-and-error tests and to adjust the MDP for pressure coring with MeBo200 within sediments consid-

ered to partially host gas hydrates (see Table A1 in the Appendix for core specifications). During that cruise the capability to achieve excellent core recovery rates as well as pressure cores with the MDPs was proven (see Sect. 3). MDP coring was additionally performed during cruise MSM57/1 with RV *Maria S. Merian* in summer 2016 off Spitsbergen (Bohrmann et al., 2017). Before deployment parts of the MDPs were modified after consideration of the test results of drillings conducted during SO247 and of technical requirements for usage with MeBo70. During MSM57/1, MDPs were used three times at two sites (Table A1 in the Appendix). While MeBo station GeoB21613-1 was carried out at a reference site expected to be virtually devoid of gas hydrates, GeoB21616-2 was performed within an active pocket and assumed to contain gas hydrates.

2.3 Handling of MDP core barrel after recovery and core processing

After the MeBo has been recovered and the MDPs were removed from the magazine, mechanical components above and below the pressure chamber were disassembled in order to make the MDP’s pressure-bearing parts accessible. An assembly of gas-tight valves and ports (modified after Dickens et al., 2003; Heeschen et al., 2007; and Shipboard Scientific Party, 1996) and a pressure sensor for continuous monitoring of the internal pressure were connected to the MDP pressure chamber. During cruise MSM57/1, pressurized fluid (gas and water) was released incrementally from the pressure chamber into a gas-tight, scaled syringe for gas sub-sampling and determinations of fluid volumes. Quantification of released fluids was carried out on-deck at atmospheric pressure and ambient temperature (ca. 2 to 6 °C).

Repeatedly, after release of a certain gas volume, gas sub-samples were taken and transferred into glass serum vials for analysis of molecular compositions (C₁–C₆ hydrocarbons, N₂, O₂, Ar; Pape et al., 2010a). Subsequent to degassing (when pressure inside the pressure chamber has dropped to atmospheric pressure), the core liner containing the depressurized sediment core was removed from the pressure chamber through the lower valve. Since the technical principle of the MDP does not comprise a transparent core liner for

subsequent core description, the sediment core needed to be transferred into a suitable liner. A piston system was used to push the core into a liner in a sliding motion. Finally, the core was processed like a conventional core (e.g., through splitting, lithological description, photography, and storage).

3 Results and discussion

The main objectives of the MDP deployments during SO247 were to identify best practice and settings for MDP pressure coring, to technically meet the requirements of both MeBo systems (MeBo70 and MeBo200), and to fit for accomplishing the main goals of cruise MSM57/1. The major objectives of that cruise were to recover cores under pressure and to subsequently carry out a controlled pressure reduction. This degassing procedure would allow for a quantitative determination of the gas in situ amount, which is largely lost when a core is recovered by conventional means.

3.1 Proof of functionality – deep-water deployments

MDPs have been deployed with MeBo200 during SO247 nine times and with MeBo70 three times during MSM57/1 (Fig. 2, Table A1 in Appendix). During SO247, recovery rates with the MDP of more than 82 % were obtained during five deployments, of which two exceeded 97 %. Virtually no sediments were recovered during two deployments only.

Two pressurized samples (GeoB20802-6 (2P): sediment core (99 % recovery rate) and GeoB20846-1 (13P): fluid sample from overconsolidated silt section) were received during SO247, both with pressure higher than in situ values (Fig. 2). Although quantitative degassing of the pressure core GeoB20802-6 (2P) could not be executed properly due to technical issues, the two main technical aspects of the MDP (piston coring, preservation of in situ pressure) have been proven to work during SO247. It should be pointed out that the deepest sediments at stations GeoB20803-2, 20824-4, 20831-3, and 20846-1 were collected with the MDP.

During and after cruise SO247, an intense evaluation of the MDP system with regard to core recovery and operation was carried out. Modifications on the sealing concept, the lifting and unlocking mechanisms, and the downstream degassing procedures as well as minor changes of the floating piston led to improvements in handling and operation of the pressure-core barrel and in core analysis. The improvements resulted in an increase of the core barrel's overall reliability and performance, which has been proven throughout MSM57/1 (Fig. 2). Standardized procedures and comprehensive documentation enabled repeated deployment of the MDP on a routine basis. This will facilitate to establish the MDP deployments as a “near conventional” operation in MeBo coring.

During MSM57/1, MDPs have been deployed three times with MeBo70 (Table A1, Appendix). During all operations pressurized samples (two sediment cores and one fluid sam-

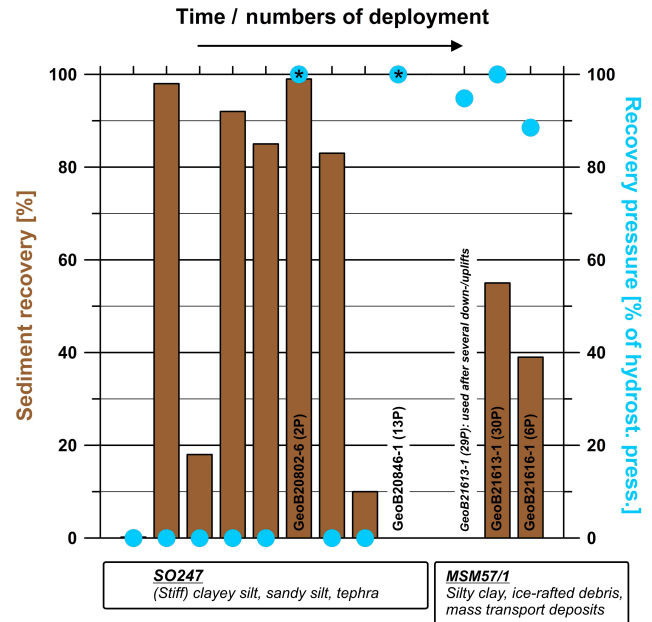


Figure 2. Overview of sediment recovery rates (in percentage of liner volume) and recovery pressure (in percentage of hydrostatic pressure at the drill site) obtained in the course of MDP deployments and modifications during cruises SO247 and MSM57/1. * = Pressure inside pressure vessel higher than hydrostatic pressure due to initial overcharge by the pressure accumulator. Specifications of drill sites are provided in Table A1 in the Appendix.

ple) were recovered. The average sediment recovery of the two pressurized sediment cores was 47.0 %. The deepest sediments at stations GeoB21613-1 and 21616-1 were collected with MDPs (sections 30P and 6P, respectively). The lack of sediment in barrel GeoB21613-1 (29P), which was initially prepared for operation during preceding stations, most likely resulted from a technical malfunction of the piston system. This was probably caused by periodically changing pressure regimes over the course of four lowerings and three liftings of MeBo before final deployment of the MDP.

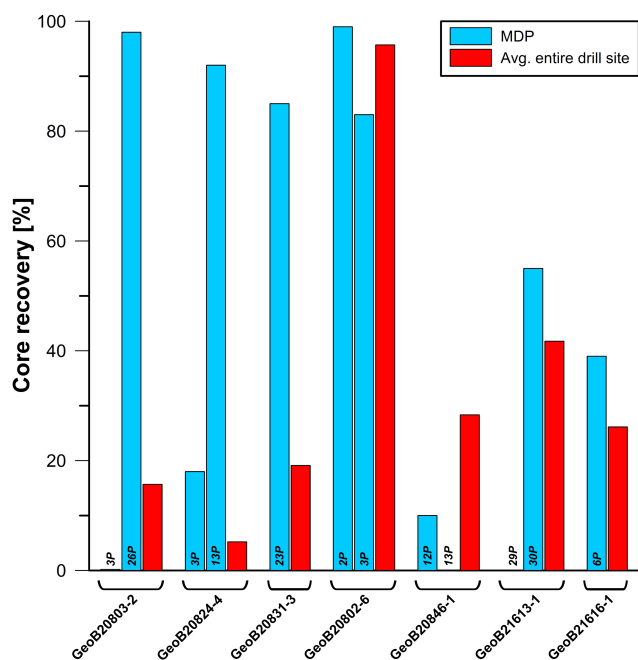
3.2 Core recoveries

Except for single MDPs at three sites (GeoB20803-2 (3P), 20802-6 (3P), and 21613-1 (29P)) and both MDPs recovered from site GeoB20846-1, core recoveries with the MDP exceeded average recoveries calculated for all barrels (conventional core barrels plus MDP) retrieved from that site (Fig. 3).

These results suggest that the floating piston system of the MDP supports the core intrusion process and, thus, leads to a relatively higher core recovery. However, since different sediment properties and drilling parameters might have affected core recoveries, further investigations are required to evaluate the overall functionality of the MDP piston system.

Table 2. Degassing characteristics of pressure cores (total fluid volume = total water volume + total gas volume).

GeoB	Section no.	Core length mm	Core volume L	Total water volume released L	Total gas volume released L	Total fluid volume released L	Volumetric fluid – sediment ratio LL^{-1}
MSM57/1							
21613-1	30P	550	0.8747	0.646	0.511	1.157	1.323
21616-1	6P	390	0.6203	0.249	0.351	0.600	0.967

**Figure 3.** Comparative overview of average core recovery rates at individual drill sites (considering conventional core barrels and MDP, in red) and recovery rates of single MDPs at same drill sites (in blue).

3.3 Degassing of MDP cores

Both pressure cores obtained during MSM57/1 were degassed quantitatively while the evolution of pressure inside the MDP pressure chamber was recorded (Fig. 4). Degassing characteristics of these cores are given in Table 2.

For both pressure cores degassed during MSM57/1, a slight saw-tooth-like shape of the pressure-time profile was observed at the initial stage of incremental gas removal (time span ca. 5–40 min). This pattern has been attributed to the presence of gas hydrates in earlier studies (e.g., Dickens et al., 2000, 2003). However, fluid-to-sediment ratios of ca. 1.3 and 1.0 LL^{-1} (Table 2), are low compared to those in gas-hydrate-bearing sediment cores (e.g., Pape et al., 2010b, 2011a, b) and do not support the presence of hydrates in these cores. Instead, temporal small-scale pressure increases dur-

ing core degassing may be attributed to sudden formation of migration pathways.

Analysis of molecular composition demonstrated that gas released from 30P nearly exclusively consisted of light hydrocarbons, which predominantly originate from thermocatalysis of organic matter in the deep subsurface ($C_1 / (C_2 + C_3) = 253$; Whiticar, 1999, Table 3). In contrast, nitrogen, oxygen, and argon were found in relatively high portions in the gas released from core GeoB21616-1 (6P). The presence of these components in the released gas was most likely due to atmospheric air that is generally required for the functionality of the MDP piston system and might be partially trapped inside the pressure chamber. Air is meant to be quantitatively released prior to the sealing of the pressure vessel, but residual amounts may still remain inside. Nevertheless, molecular compositions clearly showed that microbial hydrocarbons ($C_1 / (C_2 + C_3) = 1000$) were prevailing at that depth. Void gas samples prepared from shallower sediments recovered with conventional MeBo barrels at both sites showed very similar molecular hydrocarbon compositions (data not shown), thus demonstrating the high quality of the gas obtained with the MDP. Preliminary calculations considering fluid volumes released during degassing, methane percentage in the fluid, and assumed sediment pore volume in the core suggest that the released methane exclusively resulted from exsolution caused by pressure reduction.

The results obtained during MSM57/1 substantiate that pressure vessels with full functionality are now available for the sea-floor drill rigs MeBo70 and MeBo200.

4 Conclusions and perspectives

Pressure vessels that enable sampling of deep-sea sediments under hydrostatic pressure with the sea-floor drill rigs MeBo70 and MeBo200 were successfully deployed during two cruises in 2016. Core recovery rates usually exceeded those of the conventional corers and core preservation under pressure was achieved for three cores. Successful quantitative degassing and the quality of light hydrocarbons originating from processes in the subsurface clearly demonstrate that the MeBo pressure vessels are now suitable for routine operations.

The MDPs were mainly designed for the recovery and preservation of gas-hydrate-bearing sediments and also for

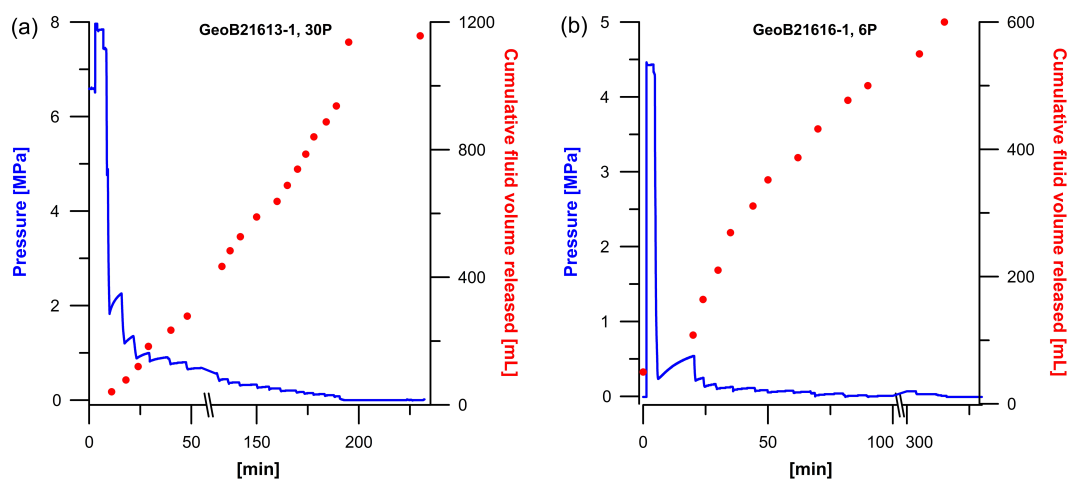


Figure 4. Degassing characteristics of two pressurized sediment cores collected with MeBo70 during cruise MSM57/1. **(a)** Pressure and cumulative fluid volume released vs. time during degassing of section GeoB21613-1 (30P). **(b)** Pressure and cumulative fluid volume released vs. time during degassing of section GeoB21616-1 (6P).

Table 3. Average molecular composition of gas released from pressure cores during MSM57/1 (100 mol % = all volatiles stated).

GeoB	Section no.	CH ₄	C ₂ H ₆	C ₃ H ₈	C ₁ / (C ₂ + C ₃)	N ₂	O ₂ + Ar
21613-1	30P	79.88	0.31	0.01	253.0	16.58	3.23
21616-1	6P	43.92	0.04	b.d.l.	1000.0	46.59	9.45

b.d.l. = below detection limit (<0.005 mol %)

the precise determination of true gas amounts. However, comparably low volumetric gas–sediment ratios obtained from pressurized cores so far show that the MDPs are not only applicable for the retrieval of gas and gas-hydrate-rich sediments but are also appropriate for collecting sediments hosting relatively small gas amounts.

Relevant components of the MDP were manufactured from titanium, which allows for the scanning of undisturbed pressure cores with non-destructive techniques (e.g., with X-rays, gamma rays, sonic waves) during future operations, as has already been done on cores retrieved with other pressure-coring tools (e.g., Riedel et al., 2006; Suzuki et al., 2015). In addition, a MDP subsampling and transfer system will enable segmentation of pressure cores and storage of core segments in smaller pressure cells for the analysis in spatially high resolution and further processing methods in the future.

Appendix A

Table A1. Overview of sections cored with MDP during SO247 (MeBo200) and MSM57/1 (MeBo70) (in chronological order). Further information on cores collected during the cruises are provided in the cruise reports (Huhn, 2016; Bohrmann et al., 2017).

Station GeoB (section no.)	Latitude (° S)	Longitude (° E)	Water depth (m)	Core top depth (m b.s.f.)	Core bottom depth (m b.s.f.)	Sediment recovery (%)	Recovery pressure (MPa)	Remarks
20803-2 (3P)	38°49.19' S	178°27.86' E	670	7.40	8.70	0.2	0.00	clayey silt
20803-2 (26P)	38°49.19' S	178°27.86' E	670	80.90	82.20	98.0	0.00	clay-rich silt
20824-4 (3P)	40°2.04' S	178°9.71' E	670	7.40	8.70	18.0	0.00	overconsolidated silt
20824-4 (13P)	40°2.04' S	178°9.71' E	670	35.40	36.70	92.0	0.00	overconsolidated silt
20831-3 (23P)	38°49.77' S	178°28.56' E	718	77.40	78.70	85.0	0.00	clayey silt
20802-6 (2P)	38°45.93' S	178°29.01' E	546	23.15	24.20	99.0	11.9*	clayey silt
20802-6 (3P)	38°45.93' S	178°29.01' E	546	24.20	24.90	83.0	0.00	clayey silt
20846-1 (12P)	40°01.50' S	178°10.70' E	550	38.90	40.00	10.0	0.00	overconsolidated silt and tephra
20846-1 (13P)	40°01.50' S	178°10.70' E	550	40.00	41.00	0.0	9.93*	overconsolidated silt and tephra
average						53.9		
21613-1 (29P)	78°59.81' N	6°57.81' E	1200	60.30	61.40	0.0	11.38	Deployed after several down- and uplifts of the tool
21613-1 (30P)	78°59.81' N	6°57.81' E	1200	61.40	62.50	55.0	12.00	silty clay
21616-1 (6P)	79°00.42' N	6°54.25' E	1210	12.80	13.90	39.0	10.71	clay
average						31.3		

* Pressure inside pressure vessel higher than hydrostatic pressure due to an initial overcharge by the activated accumulator.

Data availability. All data reported are made publicly available through the PANGAEA information system (Data Publisher for Earth and Environmental Science) sustained by the World Data Center for Marine Environmental Sciences (WDC-MARE). Data from research cruises SO247 and MSM57/1 are publicly accessible through the PANGAEA information system via <https://www.pangaea.de/expeditions/cr.php/Merian> and https://www.pangaea.de/expeditions/cr.php/Sonne_2014.

Author contributions. TP conducted degassing experiments with the MDP during cruises SO247 and MSM57/1. HJH designed, built, and modified MDP, tested them in the lab and during cruises with MeBo in 2011, prepared MDP for deployment during SO247, and proposed drill parameters. DW prepared MDP for deployment during SO247 and MSM57/1 and proposed drill parameters. EA participated in lab tests of MDP and designed technical modifications. TF supervised drilling procedures with MDP and MeBo and proposed drill parameters. KH led cruise SO247 and proposed MDP deployment depths. GB proposed development of pressure vessels for the deep-sea drill rig MeBo within the German gas-hydrate-related project SUGAR, led cruise MSM57/1, and proposed MDP deployment depths. TP prepared the paper with contributions from all co-authors.

Competing interests. The authors declare that they have no conflict of interest.

Acknowledgements. Masters and crews of SO247 and MSM57/1 as well as the MeBo teams are greatly acknowledged for their excellent support during the field campaigns. We are very grateful to the co-chief scientist of SO247, N. Kukowski, Friedrich Schiller University Jena, Germany, for providing opportunities to deploy the MeBo pressure vessels (MDPs). The authors wish to thank Andrew Wright (Geoquip Marine Operations AG), Koji Yamamoto (Technology and Research Center, Japan Oil, Gas and Metals National Corporation; JOGMEC), and the handling editor of the journal, Thomas Wiersberg, for their constructive comments on this manuscript. Design and development of the MDPs were funded by the German Federal Ministry for Economic Affairs and Energy through the collaborative project SUGAR (Submarine Gas hydrate Resources; 03SX250B).

Edited by: T. Wiersberg

Reviewed by: K. Yamamoto and A. Wright

References

Abegg, F., Hohnberg, H.-J., Pape, T., Bohrmann, G., and Freitag, J.: Development and application of pressure-core-sampling systems for the investigation of gas- and gas-hydrate-bearing sediments, *Deep-Sea Res. Pt. I*, 55, 1590–1599, <https://doi.org/10.1016/j.dsr.2008.06.006>, 2008.

Abid, K., Spagnoli, G., Teodoriu, C., and Falcone, G.: Review of pressure coring systems for offshore gas hydrates research, *Underwater Technol.*, 33, 19–30, <https://doi.org/10.3723/ut.33.019>, 2015.

Bohrmann, G. and cruise participants: R/V MARIA S. MERIAN Cruise Report MSM57, Gas Hydrate Dynamics at the Continental Margin of Svalbard, Reykjavik – Longyearbyen – Reykjavik, 29 July–7 September 2016, 204 pp., available at: <http://elib.suub.uni-bremen.de/edocs/00105895-1.pdf>, 2017.

Dickens, G. R., Wallace, P. J., Paull, C. K., and Borowski, W. S.: Detection of methane gas hydrate in the pressure core sampler (PCS): Volume-pressure-time relations during controlled degassing experiments, in: *Proc. ODP, Sci. Res.*, edited by: Paull, C. K., Matsumoto, R., Wallace, P. J., and Dillon, W. P., College Station, TX (Ocean Drilling Program), 113–126, <https://doi.org/10.2973/odp.proc.sr.164.210.2000>, 2000.

Dickens, G. R., Schroeder, D., Hinrichs, K.-U., and the Leg 201 Scientific Party: The pressure core sampler (PCS) on ODP Leg 201: General operations and gas release, in: *Proc. ODP, Init. Repts.*, edited by: D'Hondt, S. L., Jørgensen, B. B., Miller, D. J., et al., 201: College Station, TX (Ocean Drilling Program), 1–22, <https://doi.org/10.2973/odp.proc.ir.201.103.2003>, 2003.

Freudenthal, T. and Wefer, G.: Scientific Drilling with the Sea Floor Drill Rig MeBo, *Sci. Drill.*, 5, 63–66, <https://doi.org/10.2204/iodp.sd.5.11.2007>, 2007.

Freudenthal, T. and Wefer, G.: Drilling cores on the sea floor with the remote-controlled sea floor drilling rig MeBo, *Geosci. Instrum. Method. Data Syst.*, 2, 329–337, <https://doi.org/10.5194/gi-2-329-2013>, 2013.

Heeschen, K. U., Hohnberg, H. J., Haeckel, M., Abegg, F., Drews, M., and Bohrmann, G.: In situ hydrocarbon concentrations from pressurized cores in surface sediments, Northern Gulf of Mexico, *Mar. Chem.*, 107, 498–515, <https://doi.org/10.1016/j.marchem.2007.08.008>, 2007.

Hohnberg, H.-J.: Kernbohrtechnische Vorrichtung für die Unterstützung der Beprobung von Sedimenten mit Kernbohrgeräten am Bohrlochgrund von Bohrungen bei überdeckenden statischen Flüssigkeitsdrücken, wie z.B. in der Tiefsee, German Patent and Trade Mark Office (DPMA), Application number 102008049795 A1, 2010.

Huhn, K.: Cruise Report / Fahrtbericht SO247 – SlamZ: Slide activity on the Hikurangi margin, New Zealand, Wellington (NZ): 27 March 2016 – Auckland (NZ): 27 April 2016, MARUM, Center for Marine Environmental Sciences, University of Bremen, 119 pp., https://doi.org/10.2312/cr_so247, 2016.

Pape, T., Bahr, A., Rethemeyer, J., Kessler, J. D., Sahling, H., Hinrichs, K.-U., Klapp, S. A., Reeburgh, W. S., and Bohrmann, G.: Molecular and isotopic partitioning of low-molecular weight hydrocarbons during migration and gas hydrate precipitation in deposits of a high-flux seepage site, *Chem. Geol.*, 269, 350–363, <https://doi.org/10.1016/j.chemgeo.2009.10.009>, 2010a.

Pape, T., Kasten, S., Zabel, M., Bahr, A., Abegg, F., Hohnberg, H.-J., and Bohrmann, G.: Gas hydrates in shallow deposits of the Amsterdam mud volcano, Anaximander Mountains, Northeastern Mediterranean Sea, *Geo-Mar. Lett.*, 30, 187–206, <https://doi.org/10.1007/s00367-010-0197-8>, 2010b.

Pape, T., Bahr, A., Klapp, S. A., Abegg, F., and Bohrmann, G.: High-intensity gas seepage causes rafting of shallow gas hydrates in the southeastern Black Sea, *Earth. Planet. Sc. Lett.*, 307, 35–46, <https://doi.org/10.1016/j.epsl.2011.04.030>, 2011a.

- Pape, T., Feseker, T., Kasten, S., Fischer, D., and Bohrmann, G.: Distribution and abundance of gas hydrates in near-surface deposits of the Håkon Mosby Mud Volcano, SW Barents Sea, *Geochem. Geophys. Geosy.*, 12, Q09009, <https://doi.org/10.1029/2011gc003575>, 2011b.
- Riedel, M., Collett, T. S., Malone, M. J., and Expedition 311 Scientists: Expedition 311 Summary. *Proc. IODP*, 311: Washington, DC (Integrated Ocean Drilling Program Management International, Inc.), <https://doi.org/10.2204/iodp.proc.311.101.2006>, 2006.
- Shipboard Scientific Party: Explanatory notes, in: *Proc. ODP, Init. Repts.*, 164, edited by: Paull, C. K., Matsumoto, R., Wallace, P. J., et al., College Station, TX (Ocean Drilling Program), 13–41, <https://doi.org/10.2973/odp.proc.ir.164.102.1996>, 1996.
- Sultan, N., Bohrmann, G., Ruffine, L., Pape, T., Riboulot, V., Colliat, J.-L., De Prunelé, A., Dennielou, B., Garziglia, S., Himmler, T., Marsset, T., Peters, C. A., Rabiou, A., and Wei, J.: Pockmark formation and evolution in deepwater Nigeria: Rapid hydrate growth versus slow hydrate dissolution, *J. Geophys. Res.-Sol. Ea.*, 119, 2679–2694, <https://doi.org/10.1002/2013JB010546>, 2014.
- Suzuki, K., Schultheiss, P., Nakatsuka, Y., Ito, T., Egawa, K., Holland, M., and Yamamoto, K.: Physical properties and sedimentological features of hydrate-bearing samples recovered from the first gas hydrate production test site on Daini-Atsumi Knoll around eastern Nankai Trough, *Mar. Pet. Geol.*, 66, 346–357, <https://doi.org/10.1016/j.marpetgeo.2015.02.025>, 2015.
- Wei, J., Pape, T., Sultan, N., Colliat, J.-L., Himmler, T., Ruffine, L., de Prunelé, A., Dennielou, B., Garziglia, S., Marsset, T., Peters, C. A., Rabiou, A., and Bohrmann, G.: Gas hydrate distributions in sediments of pockmarks from the Nigerian margin – Results and interpretation from shallow drilling, *Mar. Pet. Geol.*, 59, 359–370, <https://doi.org/10.1016/j.marpetgeo.2014.09.013>, 2015.
- Whiticar, M. J.: Carbon and hydrogen isotope systematics of bacterial formation and oxidation of methane, *Chem. Geol.*, 161, 291–314, [https://doi.org/10.1016/S0009-2541\(99\)00092-3](https://doi.org/10.1016/S0009-2541(99)00092-3), 1999.



Contamination tracer testing with seabed drills: IODP Expedition 357

Beth N. Orcutt¹, Markus Bergenthal², Tim Freudenthal², David Smith³, Marvin D. Lilley⁴,
Luzie Schnieders², Sophie Green³, and Gretchen L. Früh-Green⁵

¹Bigelow Laboratory for Ocean Sciences, East Boothbay, ME 04544, USA

²MARUM, University of Bremen, 28334 Bremen, Germany

³British Geological Survey, The Lyell Centre, Edinburgh, EH14 4AP, Scotland, UK

⁴School of Oceanography, University of Washington, Seattle, WA 98195, USA

⁵Institute for Geochemistry and Petrology, ETH Zürich, 8092 Zürich, Switzerland

Correspondence to: Beth N. Orcutt (borcutt@bigelow.org)

Received: 5 July 2017 – Revised: 18 August 2017 – Accepted: 22 August 2017 – Published: 30 November 2017

Abstract. IODP Expedition 357 utilized seabed drills for the first time in the history of the ocean drilling program, with the aim of collecting intact sequences of shallow mantle core from the Atlantis Massif to examine serpentinization processes and the deep biosphere. This novel drilling approach required the development of a new remote seafloor system for delivering synthetic tracers during drilling to assess for possible sample contamination. Here, we describe this new tracer delivery system, assess the performance of the system during the expedition, provide an overview of the quality of the core samples collected for deep biosphere investigations based on tracer concentrations, and make recommendations for future applications of the system.

1 Introduction

IODP Expedition 357 “Atlantis Massif Serpentinization and Life” aimed to collect intact sequences of shallow mantle core for examining serpentinization and deep biosphere processes (Früh-Green et al., 2015, 2016). As such, collection of high-quality core material for geochemical and microbiological analysis was a priority, and methods for assessing the quality of the core material were needed. The use of synthetic tracers in drilling fluids to monitor for potential contamination of drill core samples for microbiological analysis has become fairly routine during microbiology-focused expeditions (Inagaki et al., 2015; Lever et al., 2006, 2013; Smith et al., 2000; Friese et al., 2017; Sauvage et al., 2016). Perfluoromethylcyclohexane (PFC) has been identified as an ideal tracer because of the large range of concentrations that are detectable (i.e., across 6 orders of magnitude) with a gas chromatograph equipped with an electron capture detector (GC-ECD) (Smith et al., 2000; Lever et al., 2006; Sauvage et al., 2016). Recent reports have also demonstrated the use of other fluorescent solutions (Friese et al., 2017; Kallmeyer, 2017). Particulate tracers, such as fluorescent beads, are used

less frequently due to problems with dispersion, dilution, and false negatives (Lever et al., 2006; Smith et al., 2000).

During seafloor drilling with a drillship such as the JOIDES Resolution or Chikyu, drilling fluids (muds) are prepared at the sea surface and injected into the drill pipe, and the concentration of PFC tracer delivered into the flush water can be closely monitored and adjusted to reach saturating conditions (roughly 1 mg L^{-1}), as described in detail elsewhere (Sauvage et al., 2016; Lever et al., 2006). Similar approaches were also recently used for platform drilling in the relatively shallow waters of the Baltic Sea on IODP Expedition 347, where PFC tracer was added to drilling muds at the platform prior to injection into the borehole (Andrén et al., 2015).

In contrast, seabed drills are remote drilling platforms that directly use bottom seawater as flushing fluid, without addition of muds or fluid connection to the surface (Freudenthal and Wefer, 2007). Therefore, in order to use PFC tracers for contamination testing with seabed drills, a new system was required for delivery of PFC tracer into the drill rig suction line for bottom seawater being injected into the bore-

hole during seabed drilling (Früh-Green et al., 2017e). Here, we describe such a drill-independent system and how it was used during seabed drilling by two seabed drill systems – the RD2 from the British Geological Survey, and the MARUM-MeBo70 from the Center for Marine Environmental Sciences at the University of Bremen (MARUM; Germany) – during IODP Expedition 357 at the Atlantis Massif.

2 Tracer delivery system

The seabed drill tracer delivery system was designed to deliver approximately $50 \mu\text{L min}^{-1}$ of pure PFC solution (Sigma Aldrich) directly into the stream of flushing water to achieve a saturating concentration of 1 mg L^{-1} for a flushing rate of $50 \text{ L seawater min}^{-1}$. The system consists of a micro annular gear pump integrated into a filter-pump-valve module with short, direct connections for precise and reproducible dosing (Fig. 1). The pump is driven by an electric motor. The flow rate is controlled by motor speed using an S-BL programmable controller. The tracer fluid is provided within a disposable intravenous solution bag. The ON/OFF 2/2 shift valve is opened when the pump is operated, and closed in off mode to prevent the tracer from accidentally being sucked out of the reservoir in the unlikely case of under-pressure in the suction line for flush water. The electronics were housed in a one-atmosphere pressure housing. A system was mounted onto each drill and controlled from the surface via a dedicated RS232 serial communication link to the sub-sea tracer controller. The tracer solution was injected into the suction line of the drill mud pump. The flow rate of PFC delivery was adjustable from 0.015 to $5 \text{ mL PFC min}^{-1}$, and it was set at a fixed rate during each deployment (Table 1). The flushing rate on the rock drills varied throughout operations but tended to range from 20 to 50 L min^{-1} .

Pumping rates were initially calculated based on the flush rate of the drill and the required concentration of tracer to be injected into the system. However, subsea trials of the system were not possible prior to the expedition to confirm this functionality. Tests for PFC concentrations on samples obtained from the first holes revealed that the concentrations achieved were below those expected and required (as described below). Accounting for blockages in lines and long flow paths from the pump to the suction pump, pumping rates were increased to try to improve concentrations, without initial success (Table 1). One pump was then taken apart, and the internal rubber paddle, responsible for opening and closing the valve supplying the PFC tracer, was found to have swollen to almost twice the size it should have been, thus blocking supply. To evaluate this situation, a different rubber paddle was immersed in PFC tracer in controlled conditions in the laboratory to see if the swelling was an adverse reaction to the tracer itself, but there was no discernible change in size of the paddle after 24 h. Nevertheless, it is likely that this swelling was a long-term reaction of the valve rubber material in deep-

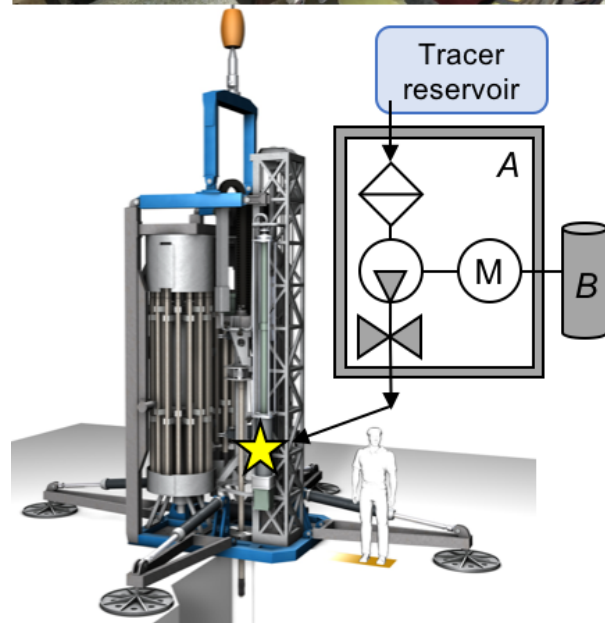
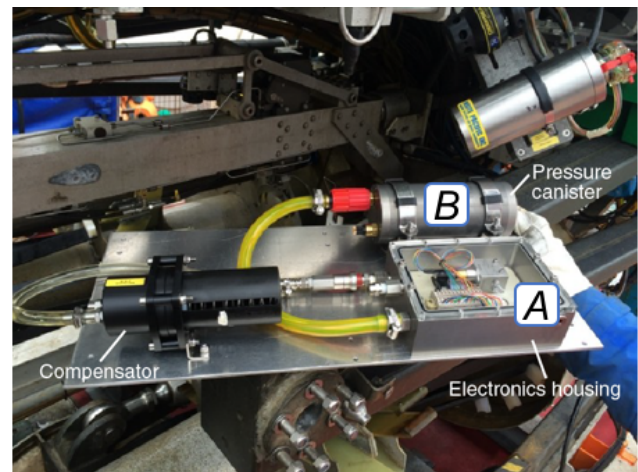


Figure 1. The drill-mounted tracer injection system during IODP Expedition 357. The top panel shows a plate on the MeBo seabed drill with the filter-pump-valve (F-P-V) module (A) in an electronics housing, pressure canister with micromotor controller (B), and oil compensator. The lower panel shows a schematic of the tracer system as mounted on the MeBo drill rig. A flexible bag with a tracer was connected to the F-P-V (A), with pumping controlled by the motor (B), to deliver the tracer to the suction and mixing chamber (star) for mixing with bottom seawater before being injected into the borehole via a displacement pump. Top panel image courtesy of Tim Freudenthal, and reproduced from Fig. F17 in Früh-Green et al. (2017e) with permission.

sea contact with either the tracer or seawater. Since the valve was only added as a safety measure to prevent uncontrolled loss of tracer during off-mode of the tracer pump, the paddle was shaved to reduce its size and allow the valve to be left in the permanently open position. Concentrations in fluid samples acquired after these changes were much improved, and

Table 1. Summary of PFC tracer system operations during IODP Expedition 357 organized by hole, including water depth in meters, drilling sequence order, drill rig, speed of delivery pump (revolutions per minute) and laboratory lower detection limits (in pg cm^{-3}) for the quantification method. ^a by drilling order number indicates deployments after the tracer delivery pump modification as described in the text. Two different detection limits for Hole 71C samples (indicated by ^b) indicates two different labs where samples were collected, with the lower value indicating the blank for the lab where sensor package and liner fluid samples were collected. Pump speeds previously reported elsewhere (Früh-Green et al., 2017e).

Hole	Water depth (m)	Drilling order	Drill rig	Pump speed	Detection limit
68A	1103	1	RD2	50	0
68B	1102	13 ^a	RD2	100	75
69A	851	2	RD2	50	0
70A	1141	3	MeBo	55	0
70B	1141	7	RD2	1500	15
70C	1141	12 ^a	MeBo	100	30
71A	1391	4	MeBo	55	20
71B	1380	11	RD2	1500	25
71C	1390	14 ^a	MeBo	50	75/500 ^b
72A	820	5	RD2	100	20
72B	820	6	RD2	100	15
73A	1430	8	MeBo	1500	15
74A	1550	17 ^a	MeBo	50	85
75A	1568	15 ^a	RD2	50	75
75B	1568	16 ^a	RD2	50	85
76A	768	9	RD2	1500	15
76B	768	10	RD2	1500	15

pumping rates for tracer injection were thus reduced to the calculated values (Table 1).

3 Tracer monitoring, sample collection, and analysis

To monitor PFC delivery during drilling operations, a variety of samples were collected from the seabed drills after drilling: core liner fluid samples, sensor package Niskin bottle samples, and exterior and interior core samples, as described in detail elsewhere (Früh-Green et al., 2017e). The sample type referred to as “liner fluid” represents a mixture of bottom water that was in the core barrel prior to being replaced by core, as well as flushing water entrained during coring. Liner fluids were collected outside on the ship deck by draining fluid from the ball valve at the top of the core prior to opening the core barrel to recover the core inside, or by draining at the lower end of the core before removing the core liner from the core barrel. In both cases, fluids were collected into a sterile 50 mL centrifuge tube, and then 10 mL of this fluid was immediately transferred to a 22 mL glass headspace vial and crimp sealed. For sensor package “Niskin water” samples, 10 mL fluid samples were collected from each of three drill-mounted Niskin bottles, which sampled the fluids flushed out of the borehole near the break-out table and bottom seawater, as described elsewhere (Früh-Green et al., 2017e). However, it is important to note that these fluid samples were often collected minutes to hours after active drilling (and flushing of the borehole) ended, so the samples likely represented a lower end-member of tracer

concentration. For shipboard core samples, when cores were transferred to the shipboard laboratory to select whole-round cores for ephemeral microbiological analyses (Früh-Green et al., 2017e), 1–5 cm^3 of core in the form of small fragments was transferred to 22 mL glass headspace vials containing 5 mL of distilled water and crimp sealed. These represented the “exterior” of the core. After flame-sterilization of the exterior surface whole-round core pieces (following the principle described elsewhere, Lever et al., 2006), “interior” samples for PFC analysis were collected in a similar manner using a flame-sterilized hammer and chisel to generate fragments from the interior of the flamed whole-round core piece. Care was taken to conduct the flame-sterilization step (which would volatilize the PFC tracer into the laboratory atmosphere) in a separate laboratory from where the samples were prepared and measured, to minimize the risk of false positives.

After shipboard collection of the above samples, the exteriors of the crimped headspace vials were rinsed with copious amounts of water, dried, and heated in a 70 °C oven for several hours prior to analysis. At the same time, a set of PFC standards was prepared under a fume hood in the same type of vial and also heated in the oven, following established tracer dilution protocols (Smith et al., 2000). It is important to note that the fume hood on the *RRS James Cook* vented into the laboratory after passing through a charcoal filter (i.e., it did not vent to the exterior of the ship), and both the oven and the GC-ECD used for analysis also vented into the room; this led to a small buildup of PFC tracer in the atmosphere of

the analysis laboratory over time. Care was taken to conduct thorough analysis of the atmospheric concentration of PFC tracer in all laboratories during analyses, both from air samples collected directly into syringes during GC-ECD analysis and from headspace vials closed in the laboratories during sample collection, to account for the possibility of false positives.

Shipboard PFC tracer analysis followed established protocols (Smith et al., 2000; Lever et al., 2006; Sauvage et al., 2016). Using a heated (70 °C) disposable plastic 3 mL syringe fitted with a two-way stopcock and a 51 mm, 22-gauge Hamilton needle, a 2 mL headspace sample from either sample or standard vials was injected into the splitless injector on Agilent 7890A GC system GC-ECD, kindly provided by Douglas Connelly of the University of Southampton. The GC-ECD was equipped with a 30 m length \times 53 μ m inner diameter \times 15 μ m coating thickness Agilent HP-AL/M column run with ultrahigh-purity nitrogen carrier gas at 4.7 psi (57 mL min⁻¹) with an initial column temperature of 120 °C for 0.5 min, followed by a 50 °C min⁻¹ ramp to 200 °C for 2.2 min. The injector temperature was set at 175 °C. Under these parameters, the PFC peak eluted at roughly 3.4 min as monitored with Agilent ChemStation Rev B.03.03 software. The concentrations of PFC tracer in samples were determined by comparing the peak area to a standard curve of peak area versus PFC tracer injected from the standards. Based on duplicate analysis of standards, the limit of detection was 2×10^{-12} g (2 pg) PFC, which is in the range of what was determined previously (Smith et al., 2000; Lever et al., 2006). Samples collected throughout the expedition were measured shipboard in batches against the same standard calibration curves. Laboratory atmosphere blanks are also reported to define lower detection limits; these values varied throughout the expedition due to buildup of volatilized tracer in the shipboard laboratory. Because of the variability in tracer pump delivery, it was not possible to convert PFC concentrations observed in the samples into the volume of flushing water potentially contaminating the core, as is commonly done. For this expedition, concentrations are reported simply as the amount of PFC tracer per volume, with PFC concentrations for samples reported in picograms PFC per cubic centimeter of sample and laboratory blanks reported as picograms PFC per milliliter air (Table 1).

In addition to shipboard assessment of tracer concentrations, frozen core samples collected for deep biosphere investigation were further subsampled for PFC tracer levels several weeks after the end of the shipboard work in shore-based laboratories (at the Kochi Core Center, Kochi, Japan, and at the Bigelow Laboratory for Ocean Sciences, Maine, USA). In some cases, the exterior of the core sample had been flame sterilized on the ship prior to freezing. Depending on the quality of the frozen core sample (i.e., an intact core whole-round versus rubbly, broken pieces), the core was treated as follows: (1) if intact, the exterior of the core sample was removed via a steam-sterilized band saw

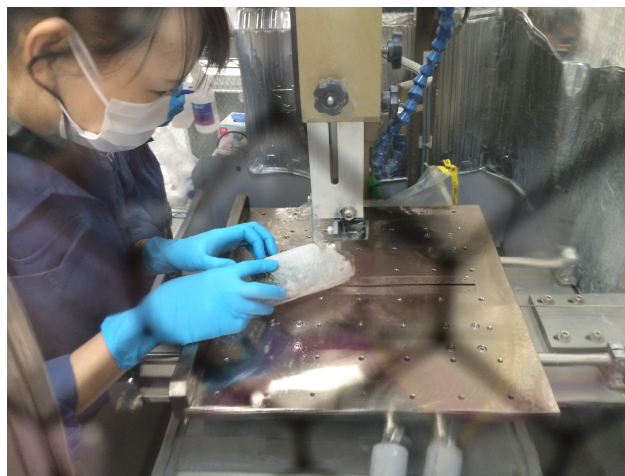


Figure 2. Example of cutting of a frozen whole-round core sample with the ultraclean diamond band saw with frozen stage inside a filtered air clean booth, available at the Kochi Core Center. Photograph by Beth Orcutt.

on a frozen stage (Fig. 2), generating “exterior” and “interior” fractions of the frozen core that were then subsampled; and (2) if rubbly, the core pieces were serially rinsed 10 times in ultrapure water within a combusted glass container. For the exterior fraction, roughly 1 cm³ of rock was transferred directly to a glass headspace vial with 5 mL water and crimp sealed. For the interior and rinsed fractions, the entire sample was first homogenized into a sand using autoclaved and/or flame-sterilized stainless-steel chisels, plates, percussion mortars, mortars, pestles, and spatulas while working between a KOACH benchtop laminar flow system (Fig. 3), and then approximately 1–2 g of sand-sized powder was transferred to a glass headspace vial with 5 mL of water and crimp sealed. It is important to note that all sample processing, as well as steam- and flame-sterilization of implements, occurred in the same laboratory, which lead to a buildup in ambient PFC concentrations in the atmosphere as assessed by collection of regular laboratory air blank samples. All of the frozen core subsamples were analyzed on a Shimadzu GC-17A system GC-ECD with a splitless injector, kindly provided by Steven D’Hondt at the University of Rhode Island Graduate School of Oceanography, following methods described elsewhere (Sauvage et al., 2016). The GC-ECD was equipped with a 15 m length \times 53 μ m inner diameter \times 15 μ m coating thickness HP PLOT Al/M column run with ultrahigh-purity nitrogen carrier gas at 30 mL min⁻¹ with an initial column temperature of 120 °C for 3.0 min, followed by a 20 °C min⁻¹ ramp to 150 °C and held for 1 min. The ECD injector and detector temperatures were 185 and 195 °C, respectively. Vials were heated prior to injection for at least 30 min at 70 °C. As there was no discernable trend in the concentration of PFC in the blank samples, the limit of detection for these batches of samples were determined from



Figure 3. Example of sample homogenization within the KOACH benchtop laminar flow system at the Kochi Core Center. Photograph by Beth Orcutt.

the averages of the laboratory blanks, which ranged from 10 to 1000 pg PFC per cm^3 air, depending on the laboratory.

4 Assessment of tracer delivery

Shipboard analysis of PFC tracer concentrations in core liner fluids and water samples collected with seabed drill-mounted Niskin bottles from the seabed drill breakout tables revealed variable success in achieving saturating PFC tracer concentrations, as documented elsewhere (Früh-Green et al., 2017a). Figure 4 provides a representative example of tracer concentrations measured in samples from Hole M0068B; similar data for other Expedition 357 holes are provided in the Supplement (Supplement Figs. S1–S16). During drilling operations at the first dozen holes, PFC delivery as measured in the fluid samples was generally low, with concentrations ranging from below the detection limit to hundreds of picograms of PFC per cm^3 . The exceptions to this were the deployments at holes M0070A and B (Supplement Figs. S4 and S5), which achieved higher concentrations of thousands of picograms of PFC cm^{-3} . Prior to the twelfth drill deployment, the tracer delivery pump internal mechanism was repaired as described above, and the subsequent tracer concentrations in the fluid samples increased by orders of magnitude. In some cases, PFC tracer was saturated in the recovered fluid samples (i.e., Hole 75B; Supplement Fig. S14). As these fluid samples represent a mixture of fluids flushed out of the borehole as well as bottom seawater, these concentrations should be viewed as lower estimates of the actual concentration of tracer in the flush waters.

Volumetric PFC concentrations on the rock samples were generally equal to or higher than the concentrations in the water samples (Fig. 4, Supplement Figs. S1–S16). High PFC concentrations were observed on exterior rock sam-

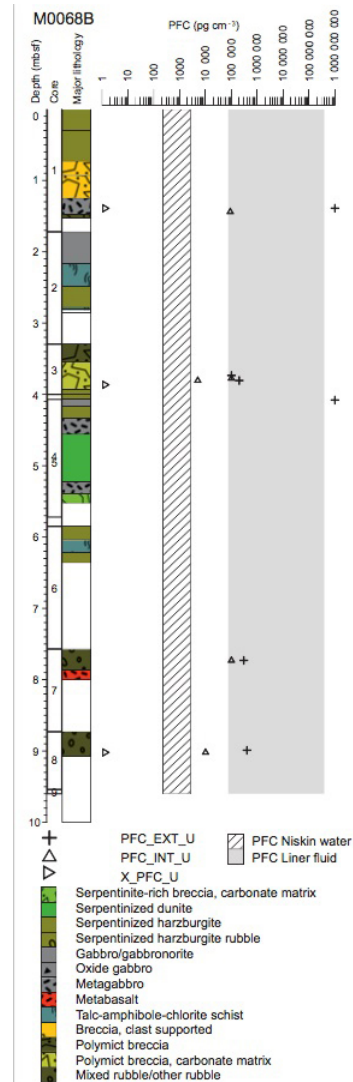


Figure 4. Summary of PFC tracer concentrations (in pg cm^{-3} on logarithmic scale) in samples collected during IODP Expedition 357 from Hole M0068B, as compared to the lithology logs from the site according to legend (Früh-Green et al., 2017a). For this figure (and all figures in the Supplement), symbols are as follows. PFC concentrations measured in fluid samples from the sensor package Niskin bottles (“PFC Niskin water”, grey shaded box) and the core liner fluids (“PFC Liner fluid”, match mark box) presented as the range of lower and upper concentrations measured in samples from each hole. PFC concentrations measured on whole-round core (WRC) samples: PFC_EXT_U (cross), exterior piece of unflamed whole-round core sample (WRC); PFC_INT_U (triangle), interior piece of unflamed WRC; X_PFC_U (arrow), homogenized unflamed WRC after serial rinsing with ultrapure water; PFC_EXT_F (circle), exterior piece of flamed WRC; PFC_INT_F (diamond), interior piece of flamed WRC; X_PFC_F (star), homogenized flamed WRC after serial rinsing with ultrapure water. Values on right-most edge of axis represent values above the maximum detection limit ($> 1 \text{ mg cm}^{-3}$), and values on left-most edge of axis represent values below the minimum detection limit (as shown in Table 1).

ples from holes M0068B (Fig. 4), M0070A/B/C (Supplement Figs. S4–S6), M0071A/B/C (Supplement Figs. S7–S9), M0075A/B (Supplement Figs. S13–S14), and M0076A/B (Supplement Figs. S15–S16). Exterior rock samples from holes M0069A (Supplement Fig. S3) and M0072A/B (Supplement Figs. S10–S11) were generally lower in PFC concentration. PFC concentrations in the one sediment core collected from M0074A were low (Supplement Fig. S12). Core samples were not collected from Hole M0073A (no core recovery).

5 Assessment of sample quality for deep biosphere investigations

The primary motivation for designing the tracer delivery system was to enable assessment of the quality of the core samples for deep biosphere investigations, and the degree to which samples might be compromised by exposure to bottom seawater or other sources. Various strategies were employed during the expedition to assess the intrusion of tracer into the interior of the core samples, including flaming of the exterior of the whole-round core with a handheld butane torch (to volatilize the PFC tracer on the exterior of the core, and presumably destroy any contaminating microbial cells), and/or physical removal of the exterior of the core with a diamond-tipped band saw (Fig. 2), and or serial rinsing of the core exterior with distilled water. Given the variable nature of the core recovered, which ranged from coherent pieces to rubble (Früh-Green et al., 2016), these strategies had varying degrees of success. Interior core samples from Hole M0068B still had high PFC concentrations, even after flaming or physical removal of the core exteriors (Fig. 4), which was expected given the very crumbly and talc-rich nature of the serpentinized samples from this core (Früh-Green et al., 2017a). By comparison, serial rinsing of whole-round cores from this hole with ultrapure water resulted in very low PFC concentrations (Fig. 4). Interior core pieces from Site M0070 holes often had lower PFC concentrations than in the exterior samples (Supplement Figs. S4–S6), suggesting limited intrusion of the tracer into the basalt breccias at this site (Früh-Green et al., 2017c). Flaming of the core material from Site M0071 was generally effective at preventing PFC intrusion into the interior of the core samples (Supplement Figs. S8–S10), which was expected considering that many of these samples were coherent (Früh-Green et al., 2017d). Site M0075 samples were very rubbly (Früh-Green et al., 2017d), and interior PFC concentrations were generally elevated while washing again seemed to have a positive effect (Supplement Figs. S13–S14). Although core samples from Site M0076 tended to be coherent, they were often rich in veins (Früh-Green et al., 2017b), which likely allowed transfer of PFC into the interiors of some samples (Supplement Figs. S15–S16).

6 Conclusions

Overall, the principle and implementation of a tracer injection system for seabed drill systems were proven to work. Following shipboard modification of the designed system, saturating concentrations of perfluoromethylcyclohexane were achievable in the drilling fluids used by the seabed drills during IODP Expedition 357, and PFC concentrations on the exterior and interior of core samples could be used as a measure to assess the quality of the sample material for detailed microbiological and geochemical analyses. With further minor developments, the system would be a reliable for use with any subsea system that required a controllable, low volume fluid injection system. One tempting new alternative for core contamination testing is the use of aqueous fluorescent particles as drill fluid tracers, which are cheaper and easier to quantify as compared to the volatile PFC tracer used in this study (Friese et al., 2017; Kallmeyer, 2017).

Data availability. PFC concentration data are provided in the Supplement. Supplement Table S1 details the concentrations in the rock samples, and Supplement Table S2 details the minimum and maximum concentrations in the fluid samples. Data are plotted by hole in Supplement Figs. S1–S16.

The Supplement related to this article is available online at <https://doi.org/10.5194/sd-23-39-2017-supplement>.

Author contributions. MB designed and built the tracer delivery system with input from TF, BNO, and DS; MB, TF, and LS deployed the system at sea with input from DS; BNO analyzed all samples with setup support from ML and LS; SG prepared figures; BNO wrote the manuscript with input from all coauthors.

Competing interests. The authors declare that they have no conflict of interest.

Acknowledgements. This technical effort benefited greatly from the advice and support of many individuals before, after, and during the expedition. Steven D'Hondt, Dennis Graham, and Mark Lever provided excellent guidance and advisement during the planning stages. Douglas Connelly and Kate Peel (University of Southampton), Dennis Graham and Steven D'Hondt (University of Rhode Island), and Tamara Baumberger, Rolf Pedersen, and Ingunn Thorseth (University of Bergen) generously provided equipment support and training. The Rock Drill 2 and MeBo Seafloor Drill Rig teams provided expert rig operations and tracer system interface, with support from Dave Smith and Carol Cotterill. Shipboard scientists Susan Lang, Yuki Morono, Marianne Quemeneur, Matthew Schrenk, and Katrina Twing graciously assisted with sample collection, and Gaye Bayrakci, Carol Cotterill,

Holger Kuhlmann, Sally Morgan, Alex Wülbers, and Ursula Röhl provided additional expedition support. Shorebased sampling was tirelessly provided by William Brazelton, Katherine Hickok, Susan Lang, Yuki Morono, Christopher Thornton, and Nan Xiao with support from Fumio Inagaki and JAMSTEC. We humbly thank the Expedition 357 core description team for tirelessly providing the data for the lithology logs. We thank Katrina Twing for comments on an earlier draft, and Susan Lang for advice on figures. This research used samples and data provided by the International Ocean Discovery Program (IODP). Funding for this work was provided by the US Science Support Program to the IODP (NSF award OCE-1450528, subaward 16(GG009393-01) to BNO), the European Consortium for Ocean Research Drilling (ECORD), and the Deep Carbon Observatory funded by the Alfred P. Sloan Foundation (Sloan-G-2015-14084-Deep Life Community subaward to BNO).

Edited by: Jan Behrmann

Reviewed by: two anonymous referees

References

- Andrén, T., Jørgensen, B. B., Cotterill, C., Green, S., Andrén, E., Ash, J., Bauersachs, T., Cragg, B. A., Fanget, A.-S., Fehr, A., Granoszewski, W., Groeneveld, J., Hardisty, D., Herrero-Bervera, E., Hyttinen, O., Jensen, J. B., Johnson, S., Kenzler, M., Kotilainen, A., Kotthoff, U., Marshall, I. P. G., Martin, E., Obrochta, S., Passchier, S., Quintana Krupinski, N., Riedinger, N., Slomp, C. P., Snowball, I., Stepanova, A., Strano, S., Torti, A., Warnock, J., Xiao, N., and Zhang, R.: Methods, in: Proc. IODP, 347, edited by: Andrén, T., Jørgensen, B. B., Cotterill, C., Green, S., and Expedition 347 Scientists, Integrated Ocean Drilling Program, College Station, TX, 2015.
- Freudenthal, T. and Wefer, G.: Scientific Drilling with the Sea Floor Drill Rig MeBo, *Sci. Drill.*, 5, 63–66, <https://doi.org/10.2204/iodp.sd.5.11.2007>, 2007.
- Friese, A., Kallmeyer, J., Kitte, J. A., Montañó Martínez, I., Bijaksana, S., Wagner, D., The ICDP Lake Chalco Drilling Science Team, and The ICDP Towuti Drilling Science Team: A simple and inexpensive technique for assessing contamination during drilling operations, *Limnol. Oceanogr. Methods*, 15, 200–211, <https://doi.org/10.1002/lom3.10159>, 2017.
- Früh-Green, G., Orcutt, B. N., Green, S. L., Cotterill, C., Morgan, S., Akizawa, N., Bayrakci, G., Behrmann, J.-H., Boschi, C., Brazelton, W. J., Cannat, M., Dunkel, K. G., Escartín, J., Harris, M., Herrero-Bervera, E., Hesse, K., John, B. E., Lang, S. Q., Lilliey, M. D., Liu, H. Q., Mayhew, L. E., McCaig, A. M., Menez, B., Morono, Y., Quéméneur, M., Rouméjon, S., Sandaruwan Ratnayake, A., Schrenk, M. O., Schwarzenbach, E. M., Twing, K., Weis, D., Whattham, S. A., Williams, M., and Zhao, R.: Eastern sites, in: Atlantis Massif Serpentinization and Life. Proceedings of the International Ocean Discovery Program, 357, edited by: Früh-Green, G. L., Orcutt, B. N., Green, S. L., Cotterill, C., and Scientists, E., International Ocean Discovery Program, College Station, TX, 2017a.
- Früh-Green, G., Orcutt, B. N., Green, S. L., Cotterill, C., Morgan, S., Akizawa, N., Bayrakci, G., Behrmann, J.-H., Boschi, C., Brazelton, W. J., Cannat, M., Dunkel, K. G., Escartín, J., Harris, M., Herrero-Bervera, E., Hesse, K., John, B. E., Lang, S. Q., Lilliey, M. D., Liu, H. Q., Mayhew, L. E., McCaig, A. M., Menez, B., Morono, Y., Quéméneur, M., Rouméjon, S., Sandaruwan Ratnayake, A., Schrenk, M. O., Schwarzenbach, E. M., Twing, K., Weis, D., Whattham, S. A., Williams, M., and Zhao, R.: Central sites, in: Atlantis Massif Serpentinization and Life. Proceedings of the International Ocean Discovery Program, 357, edited by: Früh-Green, G. L., Orcutt, B. N., Green, S. L., Cotterill, C., and Scientists, E., International Ocean Discovery Program, College Station, TX, 2017b.
- Früh-Green, G., Orcutt, B. N., Green, S. L., Cotterill, C., Morgan, S., Akizawa, N., Bayrakci, G., Behrmann, J.-H., Boschi, C., Brazelton, W. J., Cannat, M., Dunkel, K. G., Escartín, J., Harris, M., Herrero-Bervera, E., Hesse, K., John, B. E., Lang, S. Q., Lilliey, M. D., Liu, H. Q., Mayhew, L. E., McCaig, A. M., Menez, B., Morono, Y., Quéméneur, M., Rouméjon, S., Sandaruwan Ratnayake, A., Schrenk, M. O., Schwarzenbach, E. M., Twing, K., Weis, D., Whattham, S. A., Williams, M., and Zhao, R.: Northern sites, in: Atlantis Massif Serpentinization and Life. Proceedings of the International Ocean Discovery Program, 357, edited by: Früh-Green, G. L., Orcutt, B. N., Green, S. L., Cotterill, C., and Scientists, E., International Ocean Discovery Program, College Station, TX, 2017c.
- Früh-Green, G., Orcutt, B. N., Green, S. L., Cotterill, C., Morgan, S., Akizawa, N., Bayrakci, G., Behrmann, J.-H., Boschi, C., Brazelton, W. J., Cannat, M., Dunkel, K. G., Escartín, J., Harris, M., Herrero-Bervera, E., Hesse, K., John, B. E., Lang, S. Q., Lilliey, M. D., Liu, H. Q., Mayhew, L. E., McCaig, A. M., Menez, B., Morono, Y., Quéméneur, M., Rouméjon, S., Sandaruwan Ratnayake, A., Schrenk, M. O., Schwarzenbach, E. M., Twing, K., Weis, D., Whattham, S. A., Williams, M., and Zhao, R.: Western sites, in: Atlantis Massif Serpentinization and Life. Proceedings of the International Ocean Discovery Program, 357, edited by: Früh-Green, G. L., Orcutt, B. N., Green, S. L., Cotterill, C., and Scientists, E., International Ocean Discovery Program, College Station, TX, 2017d.
- Früh-Green, G., Orcutt, B. N., Green, S. L., Cotterill, C., Morgan, S., Akizawa, N., Bayrakci, G., Behrmann, J.-H., Boschi, C., Brazelton, W. J., Cannat, M., Dunkel, K. G., Escartín, J., Harris, M., Herrero-Bervera, E., Hesse, K., John, B. E., Lang, S. Q., Lilliey, M. D., Liu, H. Q., Mayhew, L. E., McCaig, A. M., Menez, B., Morono, Y., Quéméneur, M., Rouméjon, S., Sandaruwan Ratnayake, A., Schrenk, M. O., Schwarzenbach, E. M., Twing, K., Weis, D., Whattham, S. A., Williams, M., and Zhao, R.: Expedition 357 methods, in: Atlantis Massif Serpentinization and Life. Proceedings of the International Ocean Discovery Program, 357, edited by: Früh-Green, G., Orcutt, B. N., Green, S. L., Cotterill, C., and Scientists, T. E., International Ocean Discovery Program, College Station, TX, 2017e.
- Früh-Green, G. L., Orcutt, B. N., and Green, S.: Expedition 357 Scientific Prospectus: Atlantis Massif Serpentinization and Life, International Ocean Discovery Program (IODP), 357, <https://doi.org/10.14379/iodp.sp.357.2015>, 2015.
- Früh-Green, G. L., Orcutt, B. N., Green, S., Cotterill, C., and Expedition 357 Scientists: Expedition 357 Preliminary Report: Atlantis Massif Serpentinization and Life, International Ocean Discovery Program, 2016.
- Inagaki, F., Hinrichs, K. U., Kubo, Y., Bowles, M. W., Heuer, V. B., Hong, W. L., Hoshino, T., Ijiri, A., Imachi, H., Ito, M., Kaneko,

- M., Lever, M. A., Lin, Y.-S., Methé, B., Morita, S., Morono, Y., Tanikawa, W., Bihan, M., Bowden, S. A., Elvert, M., Glombitza, C., Gross, D., Harrington, G. J., Hori, T., Li, K., Limmer, D., Liu, C.-H., Murayama, M., Ohkouchi, N., Ono, S., Park, Y.-S., Philips, S. C., Prieto Mollar, X., Purkey, M., Riedinger, N., Sanada, Y., Sauvage, J., Snyder, G., Susilawati, R., Takano, Y., Tasumi, E., Terada, T., Tomaru, H., Trembath-Reichert, E., Wang, D. T., and Yamada, Y.: Exploring deep microbial life in coal-bearing sediment down to ~2.5 km below the ocean floor, *Science*, 349, 420–424, 2015.
- Kallmeyer, J.: Contamination control for scientific drilling operations, in: *Advances in Applied Microbiology*, edited by: Sari-aslani, S. and Gadd, G. M., Elsevier, Cambridge, San Diego, London, Oxford, 61–92, 2017.
- Lever, M., Alperin, M. J., Engelen, B., Inagaki, F., Nakagawa, S., Steinsbu, B. O., Teske, A., and Scientists, I. E.: Trends in basalt and sediment core contamination during IODP Expedition 301, *Geomicrobiol. J.*, 23, 517–530, 2006.
- Lever, M. A., Rouxel, O. J., Alt, J. C., Shimizu, N., Ono, S., Coggon, R. M., Shanks III, W. C., Lapham, L., Elvert, M., Prieto Mollar, X., Hinrichs, K. U., Inagaki, F., and Teske, A.: Evidence for microbial carbon and sulfur cycling in deeply buried ridge flank basalt, *Science*, 339, 1305–1308, 2013.
- Sauvage, J., Lewis, L., Graham, D., Spivack, A. J., and D'Hondt, S.: Data report: quantification of potential drilling contamination using perfluorocarbon tracer at IODP Expedition 329 sites, in: *Proceedings of the Integrated Ocean Drilling Program*, 329, edited by: D'Hon, Inagaki, F., Alvarez Zarikian, C. A., and Scientists, E., Integrated Ocean Drilling Program Management International, Inc., Tokyo, 2016.
- Smith, D. C., Spivack, A. J., Fisk, M. R., Haveman, S. A., Staudigel, H., and Party, L. S. S.: Methods for quantifying potential microbial contamination during deep ocean coring, ODP Technical Note, 28, <https://doi.org/10.2973/odp.tn.28.2000>, 2000.



Report on the ICDP workshop DIVE (Drilling the Ivrea–Verbano zone)

Mattia Pistone¹, Othmar Müntener¹, Luca Ziberna², György Hetényi¹, and Alberto Zanetti³

¹Institute of Earth Sciences, University of Lausanne (UNIL), Bâtiment Géopolis, Quartier UNIL-Mouline, 1015, Lausanne, Switzerland

²Bayerisches Geoinstitut, University of Bayreuth, 95440 Bayreuth, Germany

³Istituto di Geoscienze e Georisorse, Consiglio Nazionale delle Ricerche (CNR), Pavia, Via Ferrata, 1, 27100 Pavia, Italy

Correspondence to: Mattia Pistone (mattia.pistone@unil.ch)

Received: 7 July 2017 – Revised: 16 October 2017 – Accepted: 17 October 2017 – Published: 30 November 2017

Abstract. The Ivrea–Verbano Zone is the most complete, time-integrated crust–upper mantle archive in the world. It is a unique target for assembling data on the deep crust and the Moho transition zone and testing several hypotheses of formation, evolution, and modification of the continental crust through space and time across the Earth. The ICDP workshop Drilling the Ivrea–Verbano zone (DIVE), held in Baveno, Italy, from 1 to 5 May 2017, focused on the scientific objectives and the technical aspects of drilling and sampling in the Ivrea–Verbano Zone at depth. A total of 47 participants from 9 countries with a wide variety of scientific and/or drilling expertise attended the meeting. Discussion on the proposed targets sharpened the main research lines and led to working groups and the necessary technical details to compile the full drilling proposal. The participants of the workshop concluded that four drilling operations in the Val Sesia and Val d’Ossola crustal sections represent the scientifically most promising solution to achieve the major goals within DIVE to unravel the physico-chemical properties and architecture of the lower continental crust towards the crust–mantle (Moho) transition zone.

1 Introduction

The Drilling the Ivrea–Verbano zone (DIVE) project aims at unravelling the chemistry, physics, and microbiology of the roots of the Earth’s continental crust and the crust–mantle transition or Moho transition zone in the most complete, time-integrated crust–upper mantle archive in the world: the Ivrea–Verbano Zone (IVZ). The IVZ and the adjacent “Serie dei Laghi” (Boriani et al., 1990) expose a crustal section of the southern Alpine basement and is a southwest–northeast elongated body in the western Alps of Italy and Switzerland (Fig. 1). This body was the first region interpreted as an exposed cross section of the entire continental crust (e.g. Berckhemer, 1968; Fountain, 1976), with the lowermost part representing the laminated lower crust, known from seismic sections all over the world and characterised by multiple densely packed sets of reflectors referred to as seismic lamellae (e.g. Fountain, 1976; Rutter et al., 1993; Weiss et al., 1999).

A team of 47 scientists gathered for a workshop held in Baveno, Italy, to discuss scientific aims, drilling sites, and the technical and societal aspects of the DIVE project. Expertise of the participants ranges from petrology, geochemistry, geophysics, field geology, microbiology, scientific drilling, and drilling engineering. A series of introductory talks, plenary discussions, and working group meetings allowed ideas to be assembled and sharpened that will be used for the full drilling proposal.

A major issue that has sparked worldwide interest is the Ivrea geophysical body, a large gravimetric, magnetic, and seismic anomaly indicating that dense, mantle-like rocks are located at fairly shallow crustal levels (locally ~ 3 km depth; Berckhemer, 1968; Lanza, 1982; Kissling, 1984; Wagner et al., 1984; Diehl et al., 2009; Figs. 2–3). The Ivrea geophysical body, in its northern part, has a surface exposure, known as the Ivrea–Verbano Zone. Although some of the results on this zone are uncertain and the subject of continuing debate,

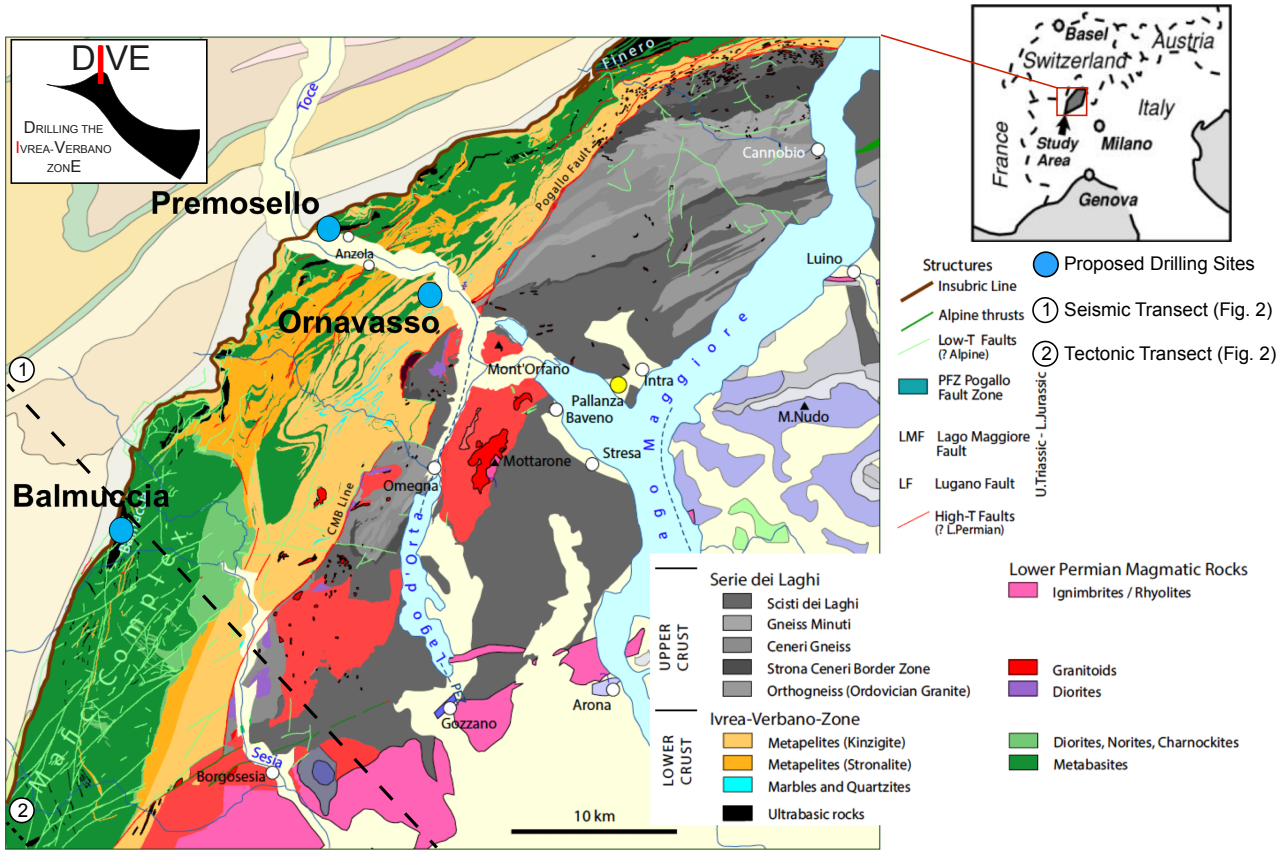


Figure 1. Overview of the geology of the IVZ and adjacent units, simplified after a compilation of James (2001) and Brack et al. (2010). The blue circles indicate the discussed drilling sites for the DIVE project. The inset figure showing the location of the IVZ in Italy is from Rutter et al. (2003).

it was clearly pointed out by the participants that work in the IVZ has played and still plays a fundamental role in shaping the debate on the origin of the lower continental crust and its transition into the mantle. Indeed, it makes an interesting case since the exposed Ivrea continental crustal section is made by two quite different sections both in composition and time. Hypotheses based on the Ivrea lower crust and crust–mantle transition zone have clearly delineated the need for additional data to resolve some fundamental yet complementary questions. This report presents the results of the workshop.

2 DIVE manifesto: project goals of the ICDP in the Ivrea–Verbano zone

The goals of the planned research are summarised below:

- i. identifying the major characteristics of the deep structure and composition of the continental crust–mantle transition zone (this requires complete characterisation of the rock properties such as mineral and bulk composition,

alteration, shear zones and faults, the relation of permeability to alteration, and fluid characterisation)

- ii. systematic compositional study of complete sections of the lower continental crust and the crust–mantle transition zone, with emphasis on crucial transitions between peridotite and metasedimentary and gabbroic rock interfaces
- iii. characterisation of physical properties of the drilled sections to refine techniques used in studies of the continental crust to improve the identification and nature of seismic reflectors (this is fundamental for up- and down-scaling observations from the kilometre-scale geophysics to centimetre-scale observations on core samples)
- iv. study of fluid–rock interaction in pristine rocks, and fluid flow and permeability along major tectonic structures such as shear zones and faults (this investigation also allows the study of the beginnings of serpentinization processes in nearly pristine mantle peridotite)

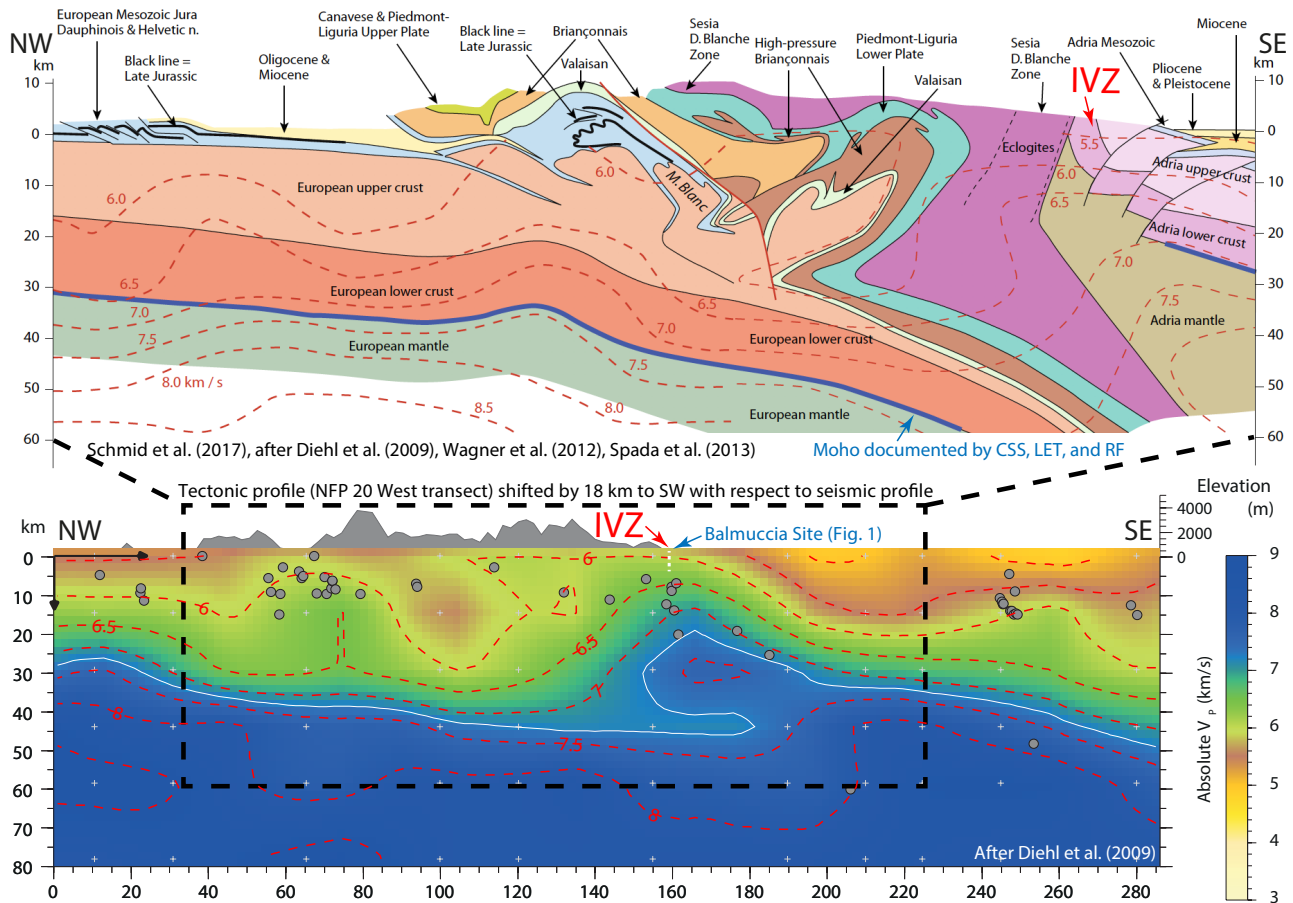


Figure 2. Northwest–southeast geological–tectonic transect (NFP 20 western transect; Schmid et al., 2017) and seismic profile (Diehl et al., 2009) across the western Alps. The two profiles are superimposed with and partly based on vertical cross sections across the final P-wave velocity model of Diehl et al. (2009), indicated by red dashed lines. The Moho (blue line in the geological-tectonic profile) is taken from a combination of controlled-source seismology (CSS), local earthquake tomography (LET), and receiver function (RF) analysis (Wagner et al., 2012; Spada et al., 2013). Data sources and traces of the profiles are reported in Schmid et al. (2017). The vertical white dashed line in the seismic profile indicates the proposed core location (up to 4 km depth) of Balmuccia site (Fig. 1). Note that the tectonic profile (NFP 20 western transect) is shifted by 18 km to the southwest with respect to the seismic profile.

- v. unravelling the extreme niches for hosting microbial life in planetary interiors, the fluid flow conditions that sustain life, as well as the hydrosphere and atmosphere on Earth, and the geochemical contexts of organic compound synthesis at depth
- vi. detailed and direct downhole geophysical monitoring of natural and human-induced seismicity, evaluation of seismic hazards near the major suture zone of the Alpine orogeny, and new insights on geothermal energy exploration
- vii. The development of a permanent educational, touristic, and research centre in the IVZ (“The ear into the Earth”).

To achieve these goals, drilling operations at three key sites in the area of the IVZ (Fig. 1) have been discussed and prioritised.

- Balmuccia, Val Sesia (peridotite sliver and gabbros of the lower crust in proximity of the Insubric Line, the structure depicted with a brown line in Fig. 1): deep drilling into the roots of a large-scale Permian magmatic system from the lower crust to the surface, with the main goal to approach the crust–mantle transition zone and benchmark it against geophysical data
- Premosello, Val d’Ossola (peridotite sliver, high-temperature shear zones): drilling into the pre-Permian continental lower crust with high lithological variability, in the fold hinges of large-scale folds to investigate peridotite–gabbro–metasedimentary interfaces

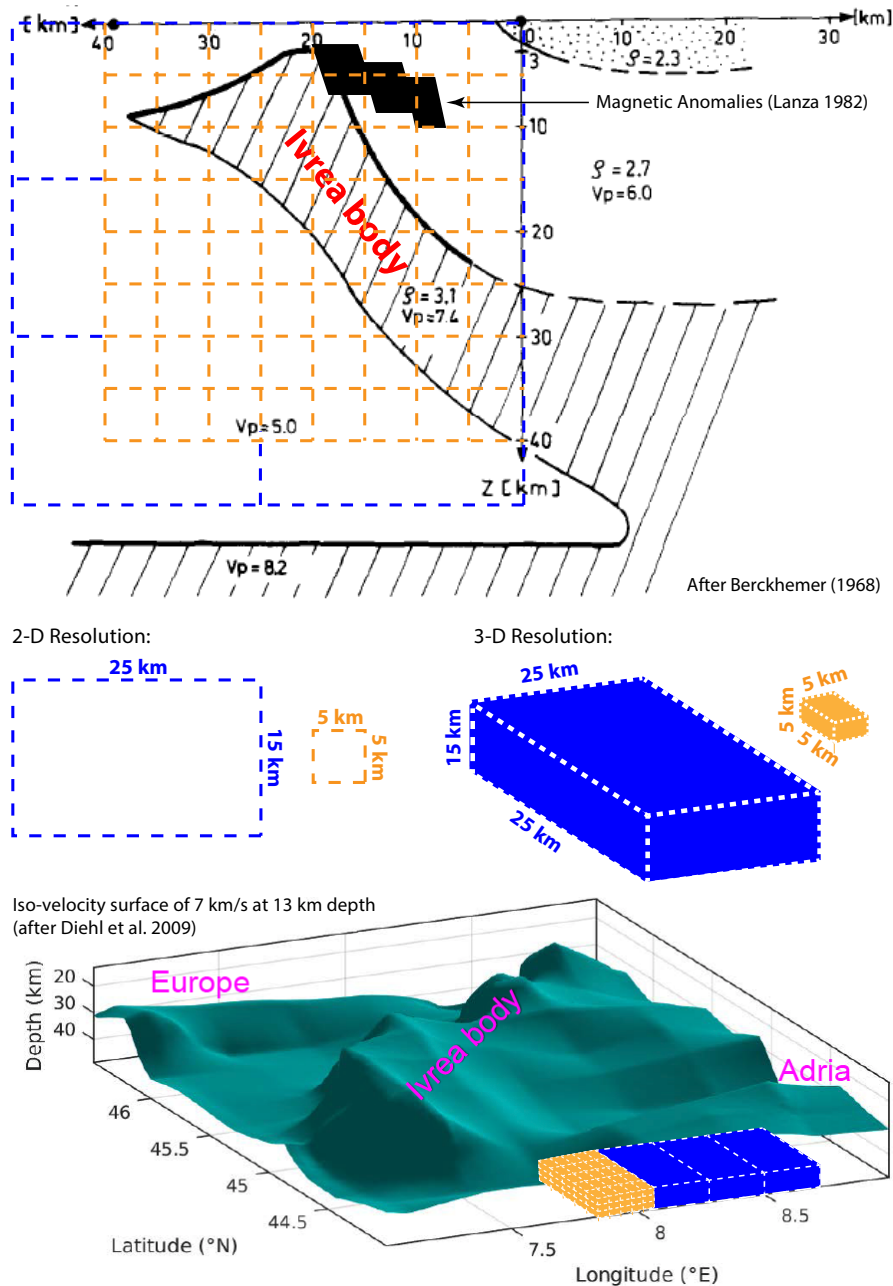


Figure 3. Cross section of the Ivrea body (“Bird’s Head model”) according to Berckhemer (1968), as determined by seismic wave velocities and gravity anomalies. Black squares are magnetically differentiated rocks with a magnetic susceptibility contrast of 5×10^{-1} CGS EMU (electromagnetic units in the centimetre–gram–second system) with respect to the surrounding lithologies (Lanza, 1982). Blue dashed grid indicates 2-D spatial seismic resolution achieved in the past (25 km \times 25 km [horizontal] \times 15 km [vertical]; Diehl et al., 2009). Orange dashed grid indicates 2-D spatial seismic resolution (5 km \times 5 km \times 5 km) to be applied in the forthcoming geophysical investigations. The higher spatial seismic resolution will allow improvements of existing 3-D geophysical models (e.g. iso-velocity surface models of Diehl et al., 2009) to image the Ivrea body at depth.

- Ornavasso, Val d’Ossola (amphibolite-facies, metasedimentary sequence in the Massone antiform): drilling into the pre-Permian heterogeneity of the intermediate to lower crust in the fold hinges of metasedimentary sequences.

In an initial phase (Phase I), each of the proposed drilling operations is planned to generate ~ 1 km of continuous coring of rocks and to sample representative sections of the Ivrea continental lower crust. A fourth drilling operation (Phase II) aimed at coring deeper into the crust–mantle transition zone

(up to 4 km) is planned as part of the second stage of drilling. The preferred site for deep drilling is the Balmuccia site but might be modified according to the results of the Phase I of drilling.

Each of these proposed sites are carefully studied by pre-drilling investigations, which include target-oriented geological site surveys aimed at determining the main structural architecture, pressure gradients in space and time across metamorphic sections, fluid and heat budgets of the crust, petro-physical properties of the lower crust, and several-kilometre-deep geophysical characterisation of the IVZ structure.

The participants of the workshop agreed that drilling is essential because drilled cores provide complete sections of the continental crust–mantle transition zone that can be compared to existing data. The outcrops of the IVZ have been investigated by the worldwide scientific community in the last 50 years, and for many models on the lower continental crust the IVZ is a reference case (e.g. Salisbury and Fountain, 1990). Specifically, the overall picture and the deep three-dimensional structure are sufficiently well known to document beyond any doubt that, in the IVZ, at shallow depth, and possibly even at the surface, representative sections of the continental lowermost crust of the Adria plate are exposed (Figs. 2–3). This, combined with continuous drilling in key sites of the IVZ, would allow unravelling the complexity of a complete lower crustal section and contributing substantially to refining hypotheses on the genesis and dynamics of the Earth's continental lower crust and Moho transition zone, on continental extension, and on the deep structure of crustal-scale magmatic plumbing systems. Continuous sampling across a number of kilometre-long drilling sections will provide access to hitherto the inaccessible, deepest portions of the continental crust, which are not exposed in the IVZ. This will in turn provide the opportunity to unravel the architecture and chemistry of the composite Moho transition zone, and, therefore, calibrate current tectonic, geophysical, and petrological models.

This ICDP workshop addressed the aspects and challenges of drilling targets, in situ well loggings, core analysis, and scientific collaborations and partnerships as well as operations, logistics, funding, permissions, outreach, education, and cooperation with national, regional, and municipal authorities. It was envisioned that drilling will be funded by the ICDP, industry, national and international science funding agencies such as the European Research Council (ERC), Swiss National Science Foundation (SNF), Italian Research Council (Consiglio Nazionale delle Ricerche or CNR), National Institute of Volcanology and Geophysics (Istituto Nazionale di Vulcanologia e Geofisica or INGV), German Research Foundation (Deutsche Forschungsgemeinschaft or DFG), Deep Carbon Observatory (DCO) Task Force 2020, US National Science Foundation (NSF), US National Aeronautics and Space Administration (NASA), European Space Agency (ESA), and Italian Space Agency (Agen-

zia Spaziale Italiana or ASI). The DIVE research plan is subdivided into five main themes as follows.

3 Petrology, geochemistry, and structural geology

The IVZ is a unique target for assembling direct data on the deep crust and the crust–mantle transition zone and testing several hypotheses of generation, construction, and evolution of the continental crust through space and time across the Earth. Drilling in Balmuccia should ultimately provide a deep borehole up to 4 km depth to approach the crust–mantle transition determined by geophysical imaging (e.g. Diehl et al., 2009; Fig. 2), or even reach it. Drilling in Premosello and Ornavasso (Fig. 1) will be planned in order to systematically cross interfaces, such as the intercalations of amphibolite to granulite facies metasedimentary and metavolcanic rocks, the transition into denser rock types (pyroxenites and/or restitic garnet-rich gneisses), and eventually the peridotitic rock types to characterise the continental Moho transition zone. Planning will be constrained by compiled site survey based on detailed geological investigations.

Petrologists and geochemists of the ICDP workshop proposed the following research themes to explore by deep drilling investigations.

1. The first theme is correlation of crustal lithostratigraphy and seismic structures with new integrated petrological and geophysical models. In continental areas the interpretation of seismic, density, and magnetic structures have largely been based on correlations with exposed lower crustal rocks. Similarly, the continental seismic Moho has been interpreted as a transition from lower crustal to mantle rocks. The IVZ provides sections of the lower continental crust with different compositions (mafic versus metasedimentary) where inter-fingering of mantle and crustal rocks are observed and, therefore, it is unclear where the seismic transition to the mantle might be found and how lateral differences in lower crustal compositions can seismically be detected (Fig. 4). Downhole variations in rock types, physical properties and alteration degree might help to better calibrate seismic models.
2. The second theme is the evaluation of budgets of carbon and heat-producing elements (U, Th, and K) of the metapelitic crust, to establish (a) similarities and differences between amphibolite facies (Kinzigite) and granulite facies (Stronalite) rocks in statistical samples along cores, and (b) mass balance of heat-producing elements from compositional and logging data, whose distributions vary within the Kinzigite formation, granulites, and the contact aureole around the Mafic Complex. The deep carbon cycle, the heat budget, and the IVZ crustal dynamics in the pre-Permian, as well as Permian period (i.e. before and after the emplacement of the Mafic

Complex and generation of granitic systems in the upper crust and volcanoes at the surface), will help reconstruct the influence of geochemistry on the potential ecology of extreme environments and determining the prohibitive and unrestrictive conditions for microbial life in the Earth's interior (e.g. Morrison et al., 2017).

3. The third theme is the identification and size-frequency distribution of shear zones and fractures to distinguish low temperature features related to exhumation from high temperature structures during accretion and/or crustal thinning.
4. The fourth theme is deformation-assisted fluid extraction processes and fluid percolation during emplacement and cooling of the lower crust.
5. The fifth theme is the quantification of chemical and physical differences and similarities between mafic and metasedimentary lower continental crust.
6. The sixth and final theme is the testing of emplacement models of deep crustal intrusions (e.g. “gabbro glacier” model; Sleep, 1975; Quick et al., 1994) or sills (e.g. “sill emplacement” model; Annen and Sparks, 2002; Solano et al., 2014). Observations along drilling transects by determining the compositional and textural variability of the gabbros in the lower crust and linking them to downhole geophysical logs will provide crucial data that will aid understanding of the mechanism of emplacement of lower crustal mafic bodies across the Earth.

4 Geophysics

During the ICDP workshop, geophysicists of different disciplines addressed the following research targets to be investigated during pre-drilling surveys, drilling operations, and complementary field experiments:

1. The geometry of mantle-derived ultramafic bodies and their transition or connection to lower crustal rocks (i.e. high-resolution refinement of the “Bird’s Head model” reported in Berckhemer, 1968; Fig. 3);
2. Quantitative assessment of the nature and scale of mineralogical variations and fabrics along a finely banded sequence;
3. The size-frequency distribution of fractures and veins and relationships to the geometry of Alpine thrusts and pre-Alpine faults, including the subsurface continuation of the Insubric Line;
4. The hydration evolution of crustal rocks with depth.

The larger-scale research objectives will be tackled in combination with the ongoing European AlpArray project (Hetényi, 2012; Hetényi and AlpArray Working Group, 2012a, b;

Molinari et al., 2016; www.alparray.ethz.ch), and a targeted, 10-station broadband seismological array operated from June 2017 (Scarponi et al., 2017).

In terms of crustal structure, the currently highest and most uniform resolution seismological image and interpretation of the IVZ is provided by Diehl et al. (2009) and subsequent works (Fig. 2). Their investigation is carried out using a 25×25 (horizontal) \times 15 (vertical) km grid (Fig. 3). If a finer-scale local earthquake P- and S-wave tomography is attempted, a dense local network with a minimum of 2 to 3 years of operation and inversion on a $5 \times 5 \times 5$ km grid is required (Fig. 3). In addition, this will be completed by existing surface tectonic studies of the IVZ (Fig. 2).

High-resolution geophysical investigation is of primary importance to approach the scale of geological knowledge; nevertheless, cross-scale connection of physical properties is not necessarily granted (see Fig. 4 for a comparison of various exposed lithologies and similar seismic wave velocities). Therefore, a multidisciplinary combination of shallow and deep geophysical investigations was proposed, ranging from active seismics (especially pre-site surveys in the Balmuccia site), passive seismology (a 10-station broadband array to investigate the Bird’s Head with receiver functions (Scarponi et al., 2017), magnetotellurics, and gravity anomalies (to map the three-dimensional buried morphology of the Ivrea geophysical body; Fig. 3) in the period 2017–2020. Drilling into the geophysically imaged volume can provide an additional approach: any fracturing process, likely enhanced by fluid circulation in and around the borehole, will be the induced source of micro-earthquakes, which is aimed at being recorded with a dedicated, targeted seismic network. In addition, once the borehole is considered complete, vertical seismic profiling (i.e. a technique devoid of blasting, employed in the recent ICDP-COSC project in Sweden; Lorenz et al., 2015) will provide an outstanding controlled-source complement to the dataset.

5 Well logging and rock physics

An international consortium of scientists will analyse the cores and conduct downhole geophysical experiments to investigate permeability, state of stress, and fracture distribution, as well as the magnetic, seismic, and resistivity properties of the lithological types in the continental lower crust and Moho transition zone.

Comprehensive downhole logging will provide a continuous, in situ, highly resolved record of key physical, chemical, and structural rock information along the entire length of the drilled lithological sequences. This, in turn, will allow for the linking of micro- to centimetre-scale observations from drill core samples to field-scale geophysical observations of the continental crust in general and in particular the IVZ. Downhole logging permits the compensation, in part, for the inevitably incomplete retrieval of

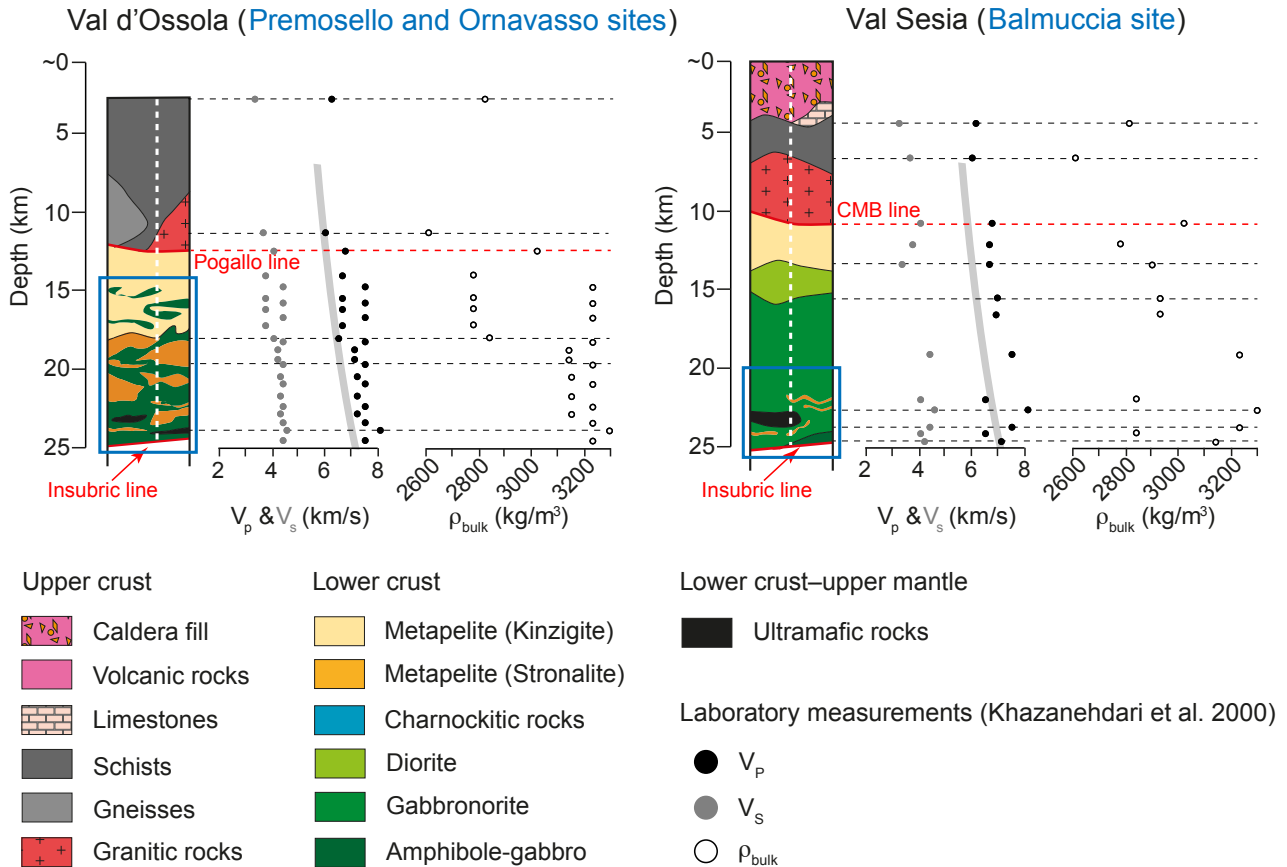


Figure 4. Schematic lithological, seismic, and density properties of bulk rocks from the main geological locations of the IVZ where the ICDP DIVE project will be targeted. Lithological data are from James (2001), Quick et al. (2003), Sinigoi et al. (2011), and Klötzli et al. (2014). Average bulk rock seismic P-wave and S-wave velocity (V_p and V_s) and density (ρ_{bulk}) data are from Khazanehdari et al. (2000). The white dashed line indicates the pathway of plotted bulk rock seismic velocity and density data for each different lithology along the cross section. Grey band shows global average V_p -depth relation for extended terrains (Christensen and Mooney, 1995). Blue squares highlight the lithologies at the drilling sites displayed in Fig. 1.

core material, although hard-rock drilling is often characterised by excellent coverage (up to 100%). Important rock physical properties to be measured by downhole logging are P- and S-wave velocities in the sonic frequency range and the electrical conductivity. The sonic measurements will be complemented by P-wave vertical-seismic-profile (VSP)-type surface-to-borehole measurements in the higher seismic frequency range. Together, these observations can then be correlated with results from corresponding crustal-scale geophysical investigations as well as petrophysical laboratory measurements on the retrieved core material.

Additional pertinent rock physical properties provided by downhole logging will be natural radioactivity, density and porosity, possibly in conjunction with neutron–neutron logging. Panoramic (360°) televiwer logging will generate high-resolution images of the structural fabric along the borehole. This does not only offer a highly resolved continuous record of key structural parameters along the entire borehole,

such as the strike and dip of the fractures, fabrics, and lithological interfaces, but also enables the construction of digital pseudo-cores, which can then be visually correlated with the retrieved core material. Combined with the standard caliper logs, such televiwer images will further permit the detection and orientation of breakouts, which, in turn, will critically constrain the nature and orientation of the prevailing present-day stress field. Petrographic studies on cores will be used to learn how geophysical logs record information about igneous rocks and interlayered metasedimentary rocks or septa in the lower continental crust and the crust–mantle transition zone, yielding a continuous record of layer spacing from the geophysical logs even where core is not recovered. This can be combined with geophysical data to identify septa-related reflectors. Finally, flow-meter logging and downhole fluid sampling and temperature measurements will provide constraints with regard to fluid flow and permeability, as well as the com-

position and origin of the fluids prevailing the pores and fractures of the probed lithologies.

Advanced packer systems could be used during the drilling process to assess possible fluid or gas discharge from permeable layers to analyse the relation between prevailing hydraulics and fluid composition with the petrology and the texture of the fluid-bearing rocks. In particular, noble gases and other transient tracers (e.g. ^3H and ^{14}C) will be analysed to trace the geochemical origin of the fluids (i.e. mantle-derived vs. crustal) and determine the water residence time. The lesson from scientific drilling in the context of nuclear waste disposal and geothermal exploration is that such fluid analyses during the drilling process are essential to analyse rock–water interactions. During the discussion, consideration was also given to keeping the boreholes open, allowing later fluid and water sampling under natural conditions after re-equilibration of drilling process disturbances.

6 Geohazards and long-term monitoring

The DIVE project will provide the opportunity to implement long-term seismic monitoring after coring (> 10 years), and possibilities for additional monitoring are being investigated (e.g. downhole temperatures, new heat flow data, dynamics of freshwater, downhole pressures, Earth magnetism, in situ microbiological tests at high pressure). Scientifically long-term seismic monitoring is necessary for an in-depth understanding of microfractures, fault reactivation, and rupturing. Data retrieved from greater depths are needed for validating existing geophysical, petrological, and geomechanical models. In situ and laboratory biological data are also an essential aspect of the drilling project, which can potentially reveal the extent and limits of the deep biosphere in the continental lower crust. Very limited data from boreholes in marine and terrestrial environments have been collected so far. The greater depth and temperature limits of the biosphere have not been reached in any borehole studies that have included a microbiological component, and the factors controlling the abundance and activities of microbes at depth and the lower depth limit of life are still poorly understood. Last but not least, the DIVE project should trigger a large-scale international network of collaborations and partnerships that could lead to the generation of a research and teaching centre of excellence in the IVZ in the long term. Specifically, it is of great importance to establish a novel international observatory in which scientists of different expertise from all over the world can visit the IVZ and integrate fieldwork, modelling, experiments, and theories to advance knowledge and technology in our society.

7 Societal impact and relevance of the IVZ

The research themes of the proposed DIVE project are collectively recognised as major focus areas for understanding

crustal processes, with implications for societal challenges such as natural hazards, energy and mineral resources, deep fluids, biosphere, and ecosystem evolution. With monitoring of the seismic activity during drilling, potentially enhanced by natural fluid circulation in the underground, the community will gain new experience from a context that is different from classical geothermal investigations such as those currently carried out in sedimentary basins. Drilling operations can represent a precious source of investment in developing education platforms for schools, university students, formation of the next generation of researchers, and the larger public. The public activities could include open days at drilling sites, press releases, and presentations in schools, universities, and interested municipalities, outlining the results of both the drilling and the subsequent work related to the core samples, as well as “Ask me anything!” or “Scientist is in”-type events. The proposed drilling sites will have a great impact on the general public, as well as the local population since all the drilling sites are within the Sesia–Val Grande geopark, which also includes the UNESCO World Heritage site of the Sesia Magmatic System, and the National Park of Val Grande. Therefore, the new data and consequent models obtained during the DIVE project will make the IVZ an even more attractive geopark for Earth sciences education and might provide unprecedented new insights into geothermal energy resources. A website will also be constructed to highlight any news of the ICDP-sponsored drilling operations “on air”.

8 Concluding remarks

Numerous issues were discussed in detail during the workshop that cannot be covered in this brief report. However, all relevant information discussed during the workshop will be used to compile the full proposal. Practical but crucial issues on sampling and coring will be elaborated during the preparation of the full drilling proposal. All discipline groups will use standardised analytical methods and will also work on a generally applicable system for data management and evaluation. More information on DIVE and its progress can be found on the ICDP DIVE project’s website (<http://www.icdp-online.org/projects/world/europe/Ivrea/>).

9 Participants of the ICDP workshop in Baveno, Italy

Bjarne Almquist, Mohsen Bazargan, George Bergantz, Théo Berthet, Peter Brack, Shuyun Cao, Tobias Diehl, Rita Economos, Donato Giovannelli, Bradley Hacker, Ulrich Harms, Jörg Hermann, Klaus Holliger, Priyank Jaiswal, Ozge Karakas, Peter Kelemen, Rolf Kipfer, Antonio Langone, Julien Leuthold, Adele Manzella, Maurizio Mazzucchelli, Michael Z. McIntire, Walter Mooney, Peter Nabelek, Benoît Petri, Simona Pierdominici, Claudia Piromallo, Silvia Pondrelli, Jan-Erik Rosberg, Matteo Scarponi, Craig

Schiffries, Anja Schleicher, Silvano Sinigoi, Thomas W. Sisson, Andrew Smye, Julien-Christopher Storck, Lorenzo Tavazzani, Riccardo Tribuzio, Lucy Tweed, Peter Ulmer, Michael Weber, and Alba Zappone.

Data availability. No data sets were used in this article.

Author contributions. OM, LZ, AZ, and MP organised and led the ICDP workshop in Baveno, Italy. GH led the working group discussions amongst the geophysicists of the ICDP workshop and initiated the 10-station broadband seismological array, which has been in operation since June 2017. MP took the lead in writing the initial draft of the manuscript. All authors contributed improvements to the final paper.

Competing interests. The authors declare that they have no conflict of interest.

Acknowledgements. ICDP is gratefully acknowledged for providing funding for the workshop in Baveno. We thank all the participants of the Ivrea ICDP workshop for their constructive input and enthusiasm, and especially Ulrich Harms for unconditional support. We are grateful to Edi Kissling for previous discussions on the geophysical Ivrea body. We acknowledge the insightful comments on the report by two anonymous reviewers. The organisers of the workshop are grateful to the late Luigi Burlini, who had already launched the idea of drilling the IVZ in 2009. MP and LZ acknowledge the support of the Swiss National Science Foundation Ambizione Fellowship and Alexander von Humboldt Postdoctoral Fellowship, respectively. Those interested in joining the DIVE project are invited to contact the authors of this article.

Edited by: Ulrich Harms

Reviewed by: two anonymous referees

References

- Annen, C. and Sparks, R. S. J.: Effects of repetitive emplacement of basaltic intrusions on thermal evolution and melt generation in the crust, *Earth Planet. Sci. Lett.*, 203, 937–955, 2002.
- Berckhemer, H.: Topographie des “Ivrea-Körpers” abgeleitet aus seismischen und gravimetrischen Daten, *Schweiz. Min. Petr. Mitt.*, 48, 235–246, 1968.
- Boriani, A., Orighi Giobbi, E., Borghi, A., and Caironi, V.: The evolution of the ‘Serie dei Laghi’ (Strona-Ceneri and Schisti dei Laghi): The upper component of the Ivrea–Verbano crustal section; southern Alps, north Italy and Ticino, Switzerland, *Tectonophys.*, 182, 103–118, 1990.
- Brack, P., Ulmer, P., and Schmid, S.: A crustal magmatic system from the Earth mantle to the Permian surface: Field trip to the area of lower Valsesia and val d’Ossola (massiccio dei Laghi, Southern Alps, Northern Italy), *Swiss Bull. Angew. Geol.*, 15, 3–21, 2010.
- Christensen, N. I. and Mooney, W. D.: Seismic velocity structure and composition of the continental crust: A global view, *J. Geophys. Res.*, 100, 9761–9788, 1995.
- Diehl, T., Husen, S., Kissling, E., and Deichmann, N.: High-resolution 3-D P-wave model of the Alpine crust, *Geophys. J. Internat.*, 179, 1133–1147, 2009.
- Fountain, D. M.: The Ivrea-Verbano and Strona-Ceneri zones, northern Italy: a cross section of the continental crust: new evidence from seismic velocities, *Tectonophys.*, 33, 145–166, 1976.
- Hetényi, G. and AlpArray Working Group: AlpArray: an initiative for broad co-operation in broadband seismology, *EPOS Newsletter*, 01/2012, 2, 2012a.
- Hetényi, G. and AlpArray Working Group: AlpArray – an initiative to advance understanding of Alpine geodynamics, *Geophys. Res. Abstr.*, 14, A-10058, 2012b.
- James, T.: A study of the geological structure of the Massiccio dei Laghi (Northern Italy), Unpublished PhD thesis, University of Manchester, 2001.
- Khazanehdari, J., Rutter, E. H., and Brodie, K. H.: High pressure/temperature seismic velocity structure of the mid- and lower-crustal rocks of the Ivrea-Verbano zone and Serie dei Laghi, NW Italy, *J. Geophys. Res.*, 105, 13843–13858, 2000.
- Kissling, E.: Three-dimensional gravity model of the northern Ivrea-Verbano zone, in: *Geomagnetic and gravimetric studies of the Ivrea zone*, edited by: Wagner, J. J. and Mueller, S., 53–61, Swiss Comm. Geophysics, Attinger SA, Neuchâtel, 1984.
- Klötzli, U. S., Sinigoi, S., Quick, J. E., Demarchi, G., Tassinari, C. C. G., Sato, K., and Günes, Z.: Duration of igneous activity in the Sesia Magmatic System and implications for high-temperature metamorphism in the Ivrea-Verbano deep crust, *Lithos*, 206–207, 19–33, 2014.
- Lanza, R.: Models for interpretation of the magnetic anomaly of the Ivrea body, *Geologie Alpine*, 58, 85–94, 1982.
- Lorenz, H., Rosberg, J.-E., Juhlin, C., Bjelm, L., Almqvist, B. S. G., Berthet, T., Conze, R., Gee, D. G., Klonowska, I., Pascal, C., Pedersen, K., Roberts, N. M. W., and Tsang, C.-F.: COSC-1 – drilling of a subduction-related allochthon in the Palaeozoic Caledonide orogen of Scandinavia, *Sci. Dril.*, 19, 1–11, <https://doi.org/10.5194/sd-19-1-2015>, 2015.
- Molinari, I., Clinton, J., Kissling, E., Hetényi, G., Giardini, D., Stipevcic, J., Dasovic, I., Herak, M., Šipka, V., Wéber, Z., Gráczner, Z., Solarino, S., the Swiss-AlpArray Field Team, and the AlpArray Working Group: Swiss-AlpArray temporary broadband seismic stations deployment and noise characterization, *Adv. Geosci.*, 43, 15–29, <https://doi.org/10.5194/adgeo-43-15-2016>, 2016.
- Morrison, S., Pistone, M., and Kohl, L.: Studying Yellowstone by integrating deep carbon science, *EOS*, 98, <https://doi.org/10.1029/2017EO076209>, 2017.
- Quick, J. E., Sinigoi, S., and Mayer, A.: Emplacement dynamics of a large mafic intrusion in the lower crust, Ivrea-Verbano Zone, northern Italy, *J. Geophys. Res.*, 99, 21559–21573, 1994.
- Quick, J. E., Sinigoi, S., Snoke, A. W., Kalakay, T. J., Mayer, A., and Peressini, G.: Geologic map of the Southern Ivrea-Verbano Zone, Northwestern Italy, U.S. Geological Survey, Reston, Virginia, VA, 2003.
- Rutter, E., Brodie, K., and Evans, P.: Structural geometry, lower crustal magmatic underplating and lithospheric stretching in the Ivrea-Verbano Zone, N. Italy, *J. Struct. Geol.*, 15, 647–652, 1993.

- Rutter, E., Brodie, K., James, T., Blundell, D. J., and Waltham, D. A.: Seismic Modeling of Lower and Mid-Crustal Structure as Exemplified by the Massiccio dei Laghi (Ivrea-Verbano Zone and Serie dei Laghi) Crustal Section, Northwestern Italy, in: *Heterogeneity in the Crust and Upper Mantle*, edited by: Goff, J. A. and Holliger, K., Kluwer Academic/Plenum Publishers, 67–97, 2003.
- Salisbury, M. H. and Fountain, D. M.: *Exposed Cross-Sections of the Continental Crust*, NATO ASI Series, Series C: Mathematical and Physical Sciences 317, Kluwer Academic Publisher, Dordrecht, Netherlands, 658 pp., 1990.
- Scarponi, M., Hetényi, G., Plomerová, J., Solarino, S., Berthet, T., Baron, L., AlpArray-Ivrea Working Group, and AlpArray Ivrea Field Team: High-resolution imaging of the Ivrea Geophysical Body: A receiver function and gravity approach, 15th Swiss Geoscience Meeting, 17–18 November 2017, Davos, Switzerland, 2017.
- Schmid, S. M., Kissling, E., Diehl, T., van Hinsbergen, D. J. J., and Molli, G.: Ivrea mantle wedge, arc of the Western Alps, and kinematic evolution of the Alps-Appenines orogenic system, *Swiss J. Geosci.*, <https://doi.org/10.1007/s00015-016-0237-0>, 2017.
- Sinigoï, S., Quick, J. E., Demarchi, G., and Klotzli, U. S.: The role of crustal fertility in the generation of large silicic magmatic systems triggered by intrusion of mantle magma in the deep crust, *Contrib. Mineral. Petrol.*, 162, 691–707, 2011.
- Sleep, N. H.: Formation of oceanic crust: Some thermal constraints, *J. Geophys. Res.*, 80, 4037–4042, 1975.
- Solano, J. M. S., Jackson, M. D., Sparks, R. J. S., and Blundy, J. D.: Evolution of major and trace element compositions during melt migration through crystalline mush: Implications for chemical differentiation in the crust, *Am. J. Sci.*, 314, 895–939, 2014.
- Spada, M., Bianchi, I., Kissling, E., Piana Agostinetti, N., and Wiemer, S.: Combining controlled-source seismology and receiver function information to derive 3-D Moho topography for Italy, *Geophys. J. Internat.*, 194, 1050–1068, 2013.
- Wagner, J. J., Klingelé, E., and Mage, R.: Regional geomagnetic study of the southern border of the Western Alps, The Ivrea body, in: *Geomagnetic and Gravimetric studies of the Ivrea Zone*, edited by: Wagner, J. J. and Müller, S., *Beitr. Geol. Schweiz Geophys.*, 21, Kümmerly & Frey, Bern, 21–31, 1984.
- Wagner, M., Kissling, E., and Husen, S.: Combining controlled-source seismology and local earthquake tomography to derive a 3-D crustal model of the western Alpine region, *Geophys. J. Internat.*, 191, 789–802, 2012.
- Weiss, T., Siegesmund, S., Rabbel, W., Bohlen, T., and Pohl, M.: Physical properties of the Lower continental crust: an anisotropic perspective, *Pure Appl. Geophys.*, 156, 97–122, 1999.



Scientific Exploration of Induced Seismicity and Stress (SEISMS)

Heather M. Savage¹, James D. Kirkpatrick², James J. Mori³, Emily E. Brodsky⁴, William L. Ellsworth⁵,
Brett M. Carpenter⁶, Xiaowei Chen⁶, Frédéric Cappa⁷, and Yasuyuki Kano³

¹Lamont-Doherty Earth Observatory, Columbia University, Palisades, NY, USA

²Department of Earth and Planetary Sciences, McGill University,
3450 University St., Montréal, QC H3A 0E8, Canada

³Disaster Prevention Research Institute, Kyoto University, Kyoto, Japan

⁴Department of Earth and Planetary Sciences, University of California-Santa Cruz,
Santa Cruz, California 95064, USA

⁵Department of Geophysics, Stanford University, 397 Panama Mall, Stanford, California 94305-2215, USA

⁶School of Geology and Geophysics, University of Oklahoma, Norman, USA

⁷CNRS, OCA, IRD, Géoazur, Sophia Antipolis, France

Correspondence to: Heather M. Savage (hsavage@ldeo.columbia.edu)

Received: 18 August 2017 – Revised: 30 October 2017 – Accepted: 3 November 2017 – Published: 30 November 2017

Abstract. Several major fault-drilling projects have captured the interseismic and postseismic periods of earthquakes. However, near-field observations of faults immediately before and during an earthquake remain elusive due to the unpredictable nature of seismicity. The Scientific Exploration of Induced Seismicity and Stress (SEISMS) workshop met in March 2017 to discuss the value of a drilling experiment where a fault is instrumented in advance of an earthquake induced through controlled fluid injection. The workshop participants articulated three key issues that could most effectively be addressed by such an experiment: (1) predictive understanding of the propensity for seismicity in reaction to human forcing, (2) identification of earthquake nucleation processes, and (3) constraints on the factors controlling earthquake size. A systematic review of previous injection experiments exposed important observational gaps in all of these areas. The participants discussed the instrumentation and technological needs as well as faults and tectonic areas that are feasible from both a societal and scientific standpoint.

1 Introduction

Understanding how earthquakes nucleate, propagate, and arrest is one of the major outstanding challenges in Earth science. The difficulty with making progress on this challenge stems from our inability to directly observe faults deep in the Earth where earthquakes nucleate, as well as our inability to test existing theory at the field scale, where we expect complex feedbacks between stress, pore pressure, and slip. These parameters could be measured by borehole and surface-based instruments during an earthquake if they were deployed near the rupture source. Previous fault zone drilling projects have probed the earthquake source soon after large events (e.g., following the 1995 Kobe, 1999 Chi Chi, 2008 Wenchuan,

and 2011 Tohoku earthquakes), and have enabled estimations of important parameters like stress during the earthquake (Ikeda, 2001; Ma et al., 2006; Fulton et al., 2013; Li et al., 2013). However, capturing the dynamics of an earthquake can only be achieved by instrumenting a fault prior to failure and monitoring it before, during, and after slip. Because earthquakes cannot be predicted, planning for a near-source deployment is extremely challenging. One possible method to ensure success is to induce failure through controlled fluid injection, similar to earthquakes induced by wastewater injection and recent small-scale (i.e., within meters of a fault zone), controlled experiments (e.g., Guglielmi et al., 2015).

Installing instruments inside the fault through fault zone drilling is the only way to obtain the small signals deep in the Earth necessary to investigate earthquake physics. An earthquake induced on a known fault through targeted fluid injection would provide an opportunity to obtain near-field information with a dense network of instruments deployed prior to the experiment. The fault could be fully characterized before the experiment with active source seismology, borehole geophysics, surface geology, and core-based investigations. An observatory of boreholes containing strain, pore pressure, temperature sensors and down-hole seismometers constructed in advance of the experiment would collect real-time data over a large frequency band (i.e., mHz to kHz) close to the source from initiation to arrest.

The recent escalation in induced earthquakes in North America makes an investigation like this a community priority. By defining the conditions necessary to induce an earthquake, the results would demonstrate how to prevent unintentionally induced earthquakes. A project of this scope requires significant community discussion and buy-in before going forward. The Scientific Exploration of Induced Seismicity and Stress (SEISMS) workshop was a first step in this direction. The overall goal of the workshop was to define the most significant scientific questions that could be addressed by in situ measurements of an earthquake with borehole observatories. In addition, we discussed technological, logistical, and societal hurdles, as well as how to overcome them. The outcome of this workshop includes focused understanding of the unanswered questions in earthquake and fault mechanics, as well as which questions could be addressed through fault zone drilling. Here, we outline the current state of understanding of earthquake physics, as articulated at the workshop, and provide a roadmap of questions that could be addressed through future fault zone drilling.

2 SEISMS meeting

2.1 Itinerary

The SEISMS workshop was held at Lamont-Doherty Earth Observatory, New York, USA, over 3 days from 29 to 31 March 2017. Attended by 86 participants from 10 countries, including representatives from industry, academia, and education, the workshop was sponsored by the International Continental Scientific Drilling Program (ICDP), the United States Geological Survey (USGS), and the Southern California Earthquake Center (SCEC). The workshop included a series of keynote talks from experts in earthquake physics, borehole instrumentation and observatories, induced earthquakes, and active earthquake experiments (Table 1), as well as group discussions concerning the need for an earthquake experiment, the scientific value of such an experiment, and the potential risks associated with inducing earthquakes.

2.2 Knowledge gaps between earthquake theory and observation

The primary goal of the SEISMS workshop was to outline and prioritize critical unresolved questions in earthquake physics. The majority of these questions are centered on our current inability to scale theory based on laboratory experiments to natural faults, as well as our inability to incorporate real-world complexity into lab experiments and models.

Much of our understanding of earthquake nucleation is based on the rate-and-state friction laws, which predict that an earthquake will begin by slipping aseismically until the rupture reaches a critical size, h^* :

$$h^* \sim \frac{\mu L}{(b-a)(\sigma-p)}, \quad (1)$$

where μ is rock shear modulus, L is the critical slip distance, σ is normal stress, p is pore pressure, and a and b are rate-and-state parameters (Rice, 1993; Scholz, 1998; Ampuero and Rubin, 2008). Because we do not know how some parameters, such as L , scale from laboratory to natural fault, the nucleation patch size is unknown, but might range in size from 0.1 to 10 m and will vary significantly depending on the effective stress resolved along the fault. It is unknown at this point whether the final earthquake size is a function of h^* . If it was, this would indicate that there is a fundamental difference between small and large earthquakes, as has been suggested when estimating other earthquake parameters such as fracture energy (Viesca and Garagash, 2015). Measurements of the nucleation length scale, accelerations, or moment release during the initial stages of slip are needed to understand the growth of earthquakes. In order to capture these signals, instrumentation would need to be essentially within meters of the slip surface. Such observations could never be made from the surface.

In addition to earthquake initiation, the processes or conditions that cause earthquakes to either arrest or propagate to larger magnitudes remain unknown, which is primarily why earthquake magnitude cannot be predicted. Structural complexity is an aspect of faults whose effects on earthquake dynamics are unknown. Geometric complexities such as non-planarity have been invoked to serve as nucleation sites (asperities) as well as boundaries to rupture propagation. Fault complexity also affects the slip during an earthquake, efficiency of energy dissipation mechanisms, and the radiation of seismic energy (Dunham et al., 2011). Furthermore, hydraulic diffusivity changes within both the fault core as well as damage zones may have significant control on pore pressure gradients throughout the rupture, and may aid in rupture arrest and the promotion of slow aseismic slip rather than fast seismic slip. In addition to geometric complexity, the controls of materials properties on different regions of the fault, such as regions of preseismic, coseismic, and afterslip, may not be constant through time or along strikes.

Table 1. SEISMS keynote talks.

Title	Speaker
Topic: Central Questions in Earthquake Physics	
The Knowns and Unknowns of Earthquake Physics	Eric Dunham
Lessons From Rangely	Barry Raleigh
Current Understanding of Induced Seismicity: Surface Observations	Elizabeth Cochran
Current Understanding of Induced Seismicity: Theory and Observations at Depth	Mark Zoback
Topic: Fault Zone Drilling and Instrumented Boreholes	
Fault Zone Drilling Experiences	Stephen Hickman
Borehole Observatories	Patrick Fulton
Topic: Drilling/Instrumentation Capabilities and Needs	
Downhole Logging Tools	Douglas Schmitt
In-Situ Experiments	Yves Guglielmi
Topic: What Would Make an Ideal Drilling Site?	
Oklahoma, USA	Brett Carpenter
British Columbia, Canada	David Eaton
Basin and Range, USA	Steven Wesnousky
Oceanic Transforms	Jeffrey McGuire and James Mori

2.3 Small- to large-scale in situ experiments and the accidental experiment of induced seismicity

Planning for the SEISMS experiment will lean heavily on the lessons learned from the Rangely experiment conducted during the 1970s (Raleigh et al., 1976). At Rangely, in situ stress measurements and measurement of the frictional strength of the faults led to successful prediction of the pore pressure needed to induce earthquakes, thereby supporting the use of the effective stress law to the scale of earthquakes and faulting. However, not all aspects of the experiment were well explained, for example, the occurrence of earthquakes far from the target fault, which required extreme hydraulic parameters using the conventional explanation. Modern thinking about elastic stresses could potentially solve these problems; however, the lack of geodetic data for the original experiment prevents a detailed analysis. Rangely also demonstrated that a well-characterized site, including tens to hundreds of observation wells, is an imperative. This included the analysis of the size of faults within the field area and minimized the risk of triggering a large earthquake. Armed with new technology in fault zone drilling and geodesy, a new-generation earthquake experiment could more directly measure fault slip and fluid pressures within both the fault core as well as the surrounding damage zone, which should enhance our ability to determine where and when failure will occur.

Recent borehole experiments have successfully induced small earthquakes ($-4.5 < M_w < -3$) in a controlled way (Derode et al., 2015; Guglielmi et al., 2015; De Barros et al., 2016). Observations of the induced earthquakes have demonstrated that the physical processes that lead to runaway slip

are complex and depend on the hydromechanical and frictional characteristics of both the fault and the surrounding rock. These experiments show that a small amount of dilatant aseismic slip can occur before seismic slip, and that earthquakes can be generated even in velocity strengthening material, which laboratory experiments suggested was unlikely (Guglielmi et al., 2015). Furthermore, several current microseismic experiments in underground mines are providing insights into the complexity in small earthquake nucleation (e.g., Yabe et al., 2015). Despite the exciting results of these studies, the earthquakes generated were limited to a small number of small magnitude events. Any change in physics from small to large earthquakes could not be captured in these experiments, and the effects of cumulative wastewater injection remain unconstrained.

Finally, the recent surge of earthquakes associated with hydrocarbon production and wastewater disposal offers new lessons. The frequency of earthquakes occurring in seismically quiet areas such as the Midwestern US and western Canada is greater than has ever been previously recorded (Ellsworth, 2013), and even moderately sized earthquakes could prove hazardous in areas that are unprepared for seismic activity. Many of the recent earthquakes are induced by human activity, but although we know that fluid injection causes induced seismicity (Raleigh et al., 1976), we cannot predict exactly when and where a particular earthquake will occur – just as with tectonic earthquakes. The scientific community should be able to contribute to this problem by defining the stress and fluid pressure conditions that are necessary to cause earthquake slip, but the measurements necessary to make these predictions do not exist. Talks and discussions on

induced seismicity at the SEISMS workshop mostly focused on the role of inherited structures and stress field characteristics in making an area more inclined to have induced seismicity. Some of the questions included the following. Are stress drops low in induced events (Sumy et al., 2017) or no different than tectonic earthquakes (e.g., Huang et al., 2017; Clerc et al., 2016)? What are pre-stress conditions on the fault within its seismic cycle, and how do they affect induced events? What role do fault damage zones play in communicating fluid pressures over large distances (Hennings et al., 2012)? What metrics are there for tracking how close a fault might be to failure during fluid injection?

2.4 Necessary components for an “active” earthquake experiment

2.4.1 Essential instrumentation

Recent fault zone drilling and other drilling projects have resulted in significant advances in borehole observatories and drilling capabilities. For instance, borehole instruments routinely include seismometers, thermistors, pore pressure sensors, and strain meters (Fulton et al., 2013; Chiaraluce et al., 2014). Increasingly, fiber optic cables are being emplaced within borehole casing and utilized as seismometers (Constantinou et al., 2016), strain meters and pressure meters (Cappa et al., 2006). To capture length scales appropriate for both the rupture tip region and fault slip patch dimension, observatory coverage across a wide range of scales will likely be required, so this type of instrumentation would be ideal for an active earthquake experiment. Finally, borehole observatories that exist on longer timescales (months–years) will need to carefully consider temperature and fluids at depth, including precursory monitoring.

2.4.2 Feasible sites

Preliminary site discussion at the SEISMS meeting focused on what would make a site feasible from both a scientific and safety standpoint. As a group, a list of criteria was developed that would be necessary for a successful site, including

1. faults that are well oriented in the current day stress field and possible to activate;
2. detailed subsurface characterization, including 3-D seismic imaging, determination of the stress and pore pressure fields, combined with surficial geologic mapping;
3. an area with low population density yet developed infrastructure (such as an oil field);
4. pre-existing and ongoing site monitoring; and
5. potential for collaboration from industry to take advantage of existing infrastructure and develop science priorities that can meaningfully contribute to hazard mitigation.

The specific sites discussed included places where induced seismicity is already occurring, like Oklahoma and British Columbia, as well as the Basin and Range, USA, and oceanic transform faults. Both terrestrial and oceanic sites were viewed favorably for an earthquake experiment (Fig. 1). Active experiments on the ocean transforms where frequent repeating events occur (McGuire et al., 2005), and continental faults where events occur much less frequently, can address different aspects of the initiation and rupture process. Also, logistical and observational constraints are very different for the two types of settings. Since there are different advantages and disadvantages for these two types of experiments, there were recommendations that proposals for both types of experiments should be worked on in parallel. Although discussion was not focused on a specific site at this time, the importance of picking a site where detailed understanding of fault structure, including the role of the damage zone in transmission of fluid pressures, number and thickness of localized slip zones, as well as friction strength, could be established before the active phase of the experiment.

2.5 Societal concerns

Safety and societal issues regarding potential induced earthquake experiments in various regions were prominent discussion topics throughout the workshop. The concept for the project would be to induce earthquakes through fluid injection, which would represent a hazardous outcome. However, there was recognition that understanding the causes of the many current human-induced earthquakes is an important issue for scientists to undertake. Given the largely unmonitored and uncontrolled way in which earthquakes are being induced in some regions, an experiment such as this would provide a valuable opportunity for the scientific community to provide some constraint on how to limit unintentionally induced seismicity.

Past examples of active geologic experiments show that communication with local officials and the public will be central to a successful project, as well as evaluation of safety risks, which would be essential for any project that might produce felt earthquakes. Outreach and education efforts will be important for any active experiment because this will likely be a high-profile project in the public eye. This should be viewed as an opportunity to provide information about earthquakes and seismic hazards. Plans for outreach activities should be started along with development of science objectives, for example by engaging local members of the public to invest in the project by helping to articulate which questions should be answered with the experiment.

3 Workshop outcomes and future directions

Participants identified three key questions at the workshop that should be targeted by the SEISMS project. They all depend on the measurement of stress, deformation, and pore

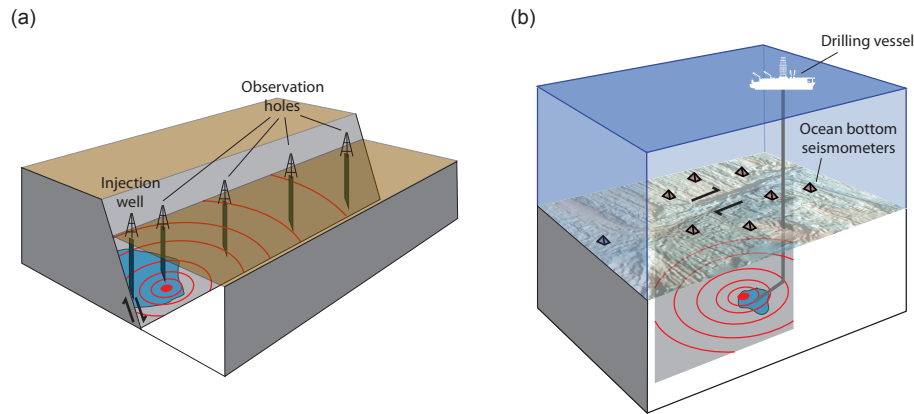


Figure 1. Potential target faults. **(a)** Continental fault observatory. Fluids pumped at the injection well will trigger an earthquake that can be recorded with seismometers, temperature sensors, strain meters, etc., at the observation holes. **(b)** Oceanic transform fault observatory. Fluid injected from a ship would trigger an earthquake on the fault that would be recorded by a network of ocean bottom seismometers (OBS in grey pyramids). Observation holes may also be drilled in advance of the injection.

pressure in the ultra-near field of an earthquake, and which therefore require a borehole observatory positioned close to the earthquake source.

3.1 Can we accurately determine when and where an earthquake is going to occur once fluid pressure is elevated?

Many induced earthquakes are associated with wastewater injection or hydraulic fracturing operations, both of which elevate fluid pressure and reduce the effective stresses at depth, promoting earthquake occurrence. However, many injection wells do not appear to induce seismicity (e.g., Cornet, 2016; Rivet et al., 2016), some wells appear to induce earthquakes at significant distances from the injector (e.g., Yeck et al., 2016; Goebel et al., 2017; Keranen et al., 2014), and some wells that directly penetrate faults have little effect on stability (Hauksson et al., 2015). These results show that even though the Rangely experiment in the 1970s seemed to demonstrate that the effective stress hypothesis describes fault failure under in situ conditions, it is still currently impossible to predict where and when an earthquake will occur, even within regions where fluid injection is taking place. This is partly because the mechanisms by which stress and pore pressure are transmitted to a fault are poorly understood. Direct fluid pressure increase and elastic stress perturbation have both been shown to be important for triggering earthquakes (e.g., Deng et al., 2016; Segall and Lu, 2015; Barbour et al., 2017), but which is more efficient, and therefore potentially more hazardous, is unknown. Induced earthquakes that occur far from an injection well indicate that fluid pressures are transmitted rapidly, highlighting the importance of complex fault zone hydrogeological structures. Furthermore, there is currently no consensus on how to predict what magnitude of earthquake could arise given a known stress or pore

pressure perturbation to a fault (e.g., McGarr, 2014; van der Elst et al., 2016). An experiment to test the response of a fault to a controlled perturbation affecting a known volume in the subsurface could elucidate the conditions necessary to induce earthquake slip, and therefore determine the limits of water injection operations appropriate for preventing unwanted induced seismicity. Important advances in technology have occurred in the nearly 50 years since the Rangely experiment. Rangely included no geodetic instrumentation and therefore could not assess the role of elasticity or creep in inducing earthquakes. Modern, digital and dense instrumentation could provide a much higher-resolution image of the earthquake locations that could address outstanding quandaries, such as the apparent location of the induced earthquakes kilometers away from the injection well.

3.2 How do earthquakes nucleate?

Laboratory-derived friction laws such as the rate-and-state equations imply that a small amount of aseismic creep should precede an earthquake. Such a precursory phase has long been sought in observational data, including foreshock sequences (e.g., Kato et al., 2012; Chen et al., 2017). More recently, geodetically measured slow slip events have been one of the more promising avenues for identifying an impending mainshock (e.g., Uchida et al., 2016). However, the scale of the precursory slip patch may be quite small, 10 m or less, and the ability to measure such a signal therefore likely depends on in situ measurements. In such a case, the larger-scale slow slip and foreshock sequences that are sometimes measured with surface instruments would be the result of more complex interactions between slip on the future rupture interface, the surrounding damage zone, potential fluid pressure changes, and heterogeneity of all of these properties along the fault (e.g., Savage et al., 2017).

3.3 What controls earthquake propagation and arrest?

All earthquakes nucleate, but not all grow to large magnitudes. This implies that some earthquakes do not propagate significantly and arrest at small magnitudes instead. Rupture propagation is thought to be a function of the initial conditions in the source region, the constitutive laws that govern frictional sliding, and the geometrical properties of the host fault. The stress field and pore pressure distribution in and around a fault are heterogeneous, and the physical characteristics of faults such as roughness and damage zone characteristics are spatially variable. Constraining all of these parameters prior to an induced earthquake would be challenging, but near-field observations of the rupture tip zone would provide an unprecedented view of the underlying physical processes.

Because the answers to the three questions outlined at the SEISMS meeting are fundamental to predicting when and where large earthquakes will occur, the workshop participants were in agreement that an earthquake experiment by fluid injection should be pursued. The next order of business is to establish potential industry partners and have a more complete discussion of potential drilling targets. More immediately, the discussions begun at the SEISMS meeting are being continued at larger conferences, including the Continental Scientific Drilling Coordination Office (CSDCO) annual meeting and the 2017 American Geophysical Union (AGU) Fall Meeting.

Data availability. No data sets were used in this article.

Competing interests. The authors declare that they have no conflict of interest.

Acknowledgements. The authors gratefully acknowledge funding for the workshop, which was provided through the following grants: ICDP CU17-0069, USGS G17AP00037, and SCEC 16234.

Edited by: Thomas Wiersberg

Reviewed by: Sukanta Roy and Kazutoshi Immanishi

References

- Ampuero, J. P. and Rubin, A. M.: Earthquake nucleation on rate and state faults—Aging and slip laws, *J. Geophys. Res.-Sol. Ea.*, 113, B01302, <https://doi.org/10.1029/2007JB005082>, 2008.
- Barbour, A., Norbeck, J. H., and Rubinstein, J. L.: The Effects of Varying Injection Rates in Osage County, Oklahoma, on the 2016 Mw 5.8 Pawnee Earthquake, *Seismol. Res. Lett.*, 88, 1040–1053, <https://doi.org/10.1785/0220170003>, 2017.
- Cappa, F., Guglielmi, Y., Gaffet, S., Lançon, H., and Lamarque, I.: Use of in situ fiber optic sensors to characterize highly heterogeneous elastic displacement fields in fractured rocks, *Int. J. Rock Mech. Min.*, 43, 647–654, 2006.
- Chen, X., Nakata, N., Pennington, C., Haffener, J., Chang, J. C., He, X., Zhan, Z., Ni, S., and Walter, J. I.: The Pawnee earthquake as a result of the interplay among injection, faults and foreshocks, *Sci. Rep.-UK*, 7, 4945, <https://doi.org/10.1038/s41598-017-04992-z>, 2017.
- Chiaraluce, L., Collettini, C., Cattaneo, M., and Monachesi, G.: The shallow boreholes at The AltotiBerina near fault Observatory (TABOO; northern Apennines of Italy), *Sci. Drill.*, 17, 31–35, <https://doi.org/10.5194/sd-17-31-2014>, 2014.
- Clerc, F., Harrington, R. M., Liu, Y., and Gu, Y. J.: Stress drop estimates and hypocenter relocations of induced seismicity near Crooked Lake, Alberta, *Geophys. Res. Lett.*, 43, 6942–6951, <https://doi.org/10.1002/2016GL069800>, 2016.
- Constantinou, A., Schmitt, D., Kofman, R., Kellett, R., Eccles, J., Lawton, D., Bertram, M., Hall, K., Townend, J., Savage, M., and Buske, S.: Comparison of fiber-optic sensor and borehole seismometer VSP surveys in a scientific borehole: DFDP-2b, Alpine Fault, New Zealand, in: SEG Technical Program Expanded Abstracts 2016 (pp. 5608–5612), Society of Exploration Geophysicists, 2016.
- Cornet, F. H.: Seismic and aseismic motions generated by fluid injections, *Geomechanics for Energy and the Environment*, 5, 42–54, 2016.
- Deng, K., Liu, Y., and Harrington, R. M.: Poroelastic stress triggering of the December 2013 Crooked Lake, Alberta, induced seismicity sequence, *Geophys. Res. Lett.*, 43, 8482–8491, 2016.
- Derode, B., Guglielmi, Y., De Barros, L., and Cappa, F.: Seismic responses to fluid pressure perturbations in a slipping fault, *Geophys. Res. Lett.*, 42, 3197–3203, 2015.
- De Barros, L., Daniel, G., Guglielmi, Y., Rivet, D., Caron, H., Payre, X., Bergery, G., Henry, P., Castilla, R., Dick, P., and Barbieri, E.: Fault structure, stress, or pressure control of the seismicity in shale? Insights from a controlled experiment of fluid-induced fault reactivation, *J. Geophys. Res.-Sol. Ea.*, 121, 4506–4522, 2016.
- Dunham, E. M., Belanger, D., Cong, L., and Kozdon, J. E.: Earthquake ruptures with strongly rate-weakening friction and off-fault plasticity, Part 2: Nonplanar faults, *B. Seismol. Soc. Am.*, 101, 2308–2322, 2011.
- Ellsworth, W. L.: Injection-induced earthquakes, *Science*, 341, 1225942, <https://doi.org/10.1126/science.1225942>, 2013.
- Fulton, P. M., Brodsky, E. E., Kano, Y., Mori, J., Chester, F., Ishikawa, T., Harris, R. N., Lin, W., Eguchi, N., and Toczko, S.: Low coseismic friction on the Tohoku-Oki fault determined from temperature measurements, *Science*, 342, 1214–1217, 2013.
- Goebel, T. H. W., Weingarten, M., Chen, X., Haffener, J., and Brodsky, E. E.: The 2016 Mw 5.1 Fairview, Oklahoma earthquakes: Evidence for long-range poroelastic triggering at >40 km from fluid disposal wells, *Earth Planet. Sc. Lett.*, 472, 50–61, 2017.
- Guglielmi, Y., Cappa, F., Avouac, J. P., Henry, P., and Ellsworth, D.: Seismicity triggered by fluid injection—induced aseismic slip, *Science*, 348, 1224–1226, 2015.
- Hauksson, E., Goebel, T. H. W., Ampuero, J.-P., and Cochran, E.: A century of oil-field operations and earthquakes in the greater Los Angeles Basin, southern California, *The Leading Edge*, 34, 650–656, <https://doi.org/10.1190/tle34060650.1>, 2015.
- Hennings, P., Allwardt, P., Paul, P., Zahm, C., Reid Jr., R., Alley, H., Kirschner, R., Lee, B., and Hough, E.: Relationship between fractures, fault zones, stress, and reservoir productivity in the

- Suban gas field, Sumatra, Indonesia, AAPG bulletin, 96, 753–772, 2012.
- Huang, Y., Ellsworth, W. L., and Beroza, G. C.: Stress drops of induced and tectonic earthquakes in the central United States are indistinguishable, *Science Advances*, 3, e1700772, <https://doi.org/10.1126/sciadv.1700772>, 2017.
- Ikeda, R.: Outline of the fault zone drilling project by NIED in the vicinity of the 1995 Hyogo-ken Nanbu earthquake, Japan, *Island Arc*, 10, 199–205, 2001.
- Kato, A., Obara, K., Igarashi, T., Tsuruoka, H., Nakagawa, S., and Hirata, N.: Propagation of slow slip leading up to the 2011 Mw 9.0 Tohoku-Oki earthquake, *Science*, 335, 705–708, 2012.
- Keranen, K., Weingarten, M., Abers, G. A., Bekins, B. A., and Ge, S.: Sharp increase in central Oklahoma seismicity since 2008 induced by massive wastewater injection, *Science*, 345, 448–451, <https://doi.org/10.1126/science.1255802>, 2014.
- Li, H., Wang, H., Xu, Z., Si, J., Pei, J., Li, T., Huang, Y., Song, S. R., Kuo, L. W., Sun, Z., and Chevalier, M. L.: Characteristics of the fault-related rocks, fault zones and the principal slip zone in the Wenchuan Earthquake Fault Scientific Drilling Project Hole-1 (WFSD-1), *Tectonophysics*, 584, 23–42, 2013.
- Ma, K. F., Tanaka, H., Song, S. R., Wang, C. Y., Hung, J. H., Tsai, Y. B., Mori, J., Song, Y. F., Yeh, E. C., Soh, W., and Sone, H.: Slip zone and energetics of a large earthquake from the Taiwan Chelungpu-fault Drilling Project, *Nature*, 444, 473–476, 2006.
- McGarr, A.: Maximum magnitude earthquakes induced by fluid injection, *J. Geophys. Res.-Sol. Ea.*, 119, 1008–1019, <https://doi.org/10.1002/2013JB010597>, 2014.
- McGuire, J. J., Boettcher, M. S., and Jordan, T. H.: Foreshock sequences and short-term earthquake predictability on East Pacific Rise transform faults, *Nature*, 434, 457–461, 2005.
- Raleigh, C. B., Healy, J. H., and Bredehoeft, J. D.: An experiment in earthquake control at Rangely, Colorado, *Science*, 191, 1230–1237, 1976.
- Rice, J. R.: Spatio-temporal complexity of slip on a fault, *J. Geophys. Res.-Sol. Ea.*, 98, 9885–9907, 1993.
- Rivet, D., De Barros, L., Guglielmi, Y., Cappa, F., Castilla, R., and Henry, P.: Seismic velocity changes associated with aseismic deformations of a fault stimulated by fluid injection, *Geophys. Res. Lett.*, 43, 9563–9572, <https://doi.org/10.1002/2016GL070410>, 2016.
- Savage, H. M., Keranen, K. M., Schaff, D. P., and Dieck, C.: Potential precursory signals in damage zone foreshocks, *Geophys. Res. Lett.*, 44, 5411–5417, 2017.
- Scholz, C. H.: Earthquakes and friction laws, *Nature*, 391, 37–42, 1998.
- Segall, P. and Lu, S.: Injection-induced seismicity: Poroelastic and earthquake nucleation effects, *J. Geophys. Res.-Sol. Ea.*, 120, 5082–5103, <https://doi.org/10.1002/2015JB012060>, 2015.
- Sumy, D. F., Neighbors, C. J., Cochran, E. S., and Keranen, K. M.: Low stress drops observed for aftershocks of the 2011 Mw 5.7 Prague, Oklahoma, earthquake, *J. Geophys. Res.-Sol. Ea.*, 122, 3813–3834, 2017.
- Uchida, N., Inuma, T., Nadeau, R. M., Bürgmann, R., and Hino, R.: Periodic slow slip triggers megathrust zone earthquakes in northeastern Japan, *Science*, 351, 488–492, 2016.
- van der Elst, N. J., Page, M. T., Weiser, D. A., Goebel, T. H. W., and Hosseini, S. M.: Induced earthquake magnitudes are as large as (statistically) expected, *J. Geophys. Res.-Sol. Ea.*, 121, 4575–4590, <https://doi.org/10.1002/2016JB012818>, 2016.
- Viesca, R. C. and Garagash, D. I.: Ubiquitous weakening of faults due to thermal pressurization, *Nat. Geosci.*, 8, 875–879, 2015.
- Yabe, Y., Nakatani, M., Naoi, M., Philipp, J., Janssen, C., Watanabe, T., Katsura, T., Kawakata, H., Georg, D., and Ogasawara, H.: Nucleation process of an M2 earthquake in a deep gold mine in South Africa inferred from on-fault foreshock activity, *J. Geophys. Res.-Sol. Ea.*, 120, 5574–5594, 2015.
- Yeck, W. L., Weingarten, M., Benz, H. M., McNamara, D. E., Bergman, E. A., Hermann, R. B., Rubinstein, J. L., and Earle, P. S.: Far-field pressurization likely caused on of the largest injection induced earthquakes by reactivating a large preexisting basement fault structure, *Geophys. Res. Lett.*, 43, 1–10, 2016.

ECORD mid-term renewal

Since January 2017, ECORD has entered into a three-step process that should lead the ECORD member countries to commit to the second phase (2019–2023) of IODP. The success of the ECORD mid-term renewal should primarily rely on ECORD's scientific and operational excellence in the international research landscape during the first phase of IODP (2013–2018), as well as the operational plans defined for MSPs, the JR, and the *Chikyu* in the second phase of IODP (2019–2023).

The first step of this process was represented by an ECORD evaluation that was conducted from January to June 2017 by the ECORD External Evaluation Committee (EEC) during a meeting that was held on 6–8 June 2017, in Bremen, Germany. The report that was delivered soon after this meeting covers all aspects of ECORD activities (science, technology, management, education, and outreach) and especially highlights the excellent ECORD scientific achievements within IODP, the need to sustain this unique and global research structure, and the need for ECORD to maintain its strengths in being able to finance and implement high-profile MSP expeditions. This report also includes a series of recommendations concerning various fields (science, education, and outreach) that the ECORD Council considered at its spring meeting that was held on June 29, 2017 in Amsterdam, the Netherlands. Among these recommendations, the ECORD Council has decided that the ECORD Managing Agency (EMA) and ESO will be administered by the Centre National de la Recherche Scientifique (CNRS) and the British Geological Survey (BGS) respectively until the end of the current programme, i.e. 2023.

The second step of this process includes a revision of the ECORD Memorandum of Understanding, based on an internal reappraisal of ECORD functioning during the first phase of IODP (2013–2018), as well as recommendations made by the EEC. The different ECORD entities have started to revise their Terms of Reference and a first draft of the new ECORD MoU should be completed soon after the upcoming ECORD Council–ESSAC meeting that will be held in Southampton, UK, on October 24 and 25, 2017. The 2019–2023 ECORD MoU should then be finalized before the end of the year and distributed to the ECORD funding agencies for approval and signature in 2018.

The third step of the ECORD mid-term renewal consists of a revision of the MoU between ECORD and the US National Science Foundation (NSF) defining the financial and operational agreement regarding the ECORD's membership in the JR Consortium and, in reciprocity, access to MSP expeditions for our

partners' scientists. Preliminary discussions between ECORD and NSF started in late 2016, have continued throughout 2017, and have led to a formal agreement between ECORD and NSF on a draft that will be finalized soon. There will be no significant change in ECORD scientists' participation in the JR expeditions during the second phase of the current programme, when the JR is expected to operate up to 10 months a year in the eastern Pacific and then in the Atlantic Ocean, the Mediterranean, Caribbean, and the Gulf of Mexico, depending on the proposal pressure concerning these regions.

No revision will be considered for the MoU linking ECORD and the Japan Agency for Marine–Earth Science and Technology (JAMSTEC) as this MoU was signed in 2013 for the whole duration of IODP. The scheduling of an engineering riserless expedition (380 “NanTroSEIZE Frontal Thrust Borehole Monitoring System”) in early 2018 and of a riser drilling expedition (359 “NanTroSEIZE: Riser Hole at C0002”) in late 2018–early 2019 respectively will create a continuity in Chikyu operations throughout the renewal time window.

U.S. convenes facility assessment workshop

On September 26–27, 2017, the U.S. Science Support Program (USSSP) sponsored the *JOIDES Resolution Assessment Workshop*, a 2-day meeting aimed at reviewing and assessing the role of the *JOIDES Resolution* drilling platform in enabling the IODP research community to carry out the objectives of the 2013–2023 IODP Science Plan, *Illuminating Earth's Past, Present and Future*. The workshop was attended by over 80 participants, including international observers, and will result in a report that provides community guidance to the National Science Foundation (NSF) as it seeks renewal of the *JOIDES Resolution* facility from the U.S. National Science Board (NSB). Responses to a wide-ranging community survey of IODP scientists were analysed by the workshop attendees both prior to and during the workshop, and will form the backbone of the report, which will review achievements and future goals by IODP theme. It will also catalogue increased efficiencies and cost-effectiveness introduced during the International Ocean Discovery Program as a result of regional operational planning and a streamlined advisory panel structure and proposal review process.

Petrophysics Summer School 2017

For the second year running a week-long summer school in petrophysics was hosted at the University of Leicester (2–7 July 2017) as a UK International Ocean Discovery Program (IODP) knowledge exchange initiative. Building on the success of the first summer school in 2016, this year's course brought together 30 participants from 10 countries (by institution; 18 by nationality) from as far away as Australia. The participant group, while predominantly comprised of graduate students, included a number of post-docs and more senior scientists, most of whom had little or no experience with petrophysics. The 6-day course combined lectures, practicals, software training, and site visits to Weatherford and the British Geological Survey (BGS) Core Store, to provide a well-rounded grounding in the fundamentals and applications of petrophysics. There was also an opportunity for participants to introduce themselves and present their research during a mini-conference held on the first day. The course received independent continuing professional development (CPD) accreditation, meaning that participants, on completion of the course, received a formal certificate indicating receipt of 36h of accredited CPD.

A pool of 14 instructors from both academia (European Petrophysics Consortium (EPC, comprising the Universities of Leicester and Montpellier), Imperial College London, JAMSTEC, Lamont-Doherty Earth Observatory of Columbia University, University of Leicester) and industry (ALS Petrophysics, BP (UK), Schlumberger Information Systems) provided training throughout the week, drawing on their many and varied experiences and including real-world examples from both commercial and IODP projects (notably, but not exclusively, Expedition 346 Asian Monsoon).

The 2nd Petrophysics Summer School was made possible via funding from the UK IODP (funded via the Natural Environment Research Council (NERC)), the European Consortium for Ocean Research Drilling (ECORD), the Aberdeen Formation Evaluation Society (AFES), and the London Petrophysical Society (LPS). Significant in-kind contributions were also made by EPC, Weatherford (Reeves Wireline Services, East Leake) and the BGS Core Store. Over half of the participants' attendance was supported via generous scholarships/bursaries from the United States Science Support Office (USSSP, 9 bursaries), ECORD (5 scholarships), and UK IODP (2 bursaries).

It is anticipated that a 3rd Petrophysics Summer School will be held in 2018 – further information will be available in January 2018 via www.iodp.rocks.

Schedules

IODP – Expedition schedule <http://www.iodp.org/expeditions/>



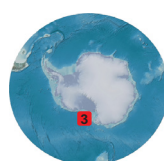
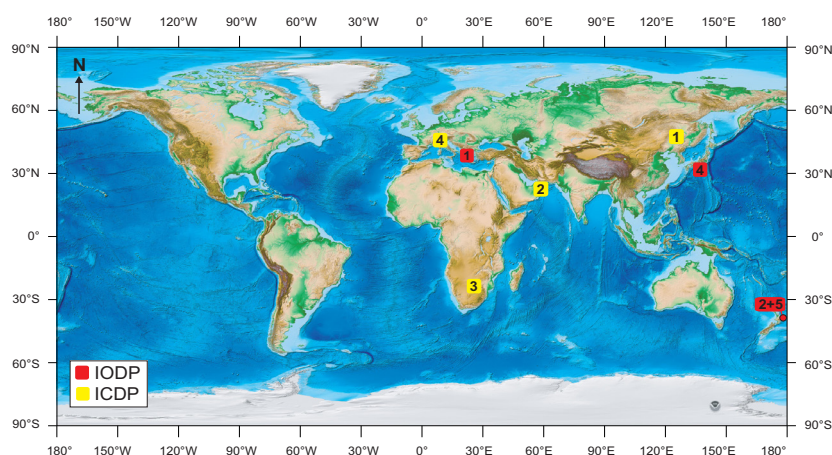
ECORD operations	Platform	Dates	Port of origin
1 381 Corinth Active Rift Development	MSP	Oct–Dec 2017	Corinth
USIO operations	Platform	Dates	Port of origin
2 372 Creeping Gas Hydrate Slides and Hikurangi LWD	JOIDES Resolution	26 Nov 2017–4 Jan 2018	Fremantle
3 374 Ross Sea West Antarctic Ice Sheet History	JOIDES Resolution	4 Jan–8 Mar 2018	Wellington
5 375 Hikurangi Subduction Margin Observatory	JOIDES Resolution	8 Mar–5 May 2018	Wellington
CDEX operations	Platform	Dates	Port of origin
4 NanTroSEIZE Frontal Thrust Borehole Monitoring System	Chikyu	12 Jan–24 Feb 2018	Shimizu

ICDP – Project schedule <http://www.icdp-online.org/projects/>



ICDP project	Drilling dates	Location
1 Songliao Basin	Apr 2014–Dec 2017	Songliao Basin, China
2 Oman Phase II	Nov 2017–Apr 2018	Oman
3 DSEIS	Apr 2017–Mar 2018	Orkney, South Africa
4 DOVE	May–Oct 2018	Alpes

Locations



Topographic/bathymetric maps courtesy of NOAA (Amante, C. and B.W. Eakins, 2009. ETOPO1 1 Arc-Minute Global Relief Model: Procedures, Data Sources and Analysis. NOAA Technical Memorandum NESDIS NGDC-24. National Geophysical Data Center, NOAA. doi:10.7289/V5C8276M).